
# INVESTIGATING THE ROLE OF GROWTH HORMONE RECEPTOR IN OESOPHAGEAL SQUAMOUS-CELL CARCINOMA

Thesis by

Boris Krivochiev

**Supervisor** A/Prof. Denver Hendricks

**Co-Supervisor** Dr. Kate Hadley



In Fulfilment of the Requirements for the Degree of Masters of Science (Med)

University of Cape Town

Cape Town, South Africa

February 2013

**PLAGIARISM DECLARATION**

1. I know that plagiarism is wrong. Plagiarism is using another's work and to pretend that it is one's own.

2. I have used the Cell Journal as the convention for citation and referencing. Each significant contribution to, and quotation in, this thesis from the work, or works of other people has been attributed and has been cited and referenced.

3. This project is my own work.

4. I have not allowed, and will not allow, anyone to copy my work with the intention of passing it off as his or her own work.

5. I acknowledge that copying someone else's assignment or essay, or part of it, is wrong, and declare that this is my own work

SIGNATURE: _____

DATE: _____

**ACKNOWLEDGMENTS**

I would like to express my sincere gratitude to the following people:

My supervisor, A/Prof. Denver Hendricks, for his excellent supervision and constant encouragement and support.

My co-supervisor, Kate Hadley, for her amazing guidance, energy, and contribution of ideas.

Members of the Cancer Research Group, for creating such a dynamic and enjoyable working environment, particularly Hapiloe Maranyane, I will miss our intense philosophical debates.

Hajira Guzgay, for her diligent management of the laboratory and the people within it.

Robert Samuels, for his valuable assistance in the laboratory.

Pauline van der Watt, Jaquiline Bracher, Nelusha Shunmoogam-Gounden and Nina Holderness-Parker, for their help in the laboratory.

Prof. Michael Waters for kindly donating the GHR expression plasmid.

The National Research Foundation and UCT for financial assistance.

**TABLE OF CONTENTS**

**Abbreviations**

| | | |
|---|---|---|
| µg | - | microgram |
| µl | - | microliter |
| µM | - | micromolar |
| $^{o}C$ | - | Celsius |
| AC | - | adenocarcinoma |
| AIDS | - | acquired immunodeficiency syndrome |
| ALS | - | acid labile subunit |
| BCA | - | bicinchoninic acid |
| BCP | - | 1-bromo-3-chloropropane |
| bp | - | base pair |
| cDNA | - | complementary DNA |
| $C_T$ | - | cycle threshold |
| DAPI | - | 4',6-diamidino-2-phenylindole |
| DEPC | - | diethylpyrocarbonate |
| DMEM | - | Dulbecco's Modified Eagle Medium |
| DMSO | - | dimethyl sulfoxide |
| DNA | - | deoxyribonucleic acid |
| EDTA | - | ethylene diamine tetra acetic acid |
| EGF | - | epithelial growth factor |
| EGFR | - | epithelial growth factor receptor |
| ERK | - | extracellular-signalling-regulated kinase |
| FAK | - | focal adhesion kinase |

| | | |
|---|---|---|
| FBS | - | foetal bovine serum |
| g | - | gramme |
| GAS | - | INFγ activated sequence |
| gDNA | - | genomic DNA |
| GHRE | - | growth hormone responsive element |
| GH | - | growth hormone |
| GHBP | - | growth hormone-binding protein |
| GHR | - | growth hormone receptor |
| GHRH | - | growth hormone-releasing hormone |
| hr | - | hour |
| HA | - | human influenza hemagglutinin |
| HIV | - | human immunodeficiency virus |
| $IC_{50}$ | - | inhibition concentration 50 |
| IGF1 | - | insulin-like growth factor 1 |
| IGFBP | - | insulin-like growth factor binding protein |
| IRS | - | insulin receptor substrate |
| JAK | - | janus tyrosine kinase |
| JH region | - | joining region |
| kDa | - | kilodalton |
| LB | - | luria broth |
| LD | - | loading dye |
| M | - | molar |
| MAPK | - | mitogen-activated protein kinase |

| | | |
|---|---|---|
| MEK | - | mitogen activated protein kinase kinase |
| mg | - | milligramme |
| min | - | minute |
| ml | - | millilitre |
| mM | - | millimolar |
| MOPS | - | 3-(N-morpholino)propanesulfonic acid |
| mRNA | - | messenger ribonucleic acid |
| nm | - | nanometer |
| nM | - | nanomolar |
| O/N | - | overnight |
| OSCC | - | oesophageal squamous-cell carcinoma |
| p | - | probability value |
| P/S | - | penicillin streptomycin |
| PBS | - | phosphate-buffered saline |
| PCR | - | polymerase chain reaction |
| PGM1 | - | phosphoglucomutase 1 |
| PI3K | - | phosphoinositide-3 kinase |
| PRLR | - | prolactin receptor |
| pTyr | - | phosphorylated tyrosine |
| qRT-PCR | - | quantitative real-time PCR |
| RHP | - | random hexomer primers |
| RIPA | - | radioimmnoprecipitation assay buffer |
| RNA | - | ribonucleic acid |

| | | |
|---|---|---|
| RT | - | room temperature |
| SCC | - | squamous-cell carcinoma |
| SDS | - | Sodium dodecyl sulphate |
| SDS-PAGE | - | Sodium dodecyl sulphate- polyacrylamide gel electrophoresis |
| sec | - | second |
| SH2 | - | Src homology 2 |
| SHC | - | Src homology 2/α collagen related |
| SHP | - | SH2 domain-containing protein tyrosine phosphatase |
| siRNA | - | small interfering RNA |
| SOCS | - | suppressor of cytokine signalling |
| STAT | - | signal transducer and activator of transcription |
| TACE | - | tumour necrosis factor-α-converting enzyme |
| TBST | - | tris-buffered saline tween 20 |
| UTR | - | untranslated region |
| V | - | volts |

**ABSTRACT**

Squamous-cell carcinoma of the oesophagus is a formidable disease which poses a significant health risk in developing countries where incidence is high and survival is low. Investigating the poorly understood mechanisms involved in oesophageal tumourigenesis may provide a platform to develop improved diagnostic techniques and therapies. The growth hormone (GH) signalling axis is important for proper cellular and organ system function. The axis has been shown to play a role in a number of cancers. Additionally, GH has shown to induce neoplasms *in vivo* while forced autocrine signalling of GH was shown to promote carcinogenesis in several *in vitro* models, highlighting the role of GH in tumourigenesis. Several studies showed that the tumourigenic effects of GH are largely mediated by its receptor, growth hormone receptor (GHR). The aim of this project is to therefore identify the role GHR in oesophageal squamous-cell carcinoma (OSCC) using an *in vitro* model. mRNA analysis showed expression of endogenous GH mRNA in a majority of OSCC cell lines tested, while nearly all expressed some form of GHR. Few, however, expressed mRNA for the more-active isoform of GHR, d3GHR, indicating GH may play a role in OSCC, and may be mediated by full-length GHR (flGHR) in a majority of cell lines. Western blotting for GHR remained largely unsuccessful, indicative of the short half-life of mature GHR and the possible insensitivity of commercially-available GHR antibodies. However, unglycosylated, immature GHR is likely detected as a 95kDa band, while mature GHR may be detected as a 120kDa band. However, a non-specific 95kDa band was also detected, thereby interfering with detection of true levels of premature GHR in OSCC cell lines. GHR knockdown by small interfering RNA indicated that the GH axis may play a role in proliferation in a subset of patients that is mediated by GHR, but does not affect responses to the chemotherapeutic agents doxorubicin and cisplatin. Additionally, the mRNA expression of GHR did not correlate with the expression of functional GHR protein in a number of OSCC cell lines. These results together indicate while GHR may play a role in a subset of patients, the role is limited to proliferation when only investigating the effects of GH on proliferation and chemoresistance. However, investigating additional markers of tumourigenesis is needed to further elucidate the role of GH/GHR signalling in OSCC. Additionally, the potential tumourigenic effects of GH mediated by prolactin receptor (PRLR) may not be ignored.

# CHAPTER ONE:

# INTRODUCTION

## 1.1 Cancer

In a report published in 2011 by the Centre for Disease Control, it was reported that cancer ranked as the second leading cause of death worldwide (Heron, 2011). Based on estimates, there were approximately 12.7 million newly-diagnosed cancer cases and 7.6 million cancer-related deaths in 2008 (Ferlay *et al*., 2010). These figures are anticipated to continue increasing due to the aging and growth of the world's population, with the incidence of cancer in the United States of America anticipated to increase 45% from the years 2010 to 2030 alone (Smith *et al*., 2009). Incidence rates in developed countries are double those seen in developing countries due to the adoption of a lifestyle more suited to the development of cancer, such as physical inactivity, smoking, and diets rich in fat (Jemal *et al*., 2011). However, cancer mortality rates in developed and developing countries remain similar, with cancer survival being poorer in developing countries. This can be attributed to a combination of late-stage diagnoses, limited access to health care, and inadequately funded government health care budgets (Jemal *et al*., 2011). Cancer therefore poses an increasing threat to health and economic systems, particularly in developing countries. This paints a bleak picture for the economically developing world, and highlights the need for cancer research within these countries. There is therefore a need to increase resources for cancer research, comparable to the levels of funding dedicated to other diseases known to play major roles in developing countries, such as tuberculosis, malaria, and HIV/AIDS.

## 1.2 The Hallmarks of Cancer

Cancer, by popular definition, is the unregulated proliferation of a population of cells. However, this simple definition does not suffice. The ever-increasing insight of the molecular mechanisms of cancer, generated by research, have shown that cancer is in fact a multifactoral disease, which ultimately manifests as uncontrolled and rapid proliferation of cells into the formation of a tumour. Yet, this would not occur unless cells developed certain characteristics to allow such unregulated growth. Hanahan and Weinberg (Hanahan and Weinberg, 2011) detailed six characteristics that normal cells would have to acquire before becoming cancerous. They also suggested that these characteristics are facilitated by the genomic instability present within pre-malignant cells that allows mutations to occur and thus the acquisition of such characteristics. The six hallmarks of cancer are as follows: sustenance of proliferative signalling, evasion of growth suppressors, resistance of cell death, enabling replicative immortality, induction of angiogenesis, and activation of invasion and metastasis, with sustenance of proliferative signalling being arguably the most fundamental trait. The process whereby these hallmarks are acquired relies heavily on the manipulation of existing intracellular signalling pathways brought about directly through genetic instability.

## 1.3Oesophageal Cancer

Given the threat posed by cancer to developing regions, oesophageal cancer is of significant concern. Oesophageal cancer is the eighth most common cancer and is the sixth leading cause of cancer death worldwide (Parkin *et al*., 1999). In 2011, an estimated 481 205 new cases of oesophageal cancer were diagnosed with 406 800 deaths attributed to the disease (Jemal *et al*., 2011), making it one of the highest mortality rates compared to other cancers. Significantly, it is estimated that 83% of new diagnoses, and 85% of deaths attributed to oesophageal cancer occurred in developing countries (Fig.1), with males being two times more at risk than females (Fig.1) (Ferlay *et al*., 2010; Jemal *et al*., 2011).

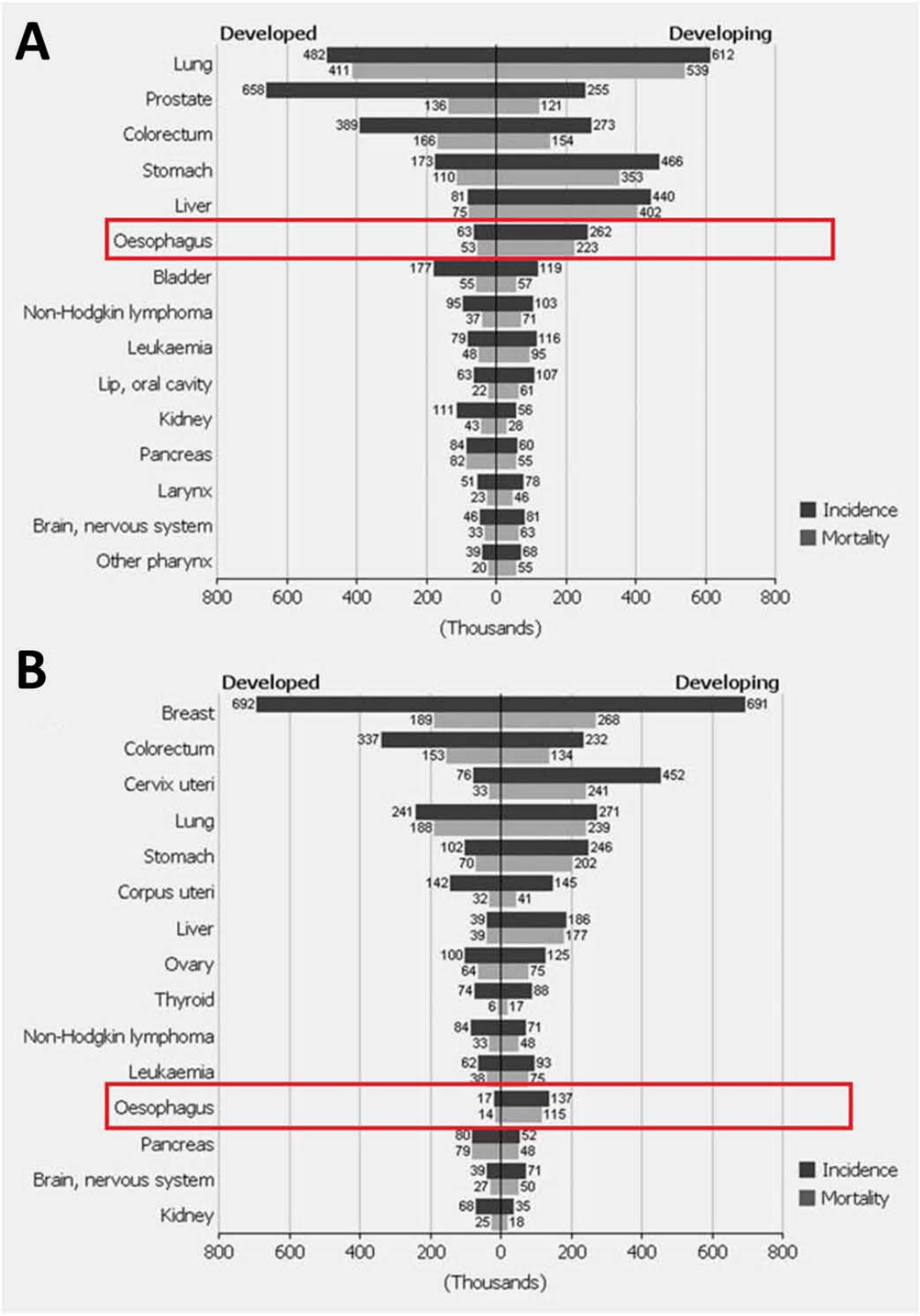


**Figure 1: Worldwide cancer incidence and mortality rates** (Ferlay *et al*., 2010)**.(A)** Estimated incidence and mortality cases (thousands) in developing and developed regions for **(A)** men, and**(B)**women.

There are two subtypes of oesophageal cancer, namely squamous-cell carcinoma (SCC) and adenocarcinoma (AC) (Daly *et al*., 2000), however, on rare occasions other carcinomas, melanomas, carcinoids, and lymphomas may also develop in the oesophagus (Enzinger and Mayer, 2003). Both subtypes share a common lineage, in that both arise from epithelial cells in the oesophagus. Yet, the two subtypes are distinct in that SCC originates from squamous cells in the epithelial layer, while AC arises from glandular cells present in the epithelium of the oesophagus. Furthermore, SCC mainly occurs in the proximal and middle oesophagus while AC occurs mainly in the distal oesophagus at the gastro-oesophageal junction (Daly *et al*., 2000; Siewert *et al*., 2001).

Geographically, oesophageal cancer is present worldwide, however, incidence rates vary greatly internationally with the higher rates found in developing countries (Fig.1). The highest incidence rates are found in Southern Africa (Fig.2) (Jemal *et al*., 2011).

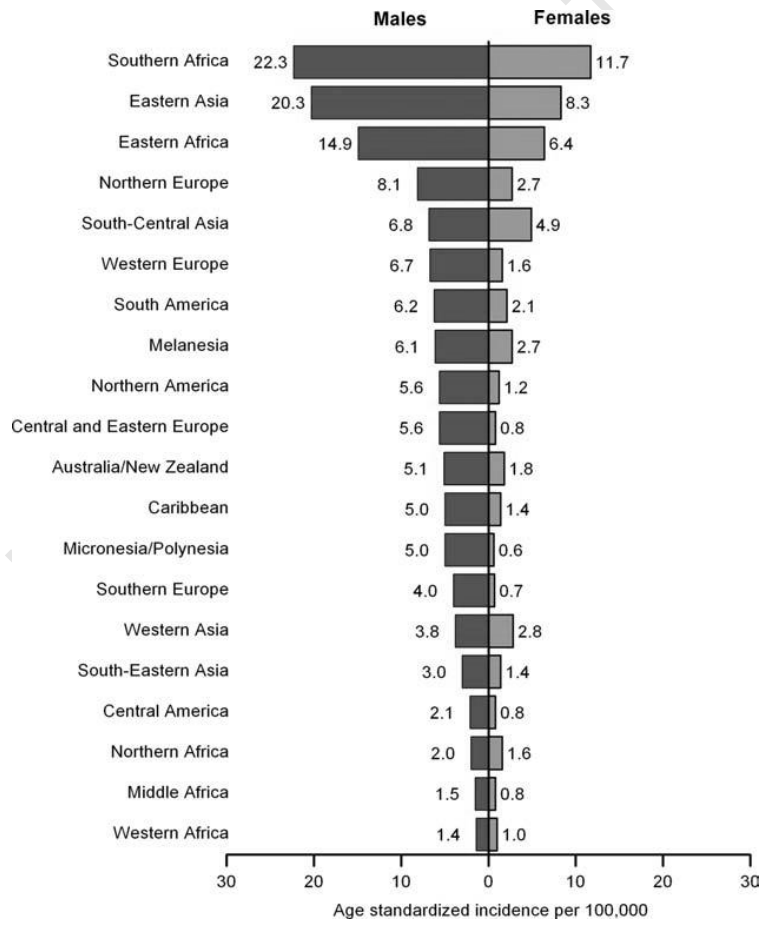


**Figure 2: Age standardised incidence of oesophageal cancer by region** (Jemal *et al*., 2011)**.** Incidence rates are indicated per 100000 per region for males and females separately.

Incidence of the two subtypes of oesophageal cancer varies internationally, with SCC occurring predominantly in developing regions, and AC being most common in developed regions. The heterogeneity of oesophageal cancer is further reflected in the different risk factors attributed to each subtype. Any factor that causes continuous irritation and inflammation of the oesophageal mucosa appears to increase the incidence of SCC. It is therefore unsurprising that tobacco smoking, alcohol consumption, and infection by human papilloma virus are possible risk factors attributed to the development of SSC (Enzinger and Mayer, 2003; Hendricks and Parker, 2002).As with SCC, there are several risk factors attributed to the development of AC, chief amongst these are Barrett's oesophagus, acid reflux, and obesity (Enzinger and Mayer, 2003; Hendricks and Parker, 2002).

Interestingly, there appears to be a genetic predisposition to developing SCC with, in a small number of cases, familial clusters being diagnosed in families with a history of nonepidermoytic palmoplantar keratoderma, a rare autosomal dominant disorder defined by a genetic abnormality at chromosome 17q25 that results in the thickening of the oesophageal mucosa (Enzinger and Mayer, 2003; Risk *et al*., 1999). Regardless of the rarity of such cases, these rare familial conditions offer insights into the mechanistic processes underlying the development of sporadic cases. Additionally, few modifications to molecular mechanisms have been described in SSC. For one, the cell cycle regulator, Cyclin D1, has been shown to be overexpressed in SSC, and its expression is shown to correlate to lymph node metastasis and survival (Nagasawa *et al*., 2001; Sarbia *et al*., 1999). Also, another cell cycle regulator, p53, has been shown to be overexpressed in half of South African patients with SSC (Chetty and Simelane, 1999). However, despite such insight into the aetiology of oesophageal cancer, specifically SSC, the molecular mechanisms behind its pathogenesis remain poorly understood.

The five-year survival rate of oesophageal cancer varies according to its stage when detected. The five-year survival rate when detected at stage 0 (a stage where abnormal cells carry a high grade of dysplasia but are not yet malignant) it is approximately 95% (Enzinger and Mayer, 2003). This drastically drops to 10%-40% when detected at stage II (abnormal cells have become malignant and have invaded the oesophageal wall), and by stage IV (distal metastasis has occurred), less than 1% of patients survive for five years (Enzinger and Mayer, 2003). Despite such low survival numbers, the five-year survival rate of oesophageal cancer is not drastically different from other cancers. However, the poor prognosis and high mortality rate when compared to other cancers may be attributed to its asymptomatic development and thus late detection (Hendricks and Parker, 2002). Therefore, in many cases oesophageal cancer is diagnosed in its late stages resulting in a low survival rate of patients and therefore its remarkably high mortality rate.

The poor prognosis of oesophageal cancer patients may also be attributed to its ineffective treatment currently being employed. Both SCC and AC initially are responsive to chemotherapy, with significant shrinkage of the tumours occurring in a majority of patients (Enzinger and Mayer, 2003). However, this response to chemotherapy typically lasts no longer than a few months, with responses to chemotherapy rarely exceeding one year (Enzinger and Mayer, 2003). This could be attributed to the presence of chemoresistant cancer stem cells present in oesophageal cancer tumours as previously demonstrated in patient tumours (Li *et al.*, 2011), and oesophageal cancer cell lines (Chen *et al.*, 2012). Surgery remains the most effective way of treating early-stage oesophageal cancer, but with its asymptomatic development and thus late detection, surgery is often ineffective (Enzinger and Mayer, 2003). Its ineffective treatment, along with its asymptomatic development, late detection, and poor understanding of the molecular mechanisms of its pathogenesis gives oesophageal cancer its distinctly poor prognosis and remarkably high mortality rate when compared to other cancers. There is therefore a need to elucidate its molecular mechanisms in order to allow for earlier detection and/or more efficient treatment of oesophageal cancer. The value of elucidating the molecular process critical for the survival of oesophageal cancer is best illustrated by the development of a drug like Herceptin®. The drug targets and facilitates the destruction of breast cancer cells that overexpress Her2/Neu, a member of the EGFR family (Cho *et al.,* 2003; Slamon *et al.,* 1989). It is anticipated that identifying critical

proteins and pathways in oesophageal cancer will facilitate the development of better therapeutics.

### 1.4 The GH/IGF1 Axis

One of the signalling axes well documented to be altered in various cancers is that of the growth hormone/insulin-like growth factor 1 (GH/IGF1) axis. It is well established that, normally, GH is extremely important for the regulation of postnatal growth and metabolism(Harvey, 2010). GH has also shown to play a role in amino acid transportation, mitogenesis, prevention of apoptosis, and differentiation and reorganisation of cytoskeletal architecture, indicating the highly pleiotropic effects of GH (Eisenhauer *et al*., 1995; Goh *et al*., 1997; Zhu *et al*., 2001). Additionally, GH plays a role in ensuring the proper function of several physiological systems such as the cardiovascular, reproductive, gastrointestinal, and renal systems. Its primary role, the regulation of postnatal growth, is largely mediated through the potent mitogen, IGF1 (Chhabra *et al*., 2011). Normally, GH is secreted by the pituitary gland into the blood stream where it is free to bind to its ubiquitously expressed receptor, growth hormone receptor (GHR).

The biosynthesis and secretion of GH is tightly regulated by several hormones secreted primarily by the hypothalamus (Fig.3). Ghrelin is a hormone secreted by the stomach just before meals (Cummings *et al*., 2002; Date *et al*., 2000; Kojima *et al*., 1999). Once secreted, ghrelin binds to its receptor present on somatotroph cells in the pituitary and induces the biosynthesis and secretion of GH by these cells (Kojima *et al*., 1999)(Fig.3). Similarly, growth hormone-releasing hormone (GHRH) is secreted by the hypothalamus and binds to its receptor expressed on somatotroph cells which also induces the synthesis and secretion of GH into the blood stream (Garcia-Fernandez *et al*., 2003; Lin-Su and Wajnrajch, 2002)(Fig.3). The synthesis of GH is directly inhibited by the hypothalamic production of somatostatin, which binds to its receptor present in the pituitary (Wehrenberg *et al*., 1982)(Fig.3).

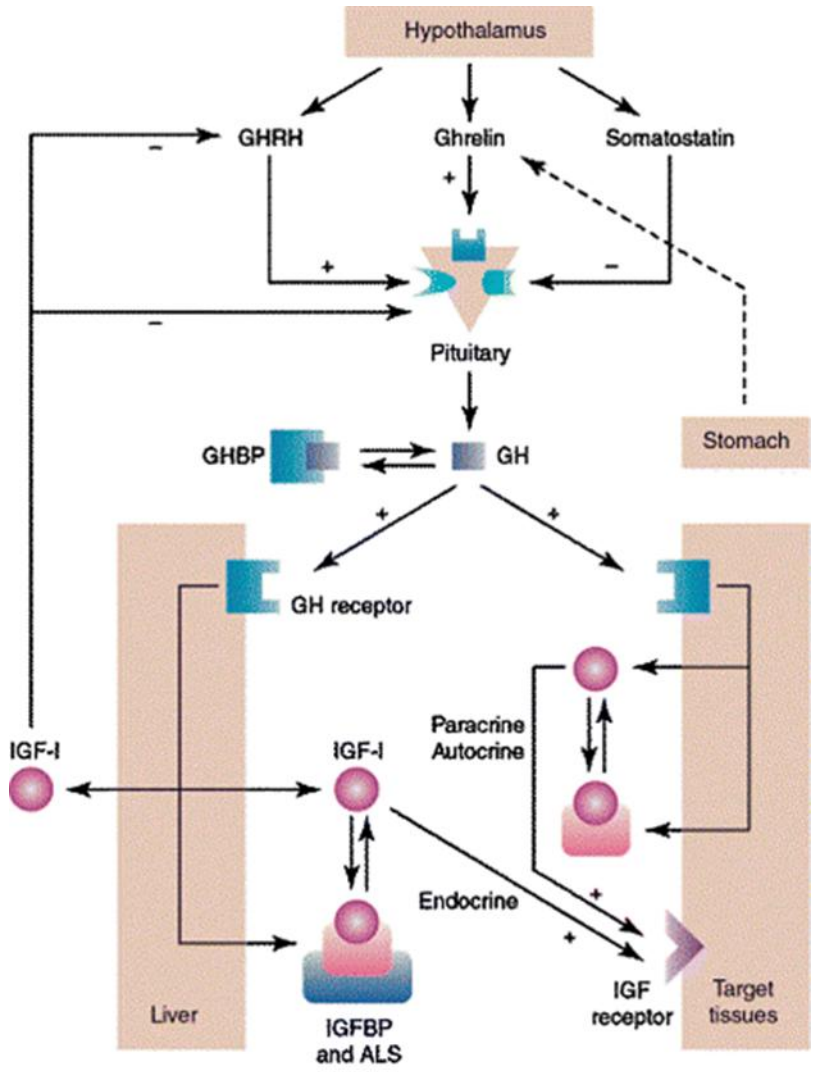


**Figure 3: The IGF1/GH axis** (Holt, 2002)**.** GH secreted by the pituitary, under the regulation of GHRH, ghrelin, and somatostatin, is free to either bind to GHBP or to its receptor expressed on target cells. Binding to its receptor, particularly on liver cells, results in the biosynthesis and secretion of IGF1, which is then free to bind to its receptor on target tissues or to IGFBP and ALS. In cells other than those of the liver, binding of GH to GHR may also induce autocrine and endocrine signalling of IGF1.

Once secreted into the bloodstream, GH may either bind to its receptor, growth hormone receptor (GHR), present on target tissues or bind to growth hormone-binding protein (GHBP) (Fig.3). Binding of GH to GHBP limits the available amount of free GH able to bind to its receptor thereby creating a GH reservoir (Baumann *et al*., 1988). It also protects GH from degradation (Baumann *et al*., 1987; Clark *et al*., 1991), and increases the hormone's short half-life in serum (Clark *et al*., 1991). If bound to its receptor, several intracellular signalling pathways are activated. These pathways converge and activate several transcription factors, the most notable being the signal transducer and activator of transcription (STAT) transcription factor family (Brooks *et al*., 2008; Frank and Messina, 2002; Zhu *et al*., 2001).

Activation of STAT transcription factors by GH induces transcription and secretion of IGF1 (Davey *et al*., 1999) (Fig.3). In addition to GHR, GH may bind to the prolactin receptor (PRLR) since both GHR and PRLR are similar in structure and function (Somers *et al*., 1994). GHR is ubiquitously expressed, but is more abundant in the liver (Frank and Messina, 2002). It is therefore unsurprising that the liver is the main origin for IGF1 synthesis and secretion (Fig.3). Once secreted by the liver, IGF1 may either act on target tissue to exert its mitogenic effects in an endocrine manner, or bind to the IGF-binding protein (IGFBP) and acid labile subunit (ALS) complex, preventing it from binding to its receptor, thus negatively regulating IGF1 downstream effects (Fig.3) (Scott *et al*., 1994). However, autocrine/paracrine signalling of IGF1 by GH binding to target tissues other than the liver cannot be excluded (Fig.3). Once secreted, IGF1 also negatively regulates GH synthesis and secretion by inhibiting GHRH.

### 1.5 Growth Hormone Receptor

The effects of GH on postnatal growth and metabolism, and on several organ systems are mediated through its receptor, GHR. GHR is a single membrane-spanning type I glycoprotein member of the cytokine receptor superfamily (Bazan, 1990; Brooks *et al*., 2008; Frank and Messina, 2002). The type I cytokine receptor family includes many other receptors, however, GHR was the first identified member of this superfamily (Cosman *et al*., 1990).

#### 1.5.1 GHR Gene Structure

The gene encoding GHR is present on chromosome 5 at position p13-p12 and spans roughly 90kb (Godowski *et al*., 1989).It includes 9 exons, exons 2 to 10 (Fig.4). Exon 2 encodes some of the 5' untranslated region (UTR), and the signal sequence (Frank and Messina, 2002) (Fig.4). The signal sequence encodes for a signal peptide that is present on all proteins designated for the secretory pathway which are either secreted from the cell, or inserted in cellular membranes (Blobel and Dobberstein, 1975). Exons 3 to 7 encode the majority of the extracellular domain of the protein(Frank and Messina, 2002) (Fig.4). Exon 8 encodes the 24-residue transmembrane region and a few residues of the extra- and intracellular domain sides flanking it (Frank and Messina, 2002) (Fig.4). Exons 9 and 10 encode for the remainder of the cytoplasmic domain, while exon 10 encodes for the 3'UTR (Frank and Messina, 2002) (Fig.4).

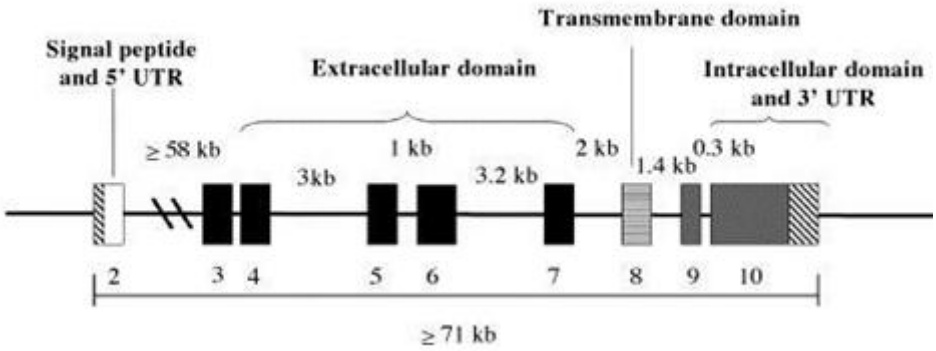


**Figure 4: Schematic of the GHR gene** (Lau *et al*., 2007)**.** Exons are numbered and are indicated as boxes. Intron sizes between exons are also indicated.

The gene is highly conserved, although, splicing of the gene varies between species. For instance, in the mouse, the gene is spliced to generate the transcript encoding GHBP (Edens *et al*., 1994). Furthermore, several human isoforms of GHR exist, arising from gene splicing, each with differing functions and ligand affinity. These isoforms will be explained in detail later. It was found that human transcripts of the gene often contained variations within the 5'UTR (Pekhletsky *et al*., 1992). Exons encoding the 5'UTR have been seen to be alternatively spliced to give rise to these 5'UTR variants (Pekhletsky *et al*., 1992). Additionally, 5'UTR splice variants appear to be tissue specific, indicating a possible complex tissue-specific regulatory role of the 5'UTR affecting the translational efficiency of the mRNAs (Edens and Talamantes, 1998; Pekhletsky *et al*., 1992).

### 1.5.2 GHR Protein Structure

As stated before, GHR is a glycoprotein of the type I cytokine receptor family (Bazan, 1990; Brooks *et al*., 2008; Frank and Messina, 2002). Its cDNA is predicted to encode a protein approximately 70kDa in size and 620 amino-acids long (Leung *et al*., 1987). However, it is commonly seen to migrate as a 120-130kDa band in reducing SDS-polyacrylamide gels when expressed in mammalian cells, due to post-translational modifications such as glycosylation and ubiquitination (Asa *et al*., 2007; Kerkhof *et al*., 2007; Stubbart *et al*., 1991; Wang *et al*., 1992). Characteristic features of the type I cytokine family of proteins include; (i) possession of a single membrane spanning domain, (ii) conserved cysteine residues in the extracellular domain, (iii) a conserved WSXWS-like motif, (iv) two conserved proline-rich domains termed Box 1 and Box 2, and (v) lack of intrinsic kinase activity.

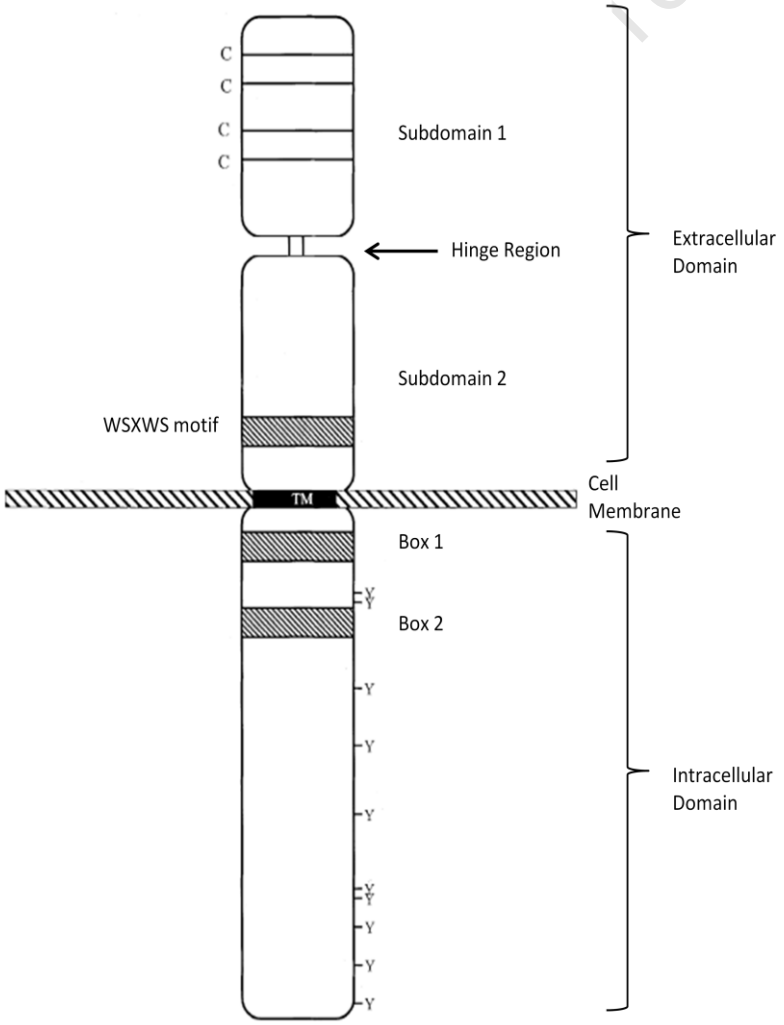


**Figure 5: Schematic of GHR protein undimerised monomer** (Zhu *et al*., 2001)**.**Extracellular, transmembrane, and intracellular domains are indicated. Cysteine residues and the WSXWS motif present in subdomain 1 and 2 are also indicated. Box 1 and 2 along with approximate relative positions of tyrosine residues (Y) present in the intracellular domain are shown.

The extracellular domain consists of two fibronectin type III β sandwich domains comprising Subdomain 1 and 2 and is predicted to extend from residues 1-246 (Fig.5) (Brooks *et al*., 2008; Frank and Messina, 2002; Zhu *et al*., 2001). The two subdomains are connected by a four residue hinge region(Fig.5)(Brooks *et al*., 2008; Frank and Messina, 2002; Zhu *et al*., 2001). Four conserved cysteine residues are present in Subdomain 1, which form two pairs that engage in forming disulphide linkages (Fig.5) (Frank and Messina, 2002; Zhu *et al*., 2001). Additionally, the WSXWS-like motif is present in Subdomain 2 (Fig.5) (Frank and Messina, 2002; Zhu *et al*., 2001). Studies have indicated that the conserved cysteine residues along with the WSXWS-like motif are both critical for the structural integrity of the receptor's extracellular domain while not being involved in GH binding (Fuh *et al*., 1990).

Unlike the extracellular domain of GHR, there is no structural data for the intracellular domain (Yang *et al*., 2007). The intracellular domain contains the two conserved proline-rich boxes and is roughly 350 residues long (Fig.5) (Frank and Messina, 2002). Box 1 is critical for the direct association of Janus tyrosine kinase 2 (JAK2) with GHR and for most other GH-stimulated intracellular functions (Brooks *et al*., 2008; Frank and Messina, 2002; Zhu *et al*., 2001). The role of Box 2 is less well defined. In addition to being rich in proline residues, Box 2 contains a short stretch of acidic residues likely to be required for optimal JAK2 interaction to Box 1, but unlike Box 1, does not serve as a direct binding site for JAK2 (Frank *et al*., 1994). Several tyrosine residues that serve as substrates for phosphorylation by JAK2 are also present in the intracellular domain of the receptor (Fig.5) (Brooks *et al*., 2008; Frank and Messina, 2002). A phenylalanine residue at position 327 has been shown to be important for GH-induced receptor internalisation and degradation (Allevato *et al*., 1995). Additionally, a conserved ubiquitin-dependent endocytosis (UbE) motif is in close proximity to the phenylalanine, and is thought to be important in mediating GH-induced receptor ubiquitination (Strous *et al*., 1996).

### 1.5.3 GHR Activation and Signalling

Two models of GHR activation by GH have been proposed. It was initially accepted that GHR exists as a monomer on the cellular surface, and that GH induces homodimerisation of these receptors (Fig.6A) (Cunningham *et al*., 1991). However, recent evidence suggest that GHR may already exist as pre-formed homodimers on the cell surface prior to GH binding (Fig.6B) (Brown *et al*., 2005; Gent *et al*., 2002).

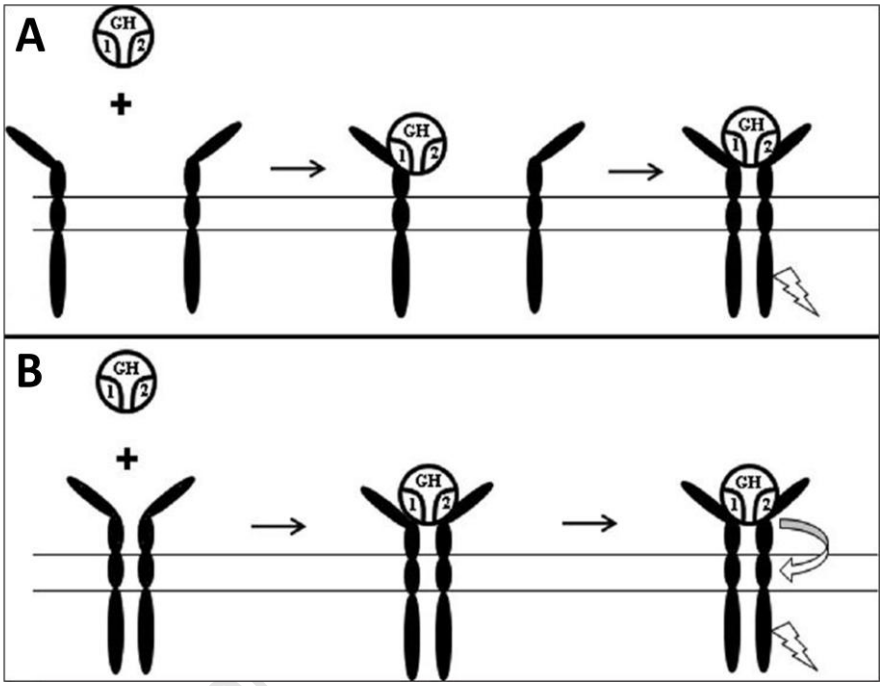


**Figure 6: Activation of GHR by GH** (Kaabi, 2012)**. (A)** Ligand-dependant dimerisation model. Binding of GHR to site 1 of GH allows binding of a second GHR monomer to site 2 of GH, thus forming homodimers. The required formation of GHR dimers results in downstream activation of the receptors. **(B)** Ligand-independent dimerisation model. Binding of GH to pre-formed homodimers of GHR results in the necessary conformational change needed for the induction of signalling.

GH possesses two binding sites; a high affinity site 1, and a lower affinity site 2 (Fig.6) (Fuh *et al*., 1992). The ligand-dependant model of GHR homodimerisation predicts that the higher affinity site 1 of GH interacts with the first receptor, which then allows for the interaction of the lower affinity site 2 to interact with a second receptor (Fig.6A) (Cunningham *et al*., 1991; Frank and Messina, 2002; Fuh *et al*., 1992). The resulting dimerisation provides the signal to generate the appropriate activation of receptor signalling (Fuh *et al*., 1992). Several lines of evidence exist that support this model; (i) self-antagonism of GHR activation by GH at high concentrations, since all available GHR monomers are bound to GH via the high affinity site 1, leaving few available GHR for site 2 binding and dimerisation (Fuh *et al*., 1992), (ii) disruption of interaction between site 2 and receptor by means of point mutation of site 2 produces antagonistic effects (Fuh *et al*., 1992), (iii) naturally occurring short isoforms of GHR lacking intracellular domains are shown to inhibit the function of full-length GHR presumably by forming non-functioning homodimers (Ross *et al*., 1997). In retrospect, the last two lines of evidence may serve as evidence for the ligand-independent dimerisation model, but at the time, was considered evidence for the ligand-dependent dimerisation model.

However, recent evidence contradicts the long-held ligand-dependant dimerisation model suggesting that GHR already exists as homodimers irrespective of GH association with the receptor. In this model, GH binds to an already formed homodimer of the receptor, resulting in a conformational change of the intracellular domain of the receptor, that in turn initiates associated tyrosine kinases and signal transduction (Fig 6B) (Brown *et al*., 2005; Gent *et al*., 2002). Evidence supporting this model includes co-immunoprecipitation studies showing that a portion of GHR exist as constitutive dimers *in vitro* (Brown *et al*., 2005; Gent *et al*., 2002). Evidence supporting the model that a conformational change of the receptor is needed for activation rather than homodimerisation includes the lack of receptor activation by dimerisation alone, and the observation that inducing a rotation of the intracellular domain by inserting alanine residues was enough to result in receptor activation (Brown *et al*., 2005).

Both models however predict that dimerisation/rotation of the receptors once bound by GH results in tyrosine kinase activation. As stated before, GHR lacks intrinsic kinase activity and therefore relies on intracellular tyrosine kinases in order to achieve signal initiation in response to GH. GHR has been shown to signal primarily through members of the Janus tyrosine kinase (JAK) family (Argetsinger *et al*., 1996). Members of the JAK family include JAK1, JAK2, JAK3, and Tyk2. Two characteristics are shared amongst these members; (i) the absence of SH2 or SH3 domains, (ii) and the presence of seven conserved JH regions, JH1-7, of which JH1 is the functional catalytic domain and JH2 is the inhibiting pseudokinase domain (Zhu *et al*., 2001).

Upon binding of GH, the dimerisation/conformational change of receptors allows for the spatial repositioning of GHR-associated JAKs bound to Box 1, which results in the disruption of the ability of JH2 domains to inhibit catalytic JH1 domains, thus leading to JAK activation (Saharinen *et al*., 2000; Zhu *et al*., 2001). Since JAK family members lack SH3 domains, which typically bind proline rich domains, it is possible that JAK kinases associate with GHR through a SH3 domain-containing adaptor protein (Finidori, 2000). Activation of receptor-associated JAK in response to GH results in JAK and GHR phosphorylation (Fig.7) (Argetsinger *et al*., 1996). GH induces mostly JAK2 phosphorylation, while JAK1 and JAK3 show minimal phosphorylation, indicating that GH signalling is primarily mediated by JAK2, and to a lesser extent by JAK 1 and JAK3 (Carter-Su *et al*., 1996; Johnston *et al*., 1994; Smit *et al*., 1996). Phosphorylation of JAK and of the intracellular domain of GHR by JAK, particularly JAK2, serves to provide docking sites for SH2 domain-containing proteins recruited to mediate downstream GH signalling by GHR.

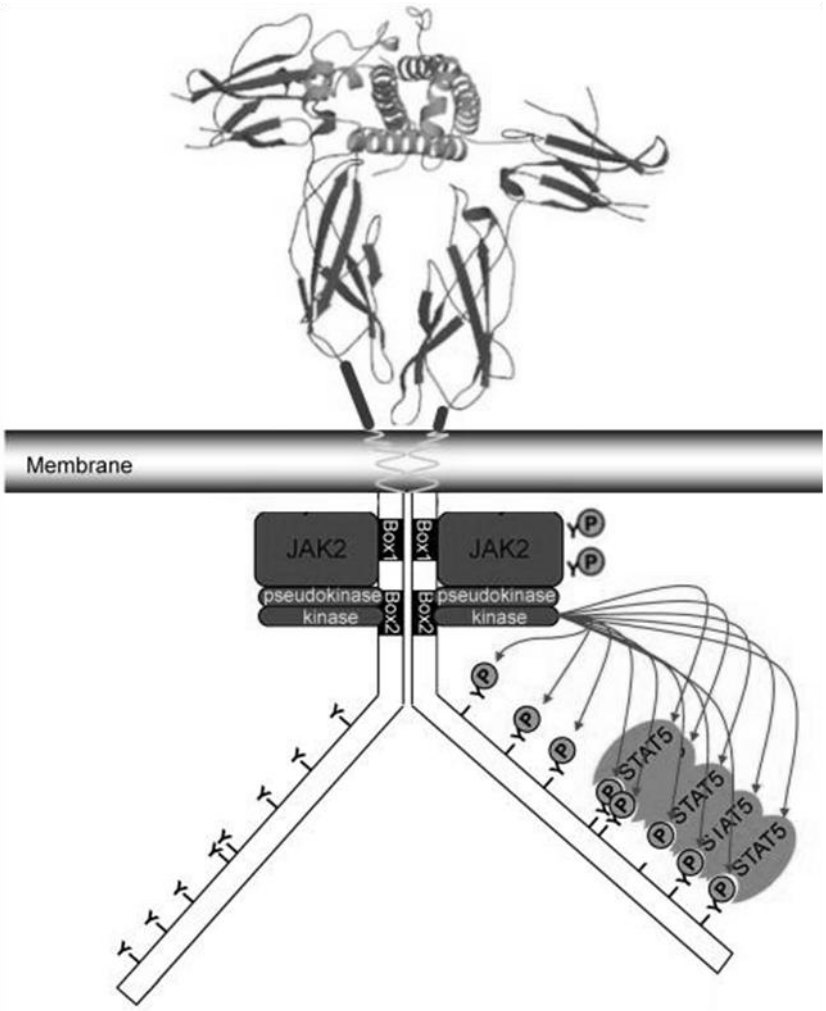


**Figure 7: JAK2 activation by GH and subsequent intracellular phosphorylation of GHR and STAT5** (Brooks *et al.*, 2008)**.**Binding of GH to GHR dimers initiates the dissociation of the pseudokinase (JH2) domain from the functional kinase domain (JH1). Phosphorylation of tyrosine residues (Y) on GHR and JAK2 then occurs, allowing for the association of SH2 domain-containing proteins, such as STAT5, to GHR, and their subsequent phosphorylation and activation by JAK2.

Several proteins are recruited and/or activated directly or indirectly by GHR using JAK to achieve downstream GH signalling. These molecules include Src homology 2/α collagen related (SHC) protein (VanderKuur *et al*., 1995), insulin receptor substrate (IRS) proteins(Yamauchi *et al*., 1998), SH2 domain-containing protein tyrosine phosphatase-1 and -2 (SHP-1 and SHP-2)(Ram and Waxman, 1997), the p58 subunit of phosphoinositide-3 kinase (PI3K ) (Moutoussamy *et al*., 1998), epidermal growth factor receptor (EGFR )(Yamauchi *et al*., 1997), and signal transducers and activators of transcription (STAT-1, -3, and -5) (Ram *et al*., 1996; Smit *et al*., 1996; Sotiropoulos *et al*., 1996) amongst others. Recruitment of the various signalling molecules results in the activation of several pathways allowing for the pleiotropic effects of GH (Fig.8).For example, association of focal adhesion kinase (FAK) to phosphorylated and thus activated JAK2 in response to GH results in activation of FAK and thus alterations to cytoskeletal structure (Zhu *et al*., 1998). Also, the MAPK/ERK and PI3K pathways are known to be activated in response to GH. The activation of ERK via the SHC, Grb2, Ras, Raf and MEK cascade is well known (Lewis *et al*., 1998). GHR has been shown to use this cascade to activate ERK1/2 (Fig.8) (Winston and Hunter, 1995). Activation of ERK1/2 ultimately results in the transcription of several genes encoding transcription factors including *c-fos*, *junB*, and *egr-1*, amongst others (Fig.8) (Hodge *et al*., 1998). GH-stimulated activation of PI3K has been shown to be mediated by GHR-activation of IRSs, specifically IRS-1 and IRS-2 (Fig.8) (Yamauchi *et al*., 1998; Yenush and White, 1997). PI3K activation then activates Akt to bring about changes in metabolism and the generation of anti-apoptotic signals (Costoya *et al*., 1999). GH-stimulated activation of PI3K has been shown to be important for cell proliferation, survival, cytoskeletal reorganisation, and cellular metabolism, further potentiating the pleiotropic effects of GH (Yenush and White, 1997).

Several genes are induced by these pathways, chief among is the *igf1* gene which encodes for the mitogen IGF1 (Murphy *et al*., 1987). Additionally, several genes encoding for suppressor of cytokine signalling (SOCS) proteins are also induced (Adams *et al*., 1998; Tollet-Egnell *et al*., 1999). Also, the genes of *c-jun* (Gurland *et al*., 1990)and *c-myc* (Murphy *et al*., 1987) that are heavily involved in proliferation are also induced by these pathways.

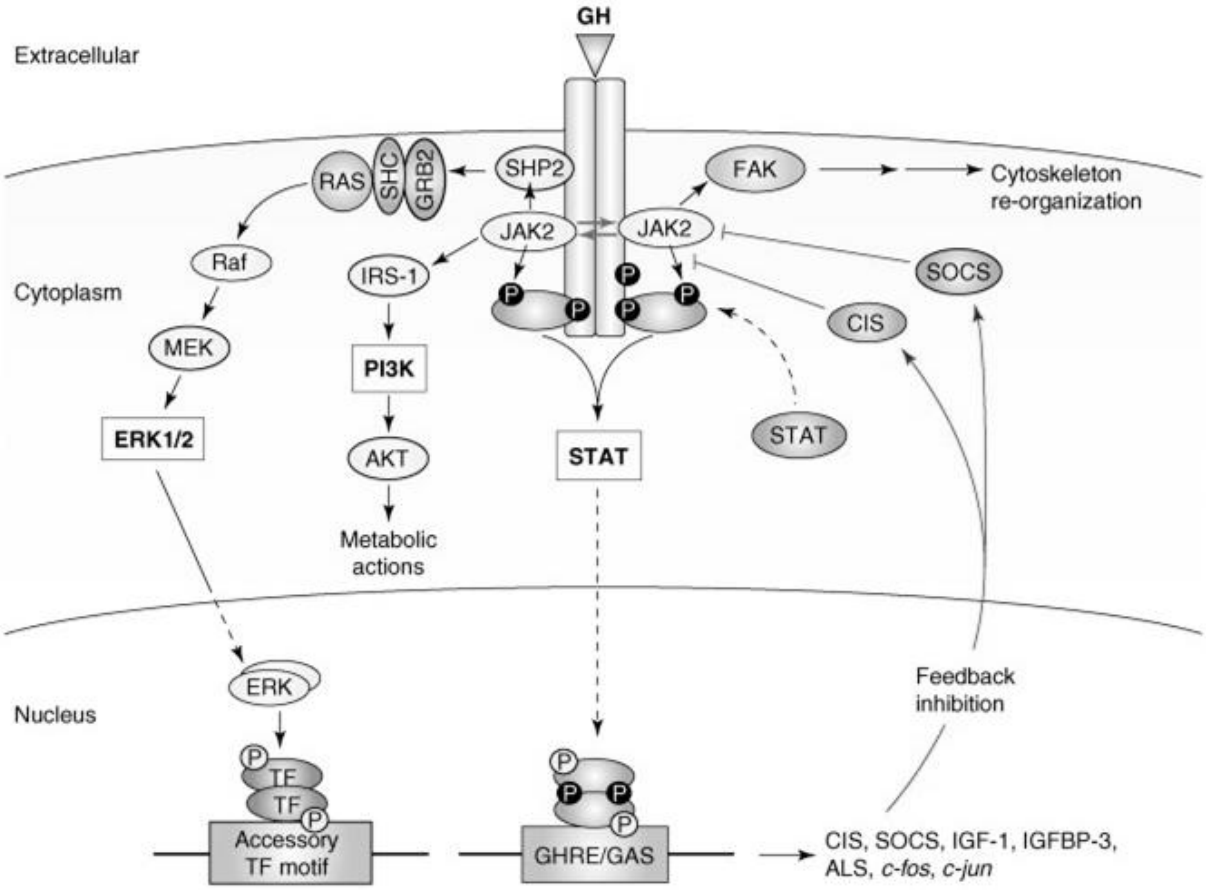


**Figure 8: Activation of several intracellular signalling pathways by GHR** (Rosenfeld *et al*., 2007)**.** Activation of GHR by GH results in JAK2 and GHR phosphorylation. This in turn provides docking sites for a number of signalling molecules, ultimately resulting in the activation of ERK1/2, PI3K, STAT, and FAK signalling pathways.

Of all the targets of GHR signal transduction in response to GH, none is more studied than the STATs. STATs are SH2 domain-containing, cytoplasmic factors that are important in binding and inducing transcription of GH-responsive genes (Herrington *et al*., 2000). STAT transcription factors are recruited to the proximity of JAKs by binding via their SH2 domains to phosphorylated tyrosine residues on the intracellular domain of GHR (Fig.7 )(Herrington *et al*., 2000; Zhu *et al*., 2001). They are then initially activated by phosphorylation by JAKs, followed by serine phosphorylation (Fig.7) (Herrington *et al*., 2000; Ram *et al*., 1996; Zhu *et al*., 2001). Several different STAT transcription factors exist, however, only STAT-1, STAT-3, STAT-5a, and STAT-5b are activated in response to GH (Sotiropoulos *et al*., 1996; Waxman *et al*., 1995a). Once activated, STAT transcription factors then dissociate from the receptor, either homo- or heterodimerise with each other, translocate to the nucleus, bind to their appropriate DNA response elements, and thereby drive transcription of various genes (Fig.8) (Ihle, 1996; Zhu *et al*., 2001). Promoter response elements to which STAT transcription factors bind include growth hormone responsive elements (GHRE) and INFγ activated sequence (GAS)-like elements(Fig.8). Genes with these response elements in their promoters include *c-fos* (Meyer *et al*., 1994)*, insulin 1* (Galsgaard *et al*., 1996)*, spi 2.1* (Bergad *et al*., 1995)*, als* (Ooi *et al*., 1997)*,* and several P450 genes encoding for members of the CYP2 and CYP 3 family (Waxman *et al*., 1995b).

In summary, GH achieves its pleiotropic cellular response by activating several complex intracellular signalling pathways. By binding to GHR, GH initiates intracellular tyrosine phosphorylation, primarily by JAK2. This then allows the recruitment and activation several different signalling molecules. These then activate multiple complex signalling pathways that affect a wide range of cellular functions. Multiple genes are also induced by this manner including genes involved in proliferation, metabolism, migration, and growth.

### 1.5.4Post-Transcriptional Regulation of GHR Protein Expression and Signalling

Considering that activation of GHR leads to alterations of such a wide variety of key cellular functions, it should be unsurprising that the GH/GHR signalling axis is tightly regulated at different levels. Firstly, as mentioned before, regulation occurs at the ligand stage; free GH available to bind GHR expressed on target tissues is already tightly regulated in serum by binding to GHBP. Other methods include inducing signalling suppressor proteins in response to GH, ligand–dependent and –independent internalisation of the receptor, shedding of the receptor at the cell surface, and interaction of full-length GHR with dominant negative isoforms of the receptor amongst others, all of which are described in more detail below.

Roughly 50% of all circulating GH is bound by GHBP thus preventing it from binding to GHR and inducing signalling (Baumann *et al*., 1988). GHBP corresponds to the extracellular domain of the full length receptor, and binds to GH in the 2:1 stoichiometry seen with GH binding to full-length GHR (Baumann *et al*., 1994; Leung *et al*., 1987). GHBP is generated differently in different species. For example, in rodents, GHBP is generated by alternative splicing of GHR mRNA resulting in the soluble form of the extracellular domain of full-length GHR (Baumbach *et al*., 1989). In humans, GHBP is derived by the proteolytic shedding of the extracellular domain of full-length GHR present on the cell surface (Alele *et al*., 1998). A known by-product of this shedding is the intracellular domain of the receptor (Alele *et al*., 1998). The proteolytic cleavage of surface-expressed GHR involves the action of tumour necrosis factor-α-converting enzyme (TACE), a known transmembrane metalloprotease (Alele *et al*., 1998; Zhang *et al*., 2000). This soluble form of the extracellular domain is then released into the bloodstream where it is free to bind GH. GHBP therefore negatively regulates GH signalling in two ways in humans; (i) it actively binds free GH in serum thereby limiting the amount of free GH able to bind to GHR, (ii) generation of GHBP results from proteolytic cleavage of full-length, surface-expressed GHR, thereby limiting GHR expression.

Furthermore, binding of GH to GHR on the cell surface not only results in signal initiation and transduction, but also the internalisation and subsequent lysosomal degradation of the activated receptor, thereby preventing over-activation of GHR (Murphy and Lazarus, 1987). Subsequent studies have shown that the UbE motif and a functional ubiquitin conjugating system is needed for ligand-induced endocytosis and degradation of the receptor (Kerkhof *et al*., 2007; Strous *et al*., 1996). Very little else is known about the process by which GH-binding leads to GHR endocytosis and degradation, however, it is proposed that binding of GH leads to the docking of ubiquitin conjugases and ligases onto the UbE motif, and the subsequent ubiquitination of GHR. Clathrin-coated endocytosis machinery is activated and results in the transport of GHR to early and late endosomes (Vleurick *et al*., 1999). The GH-GHR complex is then degraded (Strous *et al*., 1996). Additionally, there is evidence that GHR may undergo internalisation in a ligand-independent manner in similar fashion as described above (Kerkhof *et al*., 2007). By this poorly-understood mechanism, ligand-dependent and –independent GHR internalisation and degradation occurs to further regulate GHR levels and activity.

GHR signalling is also suppressed by several members of the SOCS family. SOCS members contain a central SH2 domain and a highly conserved SOCS box (Chen *et al*., 2000). The mechanism by which SOCS members suppress cytokine signalling remains poorly understood, but there is evidence that this occurs via suppression of JAK2 signalling by direct binding to the tyrosine residue (Y1007) of the activation loop of JAK2 through its SH2 domain (Yasukawa *et al*., 1999). It is suggested that this interaction inhibits the catalytic activity of JAK2 (Yasukawa *et al*., 1999). As stated before, GH is known to induce expression of SOCS-1, -2, and -3, and it is by this mechanism that GH directly results in the negative feedback of its signalling (Fig.8).

Several isoforms of GHR exist (Amit *et al*., 1997; Ballesteros *et al*., 2000; Ross *et al*., 1997; Urbanek *et al*., 1993). These isoforms will be discussed in greater detail later. Interestingly though, one of these isoforms has been shown to function as a dominant negative inhibitor of full-length GHR, adding to the several avenues already utilised to regulate signalling by GHR (Ross *et al*., 1997). This isoform of the receptor, GHR 1-279, lacks 97% of the intracellular domain, including the bulk of exon 9 and the whole of exon 10, and is therefore more akin to GHBP (Ross *et al*., 1997).It does not however lack the transmembrane region needed for cell surface anchorage, and is therefore found on the cell surface (Ross *et al*., 1997). Its suppressive effect has been shown to occur partly by suppression of downstream signalling, however, it may also exert its suppressive effects by competing with full-length GHR for GH binding when forming homodimers (Ross *et al*., 1997).

Since GHR levels are so tightly regulated by ubiquitination, it spends a very short time expressed at the cell surface as a fully-mature, glycosylated receptor. The half-life of human GHR is not clear, some studies have seen a half-life of 2 hours (Amit et al., 1997), while others showed a half-life of about 1 hour in physiological conditions (Deng et al., 2007; Pilecka et al., 2007). Its short half-life is further shortened with increasing GH availability (Deng et al., 2007), while its short half-life is further demonstrated as the half-life of rat GHR *in vivo* is 45 minutes (Gorin and Goodman, 1985). Regulation is further enforced if the receptor escapes ligand-independent ubiquitination. Binding of GH induces the expression of SOCS, while dimerisation with the GHR 1-129 isoform renders a signalling-compromised dimer. These mechanisms of GHR protein regulation remain poorly defined, but despite this, the wide range of methods used reveals insight into the complex regulation of the GHR axis.

### 1.5.5 GHR Isoforms

Besides full-length GHR, only three isoforms of GHR have been characterised. These isoforms include the d3GHR (Urbanek *et al*., 1993), 1-277 GHR (Ross *et al*., 1997), and 1-279 GHR (Amit *et al*., 1997; Ross *et al*., 1997). The isoforms are structurally unique from each other, and also have unique binding affinities and activation characteristics. The 1-277 and 1-279 GHR isoforms are structurally the most similar since both lack approximately 97% of the intracellular domain (Fig.9) (Ross *et al*., 1997). Since expression of GHR is ubiquitous, the 1-277 and 1-279 GHR isoforms are expressed in a wide variety of target tissues, including liver, adipose, muscle, heart, prostate, and kidney tissue (Ballesteros *et al*., 2000). Tissue-specific expression of the d3GHR isoform is less known and has only been reported in breast cancer cell lines and liver tissue (Decouvelaere *et al*., 1995).

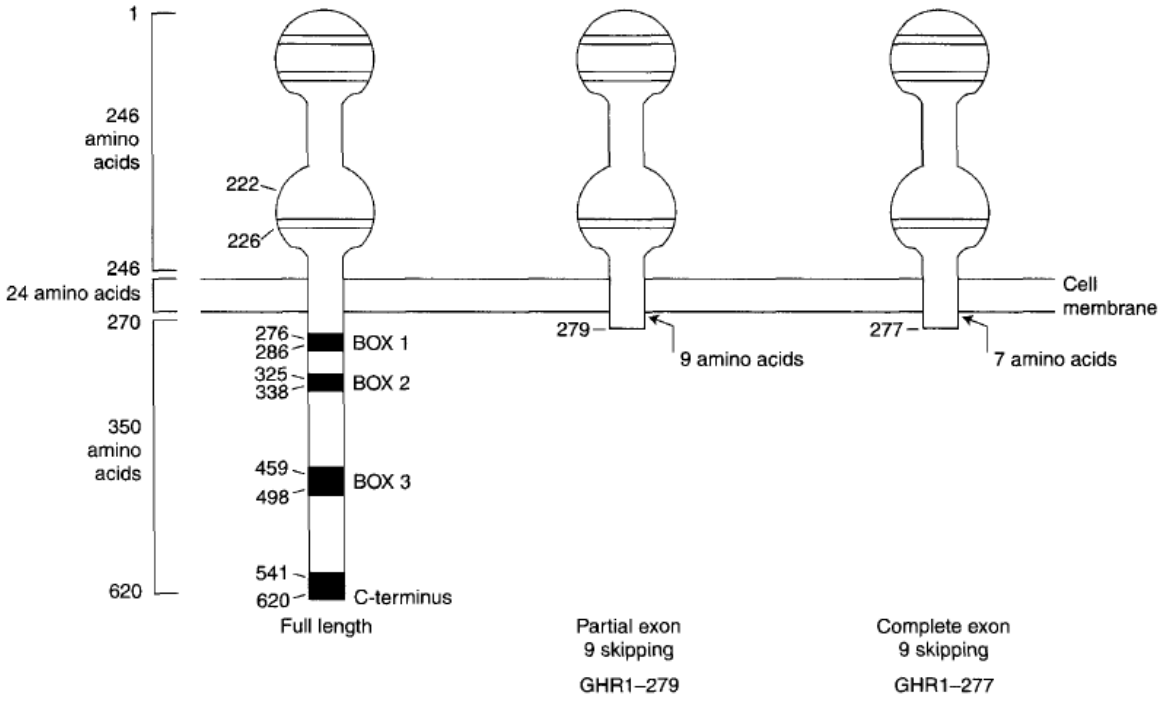


**Figure 9: Schematic of full-length GHR and the 1-277 and 1-279 GHR isoforms** (Ross, 1999)**.**

The 1-279 GHR isoform arises from utilising an alternative 3'-acceptor splice site in exon 9, which results in losing most of exon 9, and the entire exon 10, ultimately resulting in the loss of 97% of the intracellular domain. The splice site occurs 26bp downstream in exon 9, and utilisation of this splice site results in a frame shift and therefore the insertion of a premature stop codon within exon 9 (Ross *et al*., 1997).The resulting transcript encodes the whole extracellular and transmembrane domain, with only the first 9 amino acids of the

intracellular domain (Fig.9) (Ross *et al*., 1997). 1-277 GHR arises in a similar manner except that exon 9 is totally skipped, resulting in a frame shift and thus insertion of a premature stop codon in exon 10 (Ross *et al*., 1997). Once again, the resulting transcript encodes the whole extracellular and transmembrane domain, with only the first 7 amino acids of exon 10 (Fig.9) (Ross *et al*., 1997).

Of these two, similar isoforms, only the 1-279 GHR isoform has been studied further. Homodimers of this isoform undergo minimal internalisation and are not down regulated in response to GH, showing a half-life as long as 4 hours. They also showed an increased capacity to generate GHBP (Amit *et al*., 1997). Similar findings were seen in another study, however, it was also shown that the 1-279 GHR isoform had a reduced affinity for GH but increase capacity to bind GH by having more binding sites when compared to full-length GHR (Ross *et al*., 1997). It was also shown that heterodimers of 1-279 GHR and full-length GHR may exist. Given that the isoform lacks the intracellular domain, these heterodimers were unable to signal in response to GH (Ross *et al*., 1997). The 1-279 GHR isoform has therefore been shown to act as a dominant negative inhibitor of full-length GHR.

The other remaining isoform, d3GHR, arises by skipping exon 3, through homologous recombination which mimics alternative splicing between the retroviral retroelements flanking exon 3 (Pantel *et al*., 2000). The loss of exon 3 by this mechanism results in a A6D substitution in exon 2 (Dos Santos *et al*., 2004). The substitution of this highly conserved amino acid results in altered charge and hydrophobicity of the isoform compared to full-length GHR (Dos Santos *et al*., 2004). Little else is known about this isoform. Interestingly though, it has been shown by several studies that the d3GHR isoform shows increased responsiveness to GH *in vivo*, compared to full-length receptor (Binder *et al*., 2006; van der Klaauw *et al*., 2008; Dos Santos *et al*., 2004). The mechanism resulting in increased responsiveness of d3GHR remains unknown. However, it is thought that the removal of the N-terminal loop encoded by exon 3 results in a subtle conformational change in the extracellular domain that may facilitate increased responsiveness to GH binding (Dos Santos *et al*., 2004).

### 1.6 GH/IGF1 Axis in Cancer

As stated before, the GH/IGF1 axis is well described in a number of cancer models. Given that the original hypothesis of GH action on growth and proliferation was that GH stimulates the hepatic secretion of IGF1, which then functions in an endocrine manner to bind to IGF1 receptors in tissues to induce growth, it was thought that GH exerts its proliferative and growth effects through its physiological effector IGF1. IGF1 is known to act on many cell types to bring about increased proliferation and anti-apoptotic signals through its activation of MAPK and PI3K pathways respectively (Gooch *et al*., 1999). It is therefore unsurprising that elevated levels of IGF1 have shown to confer an increased risk of breast (Yee *et al*., 1989), endometrial (Elkas *et al*., 1998), pancreatic (Bergmann *et al*., 1995), lung (Minuto *et al*., 1986), colorectal (Rinaldi *et al*., 2010), and prostate cancer (Rowlands *et al*., 2009). As described previously, carcinogenesis is the multistep process whereby normal cells accumulate a number of cancerous traits through genomic "hits". Therefore, the hypothesis of the link between elevated IGF1 levels and cancer was that rather than IGF1 directly initiating carcinogenesis, it indirectly promoted carcinogenesis by increasing the pool of partially transformed cells available to receive the necessary genomic "hits" to become cancerous, and this was through the proproliferative and anti-apoptotic actions of IGF1.

GH, since it promotes the production and secretion of IGF1, also plays a role in carcinogenesis, albeit initially thought to be an indirect role. GH has been shown to be an etiologic factor in tumourigenesis. Early animal model studies have shown that GH induced neoplasms in rats (Moon *et al*., 1950), while transgenic mice overexpressing human GH showed higher incidences of tumours in mammary glands and livers (Snibson *et al*., 2001; Törnell *et al*., 1992). Also, in humans, a condition exists resulting in increased GH and therefore IGF1 levels (Chhabra *et al*., 2011). These elevated levels are as a result of either pituitary tumours, or activating mutations in the GHRH signalling cascade, which result in hypersecretion of GH by pituitary somatotroph cells (Chhabra *et al*., 2011). The condition is associated with an increased risk of colon (Ezzat *et al*., 1991), breast (Cheung and Boyages, 1997), and prostate cancer (Colao *et al*., 1998; le Roux *et al*., 2000). Given that IGF1 has been shown to play a role in these cancers, it was therefore initially thought that the tumourigenic effects of GH were indirectly mediated by IGF1 rather than directly by GH. Studies have confirmed this as mice treated with GHR antagonist resulted in a decrease of tumour volumes with a substantial decrease in serum IGF1 (Divisova *et al*., 2006). However, a study

showed that antagonism of GHR resulted in regression of meningioma xenografts in nude mice, with only a 20% decrease in serum IGF1 (McCutcheon *et al*., 2001). This indicates that GH may in fact ellicit its tumourigenic effects directly through GHR, and not via IGF1. Recently, studies have been conducted to elucidate the mechanism whereby GH may promote tumourigenesis. Such studies have shown that GH overexpression promotes proliferation (Chiesa *et al*., 2011; Kaulsay *et al*., 1999; Pandey *et al*., 2008; Segard *et al*., 2003; Zhu *et al*., 2005), anchorage-independent growth (Pandey *et al*., 2008), cell migration and invasion (Pandey *et al*., 2008), epithelial-to-mesenchymal conversion (Pandey *et al*., 2008), angiogenesis (Brunet-Dunand *et al*., 2009), and chemoresistance (Minoia *et al*., 2012; Zatelli *et al*., 2009) while inhibiting apoptosis (Segard *et al*., 2003) and differentiation (Segard *et al*., 2003), mostly within *in vivo* models. In these studies, the phenotypes achieved by overexpressed GH were seen with alterations to a wide range of cellular functions. Overexpressed GH was associated with increased transcription of several oncogenes including *hoxa1, myc,* and *jun* (Pandey *et al*., 2008). The gene encoding human telomerase, *hTERT*, and the gene encoding Cyclin D1 were also seen to be induced in response to overexpressed GH (Pandey *et al*., 2008), along with *c-fos* (Zatelli *et al*., 2009)and JNK (Minoia *et al*., 2012).

### 1.7 GHR in Cancer

GHR has been reported to be overexpressed in number of cancers, including breast (Gebre-medhin *et al*., 2001), adrenocortical (Lin *et al*., 1997), colon (Yang *et al*., 2004), and melanoma (Lincoln *et al*., 1999).Additionally, in some of the studies showing the tumourigenic effects of GH, these effects have been shown to be mediated largely by GHR, by using the GHR antagonist, G120R, that is known to bind selectively to GHR and not PRLR (Goffin *et al*., 1999; Kaulsay *et al*., 1999; Minoia *et al*., 2012; Pandey *et al*., 2008). However, the tumourigenic effects of GH have also been shown to be mediated by PRLR, albeit to a lesser extent than GHR (Xu *et al*., 2011). Given the tumourigenic effect of GH seen in various cancer cell lines, GHR antagonism was shown to inhibit tumour growth *in vitro* (McCutcheon *et al*., 2001). This, in combination with the observed tumourigenic role of GH, indicates that GH elicits its tumourigenic effects largely through GHR, however, GH signalling via PRLR cannot be completely excluded.

Interestingly, nuclear-localised GHR is a common feature of tissues and cells exhibiting a high rate of proliferation (Conway-Campbell *et al*., 2007; Lincoln *et al*., 1998). Accumulation of GHR within the nucleus has been reported in a number of cancers including B-cell lymphomas, mammary carcinoma, and melanoma (Lincoln *et al*., 1998). Full-length GHR has been demonstrated to localise to the inner and outer nuclear membranes, nucleoplasm, and chromatin to achieve its GH-stimulated function within the nucleus (Lobie *et al*., 1994). Additionally, when nuclear-localised GHR was expressed within the immortalised pro-B cell lineBaF3, aggressive metastatic tumours were generated *in vivo* when injected into mice (Conway-Campbell *et al*., 2007). These findings suggest a role for nuclear-localised GHR in tumourigenesis. Further circumstantial evidence is the observation that 75% of women with uterine cervical neoplasms showed nuclear GHR expression (Dehari *et al*., 2008).

### 1.8 Project Aim and Objective

The aim of this project is to investigate the role of GHR in oesophageal squamous-cell carcinoma (OSCC) carcinogenesis. This is based on the observations that GH plays a role in a number of cancers, and that its carcinogenic effects is largely mediated through GHR. This will be done by;

(1) Investigating the expression of GHR and GH mRNA in a panel of OSCC cell lines.
(2) Investigating the expression of GHR protein in a panel of OSCC cell lines.
(3) Investigating the effect of GHR knockdown on carcinogenesis by measuring proliferation and response to chemotherapeutic drugs.

# CHAPTER TWO

# GH & GHR EXPRESSION

To investigate the potential role of GHR and autocrine GH, OSCC cell lines underwent mRNA analysis for the identification of GH and GHR mRNA expression by means of PCR, followed by immunoblotting and immunocytochemistry. The human breast cancer cell line T47D was used as the positive control for the mRNA expression of GH, GHR (Decouvelaere *et al*., 1995), and d3GHR. mRNA expression of GH and d3GHR have not been shown previously in T47D, however, while conducting initial PCRs, it was found that the expected PCR products for GH and d3GHR cDNA were amplified from T47D cells. Thus, T47D from then on served as the positive control for all PCRs.

## 2.1 mRNA Expression Profile

### 2.1.1 Primer Design

To identify the expression of GH, full-length GHR (flGHR), and the d3GHR isoform, gene-specific primers that have previously been published were used. All primers used were intron-spanning and thus were able to distinguish between genomic DNA (gDNA) and cDNA reverse transcribed from messenger RNA (mRNA). The GH-specific primers were directed towards selected regions within exons 3 and 5 (Kaulsay *et al*., 1999). The flGHR-specific primers were specific for flGHR cDNA and excluded amplification of cDNA of the 1-277, and 1-279 GHR splice variants, but allowed amplification of d3GHR cDNA (Fig.10). These primers were directed towards regions within exon 6 and 9 (Kaulsay *et al*., 1999). The d3GHR-specific primers were directed towards exons 2 and 5 and amplified cDNA from all splice variants, from which d3GHR cDNA could be distinguished on the basis of size (Sobrier *et al*., 1993) (Fig.10).

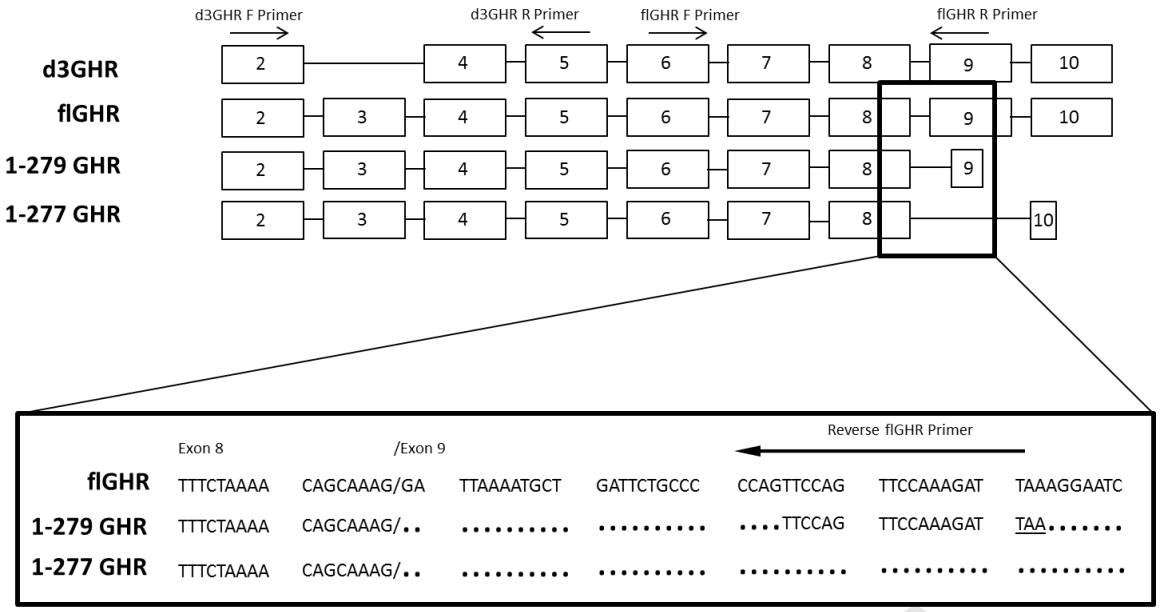


**Figure 10: Annealing position of the GHR primers used.** Exons are shown as boxes, primers as arrows, exon boundaries as slashes, deleted sections by periods, and inframe stop codons underlined.

Since the flGHR forward primer anneals within exon 6, and since exon 6 is unaltered in flGHR, 1-277, and 1-279 GHR, the flGHR-specific reverse primer had to be able to distinguish between flGHR and the mentioned isoforms. Hence, the reverse primer anneals in a portion of exon 9 that is completely lost in the 1-277 GHR isoform, and partly lost in the 1-279 GHR isoform (Fig.10). Specifically for the 1-279 GHR isoform, the primer did anneal to the very little of exon 9 that remained in the 1-279 isoform, however, the first 4 nucleotides of the 3' end of the primer did not anneal, therefore preventing the amplification of 1-279 GHR mRNA. Since d3GHR primers annealed to exons 2 and 5, and since exon 3 was lost in the d3GHR isoform and present in all other isoforms of GHR, these primers were only able to distinguish d3GHR from all other isoforms (Fig.10).

### 2.1.2 DNase Treatment

As stated above, all primers used did span introns, thus allowing the distinction between gDNA and mRNA. Of the 4 PCRs done (GH, flGHR, d3GHR, GAPDH), only the GH-specific primers were able to generate a gDNA product small enough to be effectively amplified and observed following agarose gel electrophoresis (Fig.11A). Sizes for gDNA bands using the 4 gene-specific primers were 688bp, 27 736bp, 129 186bp, and 5 210bp for GH, flGHR, d3GHR, and GAPDH gene-specific primers respectively. Contamination by gDNA in RNA preparations was first detected by GH PCR (Fig.11A). The other gene-specific primers generated extremely

large gDNA products that were unable to be visualised following agarose gel electrophoresis. An appropriate DNase treatment protocol was implemented to remove contaminating gDNA.

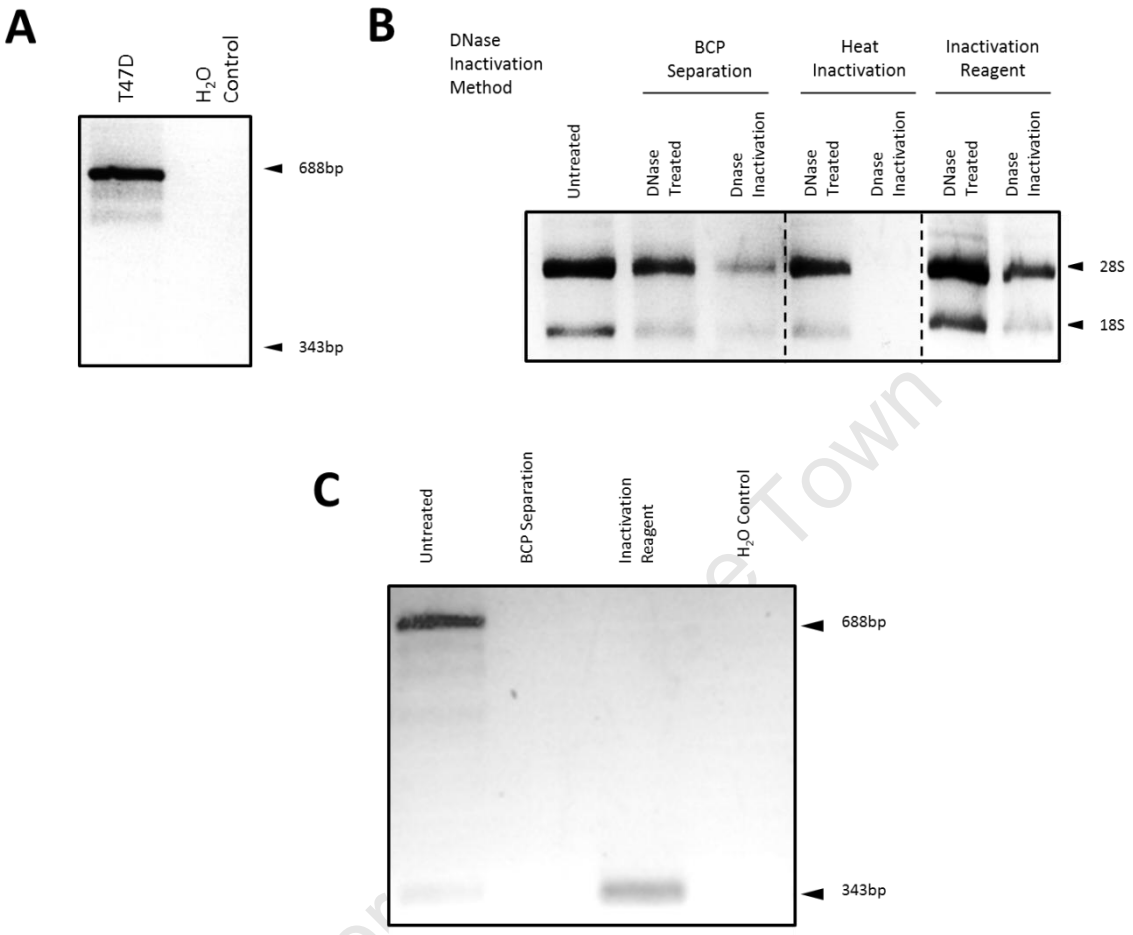


**Figure 11: Identification and removal of gDNA contamination following RNA isolation. (A)** RNA from T47D was isolated, DNase treated, converted into cDNA, amplified by PCR, electrophoresed, and visualised as in materials and methods.PCR using GH-specific primers indicating gDNA contamination product band.**(B)** RNA after DNase treatment and inactivation by three different methods; (i) 1-bromo-3-chloropropane separation, (ii) heat inactivation, (iii) addition of Inactivation Reagent. 1µg of untreated, DNase-treated, and DNase-inactivated RNA was loaded on an RNA gel and electrophoresed as in materials and methods. However, 2µg of DNase-treated RNA was loaded in the DNase treated lane of the Inactivation Reagent method. Dotted lines indicate where different images of different RNA gels have been attached. **(C)** GH PCR following DNase treatment and inactivation by BCP separation and addition of Inactivation Reagent. DNase-treated RNA then underwent cDNA conversion and GH PCR as in materials and methods.

RNA was incubated with a commercially available DNase which was then inactivated by one of the following three methods; (i) by means of 1-bromo-3-chloropropane (BCP) separation, (ii) by heat inactivation, (iii) by the addition of the Inactivation Reagent supplied with the DNase treatment kit. Spectrophotometric analysis indicated a 5% loss of RNA directly following DNase treatment, and this is further supported by the visual loss in intensity of 28S and 18S bands following RNA gel electrophoresis (Fig.11B). This loss is most likely due to handling of the sample during DNase treatment as evaporation and/or degradation may take place during the incubation step of the digest.

Spectrophotometric analysis after DNase treatment and inactivation indicated that there was a 90%, 100%, and 13% loss of starting RNA material when the DNase enzyme was inactivated by BCP separation, heat inactivation, and the addition of Inactivation Reagent, respectively. This loss was further confirmed by visual inspection of the of 28S and 18S bands following electrophoresis(Fig. 11B).

RNA treated with DNase and then inactivated by either BCP precipitation or addition of Inactivation Reagent then underwent cDNA conversion and GH PCR as described in materials and methods. The 688bp band was once again observed before DNase treatment indicating possible gDNA contamination, with the desired 343bp also being observed, albeit at low levels (Fig.11C). Following DNase treatment and DNase inactivation by BCP separation, no bands were seen to be amplified (Fig.11C), probably due to the significant loss of RNA using this method. However, following DNase treatment with inactivation by means of Inactivation Reagent, only the desired 343bp band possibly corresponding to GH mRNA was seen (Fig.11C). Sequencing of this band at a later stage indicated the 343bp band is human GH (Appendix A). The loss of the 688bp band following DNase treatment indicates that it does correspond to gDNA contamination within the RNA preparation, and that it is effectively removed with DNase treatment. The increase in intensity of the 343bp band could be as a result of a more efficient PCR reaction following the removal of gDNA contamination. This allows for the finite amounts of primers and nucleotides added to the PCR reaction to amplify only cDNA targets rather than both cDNA and gDNA targets. However, PCR for a housekeeping gene was not included here, and therefore the increase in the 343bp band due to variable levels of starting template material between samples may not be excluded.

### 2.1.3 GH & GHR mRNA Expression

Since an appropriate DNase treatment protocol was established, RNA isolated from a panel of OSCC cell lines and fibroblast cells was DNase treated, reverse transcribed, and finally amplified by PCR with the gene-specific primers for GH, flGHR, and d3GHR (Fig.12).A panel of nine human OSCC cell lines (WHCO1, WHCO5, WHCO6, Kyse 30, Kyse 70, Kyse 150, Kyse 180, Kyse 450, Kyse 520), and two normal human fibroblasts cells (DMB and $FG^{0}$) was used.

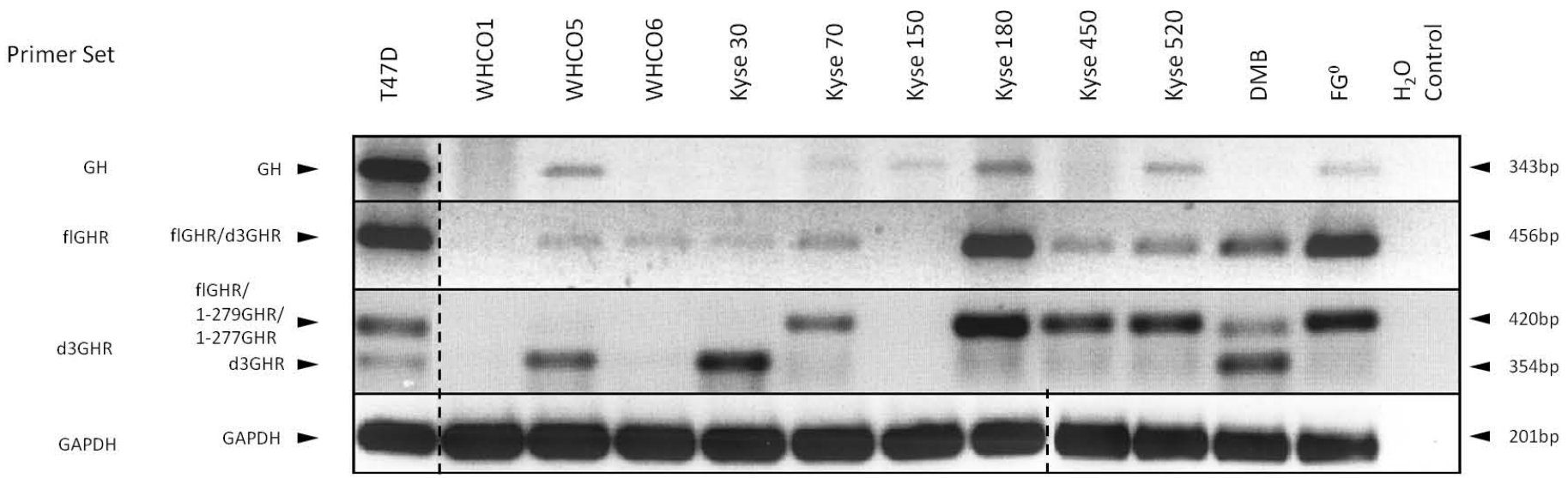


**Figure 12: mRNA expression of GH and GHR in OSCC cell lines and immortalised fibroblast cells.** RNA was isolated, DNase treated, and converted into cDNA as described in materials and methods, followed by PCR using gene-specific primers for GH, flGHR, d3GHR, and GAPDH. PCR products were then electrophoresed in a 2% agarose gel and visualised as described in materials and methods. Dotted lines indicate where lanes have been omitted. Using the flGHR primer set, a band of 456bp corresponding to flGHR and d3GHR cDNA was amplified. Using the d3GHR primer set, a 420bp band corresponding to flGHR, 1-279, and 1-277GHR was amplified, along with a 354bp band corresponding to d3GHR cDNA was amplified.

PCR for the housekeeping gene GAPDH amplified the expected 201bp product in all cell lines, indicating that the cDNA was of reasonable quality (Fig.12). As expected, following PCR for GH and flGHR in T47D, products of 343bp and 456bp in size were generated respectively (Fig.12). Sequencing of these PCR products revealed that the 343bp and 456bp products corresponded to human GH and GHR (flGHR and d3GHR) respectively (Appendix A). Using d3GHR-specific primers generated 420bp and 354bp products in T47D (Fig.12). Sequencing of these two products indicated that the 420bp correlated to GHR, either flGHR, 1-279, or 1-277 GHR, while the 354bp correlated to d3GHR mRNA (Appendix A).

PCR using the GH-specific primers showed amplification of the expected 343bp band in five of the nine OSCC cell lines (WHCO5, Kyse 70, Kyse 150, Kyse 180, and Kyse 520), conclusively showing ectopic expression of GH mRNA in these cell lines (Fig.12). Interestingly, of the fibroblast cell lines, $FG^0$ also showed GH mRNA expression (Fig.12). The 456bp band correlating to both flGHR and d3GHR mRNA was seen in seven of the nine OSCC cell lines tested (WHCO5, WHCO6, Kyse 30, Kyse 70, Kyse 180, Kyse 450, and Kyse 520) while both fibroblast cell lines also expressed flGHR and/or d3GHR (Fig.12). Using the d3GHR-specific primers that are able to distinguish between GHR and d3GHR indicated that GHR was expressed in five of the nine OSCC cell lines (WHCO5, Kyse 70, Kyse 180, Kyse 450, and Kyse 520) and in both of the fibroblast cell lines (Fig.12). Whether this correlated to flGHR, 1-279, or 1-277GHR could not be determined. However, given that in previous studies it was found that 1-279 and 1-277 GHR made up 10% and less than 1% of total GHR mRNA transcripts respectively in human liver cells (Ross *et al*., 1997), it can be argued that the 420bp product corresponds mostly to flGHR mRNA. d3GHR mRNA was only conclusively seen to be expressed in three of the OSCC cell lines (WHCO5, WHCO6 and Kyse 30), and only in DMB of the normal fibroblast cell lines (Fig.12).d3GHRmRNA was seen to be expressed by WHCO6 when performing the second d3GHR PCR (data not shown).

Since GHR is a ubiquitously expressed receptor, it should be unsurprising that it is expressed in a majority of OSCC cell lines and in both the normal fibroblast cell lines. However, it is interesting to note that of the seven OSCC cell line shown to express GHR, only two express mRNA for the d3GHR isoform. With the ectopic expression of GH mRNA shown in a majority of OSCC cell lines tested, along with the expression of GHR mRNA, indicates a possible role of the autocrine GH/IGF1 axis in OSSC that is mediated through flGHR in the majority of cell

lines tested. This could also be true for the fibroblast cells used here since $FG^0$ also showed extra-pituitary expression of GH mRNA. Additionally, the detection of d3GHR in two of the nine OSCC cell lines tested indicates that d3GHR may play a role in a subset of patients, since these cell lines originate from patients.

### 2.2 GHR Protein Expression

#### 2.2.1 Western Blotting on Cell Lines Transiently Overexpressing GHR

Since a cell line that had previously been shown to express GHR was not available, western blots were optimised using lysate from cells transiently overexpressing GHR as a positive control. Both GHR antibodies (Mab 263 and B12) were tested by straight immunoblotting using lysates from the overexpressing cell lines (Fig.13)

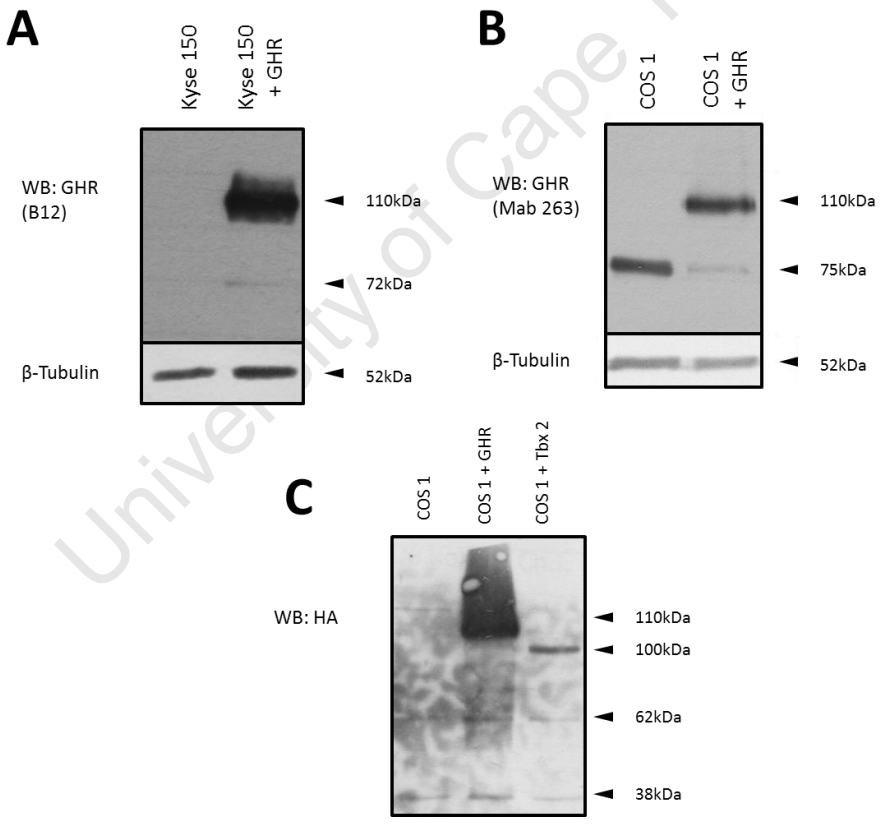


**Figure 13: Characterising the GHR protein band using cell lines transiently overexpressing GHR.** Protein from Kyse 150 and COS 1 cells that were transiently transfected with GHR was isolated, and analysed by western blot as described in materials and methods. β-Tubulin was included as a control for protein loading. Sizes of bands are indicated. Depicted results are representative of two separate experiments. **(A)**Protein isolated from GHR-overexpressing (Kyse 150+GHR) and non-overexpressing Kyse 150 cells (Kyse 150) was electrophoresed and underwent immunoblotting with the GHR antibody B12. **(B)** Protein isolated from GHR-overexpressing (COS 1+GHR) and untransfected COS 1 cells (COS 1) was electrophoresed and underwent immunoblotting with the GHR antibody Mab 263. **(C)** Protein isolated from GHR-overexpressing (COS 1+GHR) and untransfected COS 1 cells (COS 1) was electrophoresed and underwent immunoblotting for the HA tag. Additionally, as a control for the HA antibody, COS 1 cells were transfected with a Tbx2 expression plasmid known to encode HA-tagged Tbx2 protein (COS 1+Tbx2).

Kyse 150 cells, previously shown not to express GHR mRNA, were transiently transfected with the GHR expression plasmid (GHR-pcDNA3.1). Lysates from untransfected and overexpressing cells underwent SDS-PAGE electrophoresis and immunoblotted with the B12 GHR antibody. GHR overexpression resulted in the detection of two protein bands at 110kDa and 72kDa in size (Fig.13A). The 110kDa band likely corresponds to full-length GHR. Since the B12 antibody recognises the intracellular domain of GHR, the 72kDa band was likely the cytoplasmic tail remnants following cell-surface cleavage of GHR, since previously a similar sized band was detected using a similar antibody as the cytoplasmic remnant (Schantl *et al*., 2004). The 72kDa band seen following GHR overexpression is unlikely to be a splice variant of GHR as alternative splicing of cDNA-containing plasmids is highly unlikely. Also, the induction of the 72kDa band due to the stresses of transfection was also disproved when transfecting with empty pcDNA3.1 vector (Appendix A). Similar results were seen when immunoblotting GHR-overexpressing and untransfected COS 1 cells with the Mab 263 antibody, except that a 75kDa band was seen in untransfected cells, while overexpression introduced only a 110kDa band (Fig.13B). Interestingly, this 75kDa band decreased in intensity following GHR overexpression. Since β-Tubulin immunoblotting shows even protein loading, the decrease in the 75kDa band is quite intriguing.

Since the GHR protein encoded by the GHR-pcDNA3.1 plasmid is HA-tagged, protein lysates from COS 1 overexpressing and untransfected cells were immunoblotted with an antibody directed against the HA tag (Fig.13C). Once again, a 110kDa band was detected following GHR overexpression with two other protein bands being observed at 62kDa and 38kDa. However, detection for HA-tagged proteins failed to identify any proteins at 72kDa in size indicating that the HA tag was likely attached on the extracellular domain of GHR as the 72kDa band likely corresponded to the intracellular domain of GHR. Since information on the cloning of the GHR-pcDNA3.1 plasmid was unavailable, this is the likely scenario. As a control for the HA antibody, COS 1 cells were transfected with an expression plasmid known to encode for HA-tagged Tbx2 protein (Fig.13C). Tbx2 overexpression resulted in the detection of the expected 100kDa band. Control for loading was not conducted, however, based on the even intensity of the non-specific bands between lanes, it may be inferred that loading was even. This implies that all bands observed are as a result of transfection and not because of uneven loading. This, together with the introduction of the expected 100kDa

band following Tbx2 transfection, indicated that the system for transfection and immunoblotting, was functional.

Given that all three antibodies detected a 110kDa band following GHR overexpression, and that protein loading is even, the 110kDa is most likely GHR, even with the size being smaller than the reported 120-130kDa size for mature GHR (Asa *et al*., 2007; Kerkhof *et al*., 2007; Ross *et al*., 1997; Stubbart *et al*., 1991; Wang *et al*., 1992). To further support this, 100 copies of the GHR-pcDNA3.1 expression plasmid underwent PCR using the flGHR-specific primers, and the PCR product sequenced. Sequencing revealed that the insert of the plasmid was in fact human GHR cDNA (Appendix A).

### 2.2.2 Expression of GHR in Oesophageal Squamous-Cell Carcinoma Cell Lines

Since immunoblotting on GHR overexpressing cell lines indicated that GHR was detected at 110kDa using both GHR antibodies, crude protein lysate extracts from OSCC cell lines and fibroblast cells were then tested for GHR protein expression using both GHR antibodies (Fig.14). Protein lysate from GHR-overexpressing Kyse 150 cells (Kyse 150+GHR) was analysed, while T47D cells was included as a positive control as T47D cells have previously been shown to express GHR protein by western blotting (Xu *et al*., 2011).

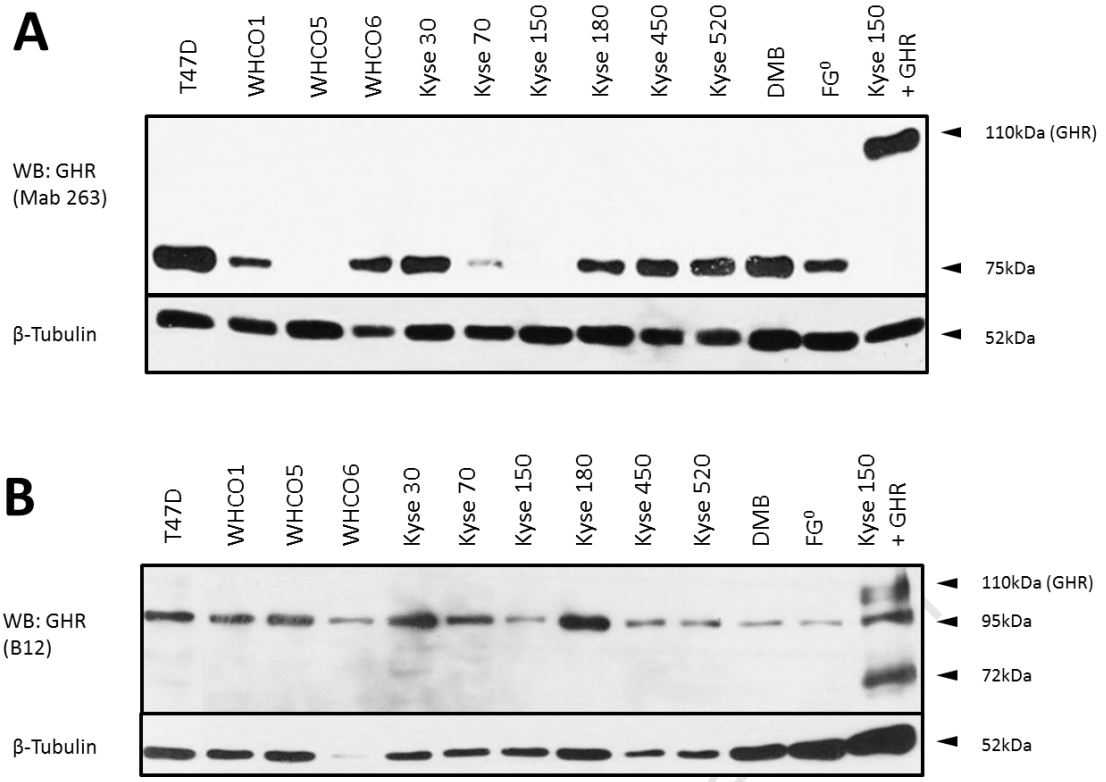


**Figure 14: GHR expression in OSSC cell lines and fibroblast cells.** 30µg of crude lysate from indicated cell lines were immunoblotted for GHR as described in materials and methods. β-Tubulin was included as a control for protein loading. Sizes of bands are indicated. Depicted results are representative of two separate experiments.**(A)** Immunoblotting with the GHR antibody Mab 263. **(B)** Immunoblotting with the GHR antibody B12.

Once again, the expected 110kDa band was observed following GHR overexpression (Kyse 150+GHR lane) and detection with the Mab 263 antibody (Fig.14A). However, this band was not seen in any of the other cell lines tested when probed with the same antibody. A 75kDa band was seen in all but two cell lines (WHCO5 and Kyse 150) (Fig.14A). The possibility of the 75kDa band being an isoform of GHR, or perhaps an unglycosylated, precursor form of the receptor, may not be excluded. The epitope for the Mab 263 has been previously mapped and found to lie around the binding region of GH (Wan *et al*., 2003), and therefore should be able to detect both 1-279 and 1-277 GHR isoforms along with flGHR. However, since 1-279GHR was detected at 55-60kDa, and since one would expect to observe 1-277GHR at a similar size, it is unlikely that the 75kDa band detected above was an isoform previously characterised (Ross *et al.*, 1997).

Immunoblotting with the B12 antibody once again detected the 110kDa and 72kDa bands following GHR overexpression (Kyse 150+GHR lane) (Fig.14B). Neither of these two bands were seen in any other of the cell lines, although, this may be a result of the uneven protein loading between lanes as evidenced by β-Tubulin immunoblotting (Fig.14B). Even with the uneven loading, a 95kDa band was seen in all cell lines tested (Fig.14B). Another study convincingly showed that using the same antibody, the 95kDa band was deemed to be GHR (Arturi *et al*., 2011), despite the band's size being far below the 120-130kDa size other studies showed to be GHR (Asa *et al*., 2007; Kerkhof *et al*., 2007; Ross *et al*., 1997; Stubbart *et al*., 1991; Wang *et al*., 1992). The same study did not indicate whether the 95kDa band was mature, full-length GHR, an isoform, or a precursor of GHR. Regardless of T47D having been reported to express GHR at 120kDa (Xu *et al*., 2011), this was not seen here using either of the GHR antibodies, possibly indicating a low sensitivity of these antibodies that are only able to detect GHR by means of western blot when overexpressed.

Given the possible insensitivity of the GHR antibodies, it was thought that 30µg of crude protein lysate may be insufficient to detect the 110kDa GHR band. 100µg of crude protein lysate was then immunoblotted with both GHR antibodies (Fig.15).

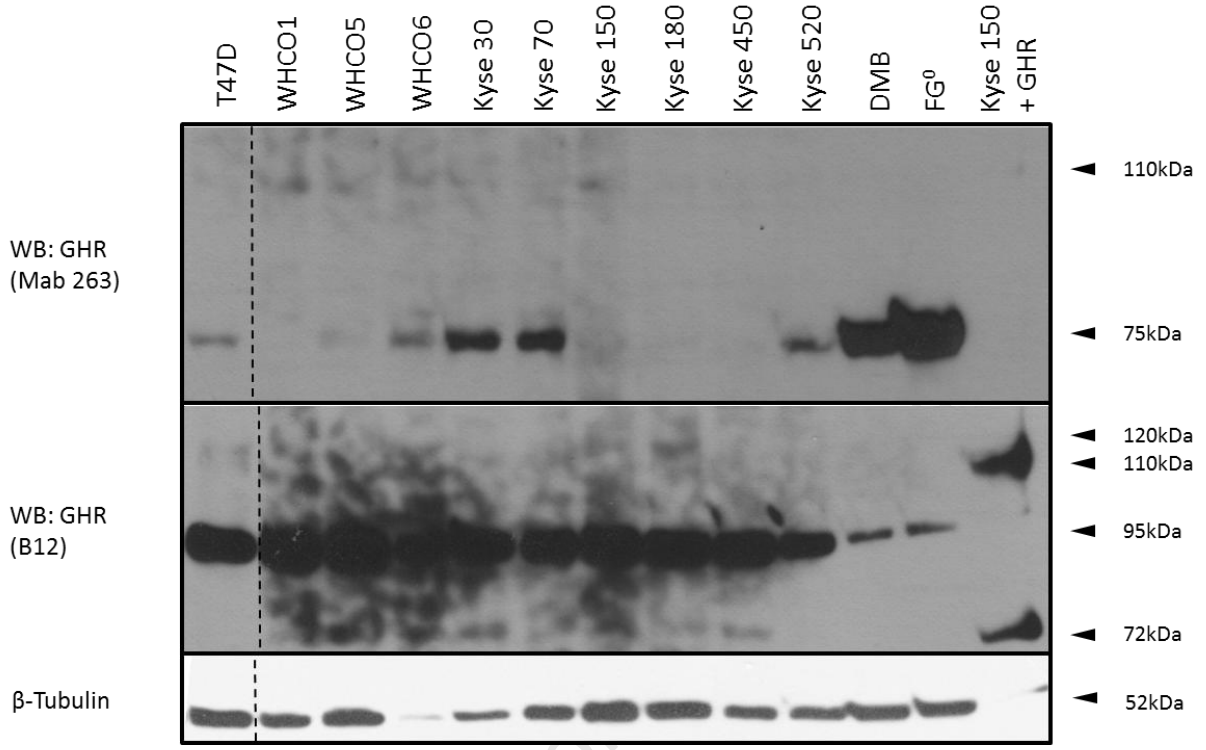


**Figure 15: GHR expression in OSSC cell lines and fibroblast cells.** 100µg of crude protein lysate from cell lines indicated was analysed by immunoblotting with the two GHR antibodies as described in materials and methods. Only 15µg lysate from the overexpressing cell line (Kyse 150+GHR) was used. The same nitrocellulose membrane was probed with the Mab 263 antibody, stripped, and then probed with the B12antibody. β-Tubulin was included as a control for protein loading. Sizes of bands are indicated. **(A)** Immunoblotting with the GHR antibody Mab 263. **(B)** Immunoblotting with the GHR antibody B12.

Once again, when probing with the Mab 263 antibody, a faint 110kDa band was observed following overexpression (Kyse 150+GHR lane), better visible at longer exposures (data not shown). A 75kDa band was seen in a majority of cell lines (Fig.15, top panel). However, despite uneven loading, a faint 110kDa band was seen in WHCO1, WHCO5, WHCO6, Kyse 30, and Kyse 150, indicating possible GHR protein expression in these cell lines (Fig.15, top panel). This would not, however, follow the expression profile of GHR mRNA as the Kyse 150 cell line had previously been shown not to express detectable GHR mRNA (Fig.12). The expression profile of the 75kDa band does not follow that observed in Fig.14, possibly due to incomplete solubilisation of membrane proteins in an effort to obtain a high concentration of protein in lysate preparations.

Stripping and reprobing of the same nitrocellulose membrane with the B12 GHR antibody once again revealed the detection a 110kDa and a 72kDa band following GHR overexpression (Kyse 150+GHR lane), and a 95kDa band in all cell lines tested (Fig.15, middle panel). However, with the increased loading of protein, a 120kDa band was now detected in T47D and Kyse 180 cells (Fig.15, middle panel), following the mRNA expression profile since these two cell lines have been shown to express the highest levels of GHR mRNA (Fig.12). Since the size of this band would be consistent with previous studies that detected mature GHR at 120kDa, it would suggest possible expression of mature GHR protein in these two cell lines. The inability to detect either the 110kDa or 120kDa band in other cell lines despite showing mRNA expression in the majority in these cell lines could reflect the possible insensitivity of these GHR antibodies and/or the low levels of the mature GHR protein in these cells. Regardless of the possibility of incomplete solubilisation of membrane proteins, the 95kDa band was once again seen as before (Fig.14B), indicating that this band is likely a cytosolic protein. Additionally, when probing higher amounts of crude lysate, it was revealed that the intracellular domain of GHR (detected at 72kDa) was present in WHCO1, WHCO5, WHCO6, Kyse 30, Kyse 180, and Kyse 450 cells.

### 2.2.3 GHR Localisation by Immunocytochemistry

The inability to detect endogenous levels of GHR in denaturing gels could be due to the need of GHR to be in its native, non-denatured state to be detected by these GHR antibodies, although this is not discussed in the literature. To test this, GHR expression was investigated by immunocytochemistry. Additionally, as mentioned previously, several studies suggest a possible role of nuclear-localised GHR as a mechanism for tumourigenesis. Immunocytochemistry was employed to investigate the subcellular localisation of GHR in OSCC (Fig.16).

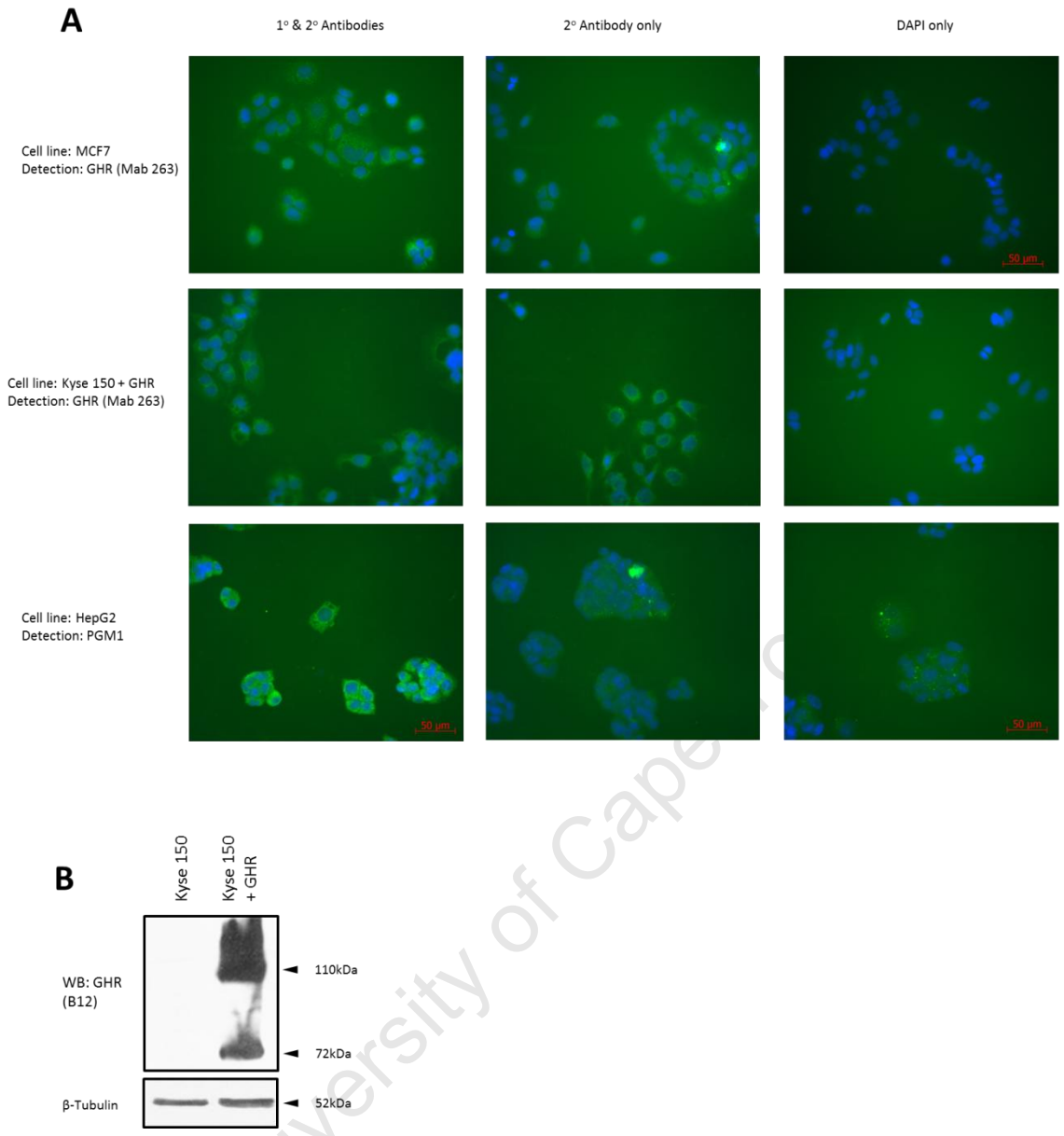




**Figure 16: Detection of GHR by immunocytochemistry.** Cells were incubated with primary and secondary antibody (1°& 2° antibodies), secondary antibody only (2° antibody only), and DAPI only. MCF7 and Kyse 150+GHR cells were tested for GHR detection by means of immunocytochemistry (top and middle panels respectively). Differing protocols for fixation, blocking, and antibody incubation, as described in materials and methods, gave similar results as above. To investigate for normal levels of signal with functioning antibodies, HepG2 cells were processed in the same manner as the cell lines used for GHR detection except that PGM1 was detected for (lower panel). **(B)** Western blot analysis indicating that the Kyse 150+GHR cells used in detecting GHR by means of immunocytochemistry were successfully transfected with GHR.

Firstly, to investigate whether the system is functional, GHR immunocytochemistry was conducted on the human breast cancer cell line, MCF 7; a cell line previously shown to exhibit detectable levels of nuclear-localised GHR (Lincoln *et al*., 1998) (Fig.16A, top panel). The Mab 263 antibody was used since it had been previously used to investigate the localisation of GHR (Gebre-medhin *et al*., 2001; Lincoln *et al*., 1999). Incubation with $1^{o}$ and $2^{o}$ antibodies resulted in a low intensity signal (Fig.16A, top panel), that was similar in signal strength when incubating with $2^{o}$ antibody only. No signal was observed when neither $1^{o}$ nor $2^{o}$ antibody was used, other than the nuclear DAPI signal (Fig.16A, top panel). This indicated that signal seen when incubating with $1^{o}$ and $2^{o}$ antibodies was likely due to the non-specific binding of the $2^{o}$ antibody (as evidenced by incubation with $2^{o}$ only), rather than localisation of GHR. Using differing fixing, blocking, and incubation conditions as described in materials and methods gave similar results.

Conducting immunocytochemistry on Kyse 150 cells transiently overexpressing GHR (Kyse 150+GHR) gave similar results as above (Fig.16A, middle panel). Additionally, using the differing fixing, blocking, and incubation conditions as described in materials and methods also gave similar results. Kyse 150 cell were shown to be successfully overexpressing GHR as evidenced by immunoblotting with the B12 GHR antibody (Fig.16B).

To test whether the lack of signal was a reflection of a general technical problem, or confined to GHR detection, the human hepatoma cell line, HepG2, were used to detect for phosphoglucomutase 1 (PGM1) localisation. Our laboratory has previously demonstrated that PGM1 is normally localised in the cytosol (unpublished data), as observed when incubated with $1^{o}$ and $2^{o}$ antibody (Fig.16A, bottom panel). Furthermore, the signal is significantly weaker when incubating with $2^{o}$ only, indicating that the high signal when incubating with $1^{o}$ and $2^{o}$ antibodies is due to the specific binding of the $1^{o}$ antibody to its epitopes present on PGM1. HepG2 cells were prepared in the same manner as for GHR detection, indicating that the system allowed for efficient fixing, binding of antibody, and detection of signal. These results suggest the possible insensitivity of these GHR antibodies, particularly the antibody used for GHR immunocytochemistry, Mab 263. Additionally, a high level of background signal was due to long exposure (Fig.16).

## 2.3 Characterisation of the GHR Protein Bands

### 2.3.1 Investigation of Protein Glycosylation

One of the many post-translational modifications proteins are subjected to before becoming mature, functional proteins is glycosylation. Glycosylation serves a wide spectrum of purposes, including the maintenance of the structural integrity of the protein (Varki *et al*., 2009). Glycosylation is the process of attaching glycan chains to specific sites within the protein (Varki *et al*., 2009). Several classes of glycans exist, the most common being *N*-linked glycans that are attached to specific asparagine side-chains within the protein (Varki *et al*., 2009).

It has been previously shown that mature GHR is N-link glycosylated, and that removal of these glycan chains by means of digestion with specific amidases resulted in a significant increase in GHR motility through SDS-PAGE gels (Asa *et al*., 2007). To investigate whether the 95kDa and 75kDa bands detected with the B12 and Mab 263 GHR respectively are either isoforms or precursor GHR proteins, Kyse 150 cells overexpressing GHR were treated with tunicamycin (Fig.16), an antibiotic known to inhibit several enzymes that catalyse the first steps of N-linked glycoprotein synthesis (Heifetz *et al*., 1978). This would also serve to confirm whether the 110kDa band is in fact mature, fully-glycosylated GHR.

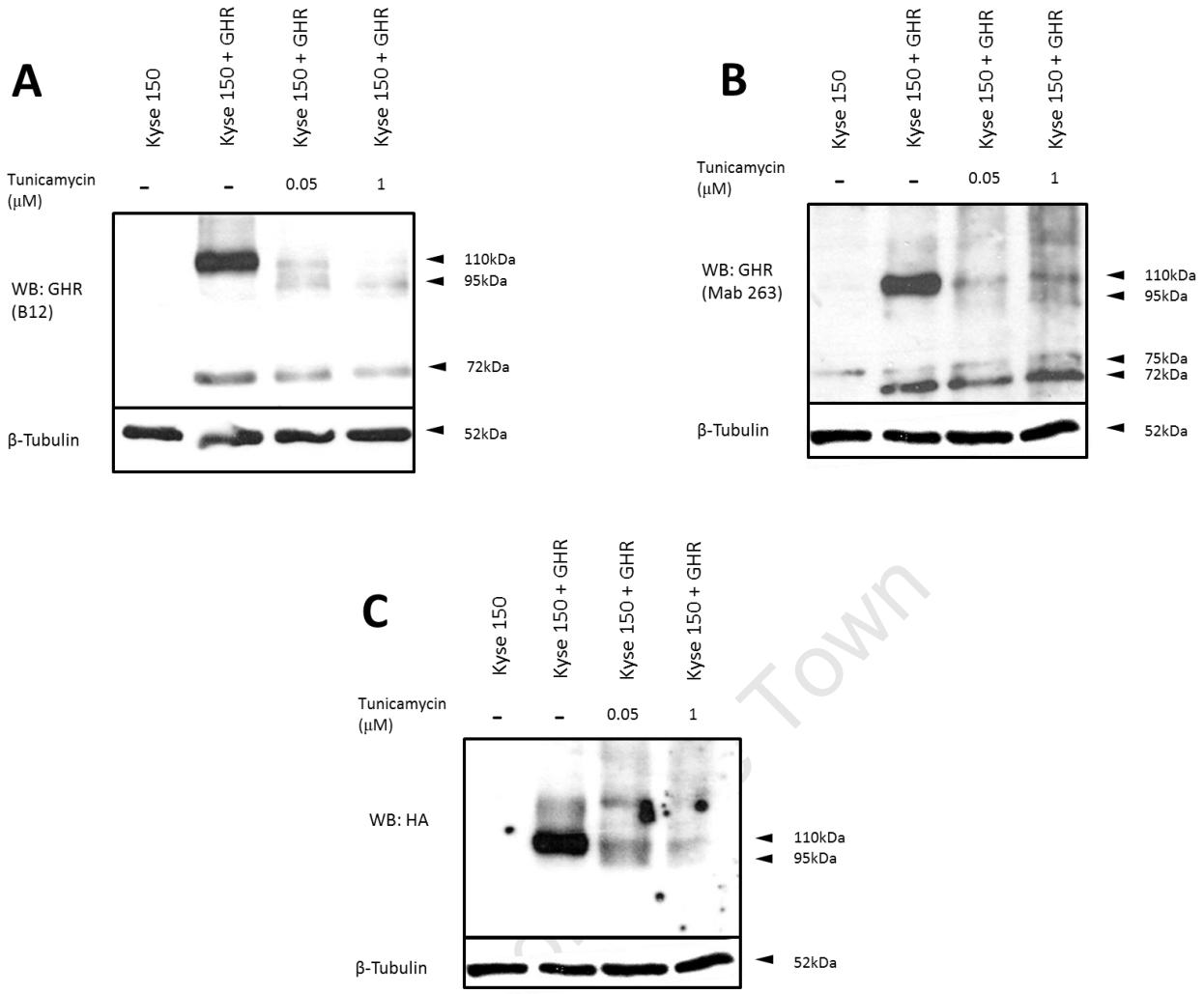


**Figure 17: Tunicamycin treatment of GHR overexpressing Kyse 150 cells.** Kyse 150 cells were induced to transiently overexpress GHR by means of transfection. The overexpressing cells were then treated with tunicamycin (0.05μM and 1μM) for 24hrs, as described in materials and methods. β-Tubulin was included as a control for protein loading. Sizes of bands are indicated. Depicted results are representative of two separate experiments.**(A)** Immunoblotting with the B12 antibody. **(B)** Immunoblotting with the Mab 263 antibody. **(C)** Immunoblotting with the anti-HA antibody.

As previously observed (Fig.13A, 14B, 16B), overexpression of GHR was associated with the expression of the 110kDa and 72kDa bands when immunoblotted with the B12 GHR antibody (Fig.17A). Treatment with increasing concentrations of tunicamycin resulted in decreased levels of the 110kDa while the 95kDa band increased in intensity (Fig.17A). The 95kDa band was also observed in untransfected cells (Kyse 150 lane) at longer exposures (not shown). There was no increase in the introduced 72kDa band. These results suggest that the 110kDa and 95kDa bands detected with the B12 antibody could possible correlate to fully-glycosylated GHR, and unglycosylated, precursor GHR respectively. The 72kDaband observed after GHR transfection and its unresponsiveness to tunicamycin treatment could indicate that the intracellular domain of GHR is unglycosylated, which is to be expected as only extracellular domains are glycosylated. The low levels of the unglycosylated, precursor form of GHR following inhibition of glycosylation compared to the high levels of glycosylated GHR when overexpressed indicate that the precursor form may have a short half-life, shorter than the 24hrs of tunicamycin treatment. However, this may be highly unlikely given since preventing glycosylation may also affect transcription and/or translation machinery.

Similar results were found when immunoblotting with the Mab 263 antibody (Fig.17B). Once again, the 110kDa band decreased with tunicamycin treatment. However, a 95kDa band, previously not seen when detecting with this antibody, increased in intensity in response to treatment with tunicamycin (Fig.17B). Given that the blot was probed with B12 and stripped prior to reprobing with the Mab 263 antibody, and given that the 72kDa band is seen when probing with Mab 263 (a band not previously seen when immunoblotting with Mab 263), incomplete stripping of the membrane prior to reprobing with Mab 263 may not be excluded. However, the 75kDa failed to respond to tunicamycin treatment, indicating that it was unlikely to be a GHR isoform as one would expect it to be glycosylated, or a precursor, unglycosylated form of GHR, as it did not increase in intensity following inhibition of glycosylation. Given that GH binds to PRLR, and that Mab 263 binds within the binding region for GH, it could be possible that the Mab 263 antibody could detect PRLR. However, the 75kDa band does not correlate to any size of known PRLR isoforms (Gadd and Clevenger, 2006), thus inferring that the 75kDa band is unlikely PRLR. These results indicated that the 75kDa band is likely to be a non-specific protein band detected by Mab 263.

In agreement with the results described above, when immunoblotting with the HA antibody, the 110kDa band observed following GHR overexpression once again decreased in intensity with increasing concentrations of tunicamycin (Fig.17C). A 95kDa band was observed following treatment with tunicamycin, a band not previously observed when immunoblotting with this antibody (Fig.16C). These results suggest that the 110kDa band observed following GHR overexpression is likely to be mature, full-glycosylated GHR, while the 95kDa band observed following treatment with tunicamycin is likely to be unglycosylated, precursor GHR. This further could imply that the 95kDa band observed in all cell lines when immunoblotting with the B12 antibody may well be a precursor form of GHR. Since protein loading was even, the different intensities of the different bands were not attributed to protein loading. It should be mentioned that the 95kDa band is still significantly larger than the predicted 72kDa size of GHR based on its amino acid sequence. This could be as a result of other possible post-translational modifications GHR is subjected to such as O-linked glycosylation or ubiquitination, or may reflect formation of protein complexes resistant to SDS-PAGE conditions, neither of which are investigated in the literature.

### 2.3.2 GHR Knockdown

To confirm whether the 95kDa band observed, specifically when immunoblotting with the B12 antibody, was related to GHR, GHR was knocked down in the Kyse 180 cell line using commercially available small interfering RNA (siRNA) (Fig.18). The siRNA binds to exon 5 of GHR mRNA, and should therefore knock down flGHR along with all other known isoforms of GHR.

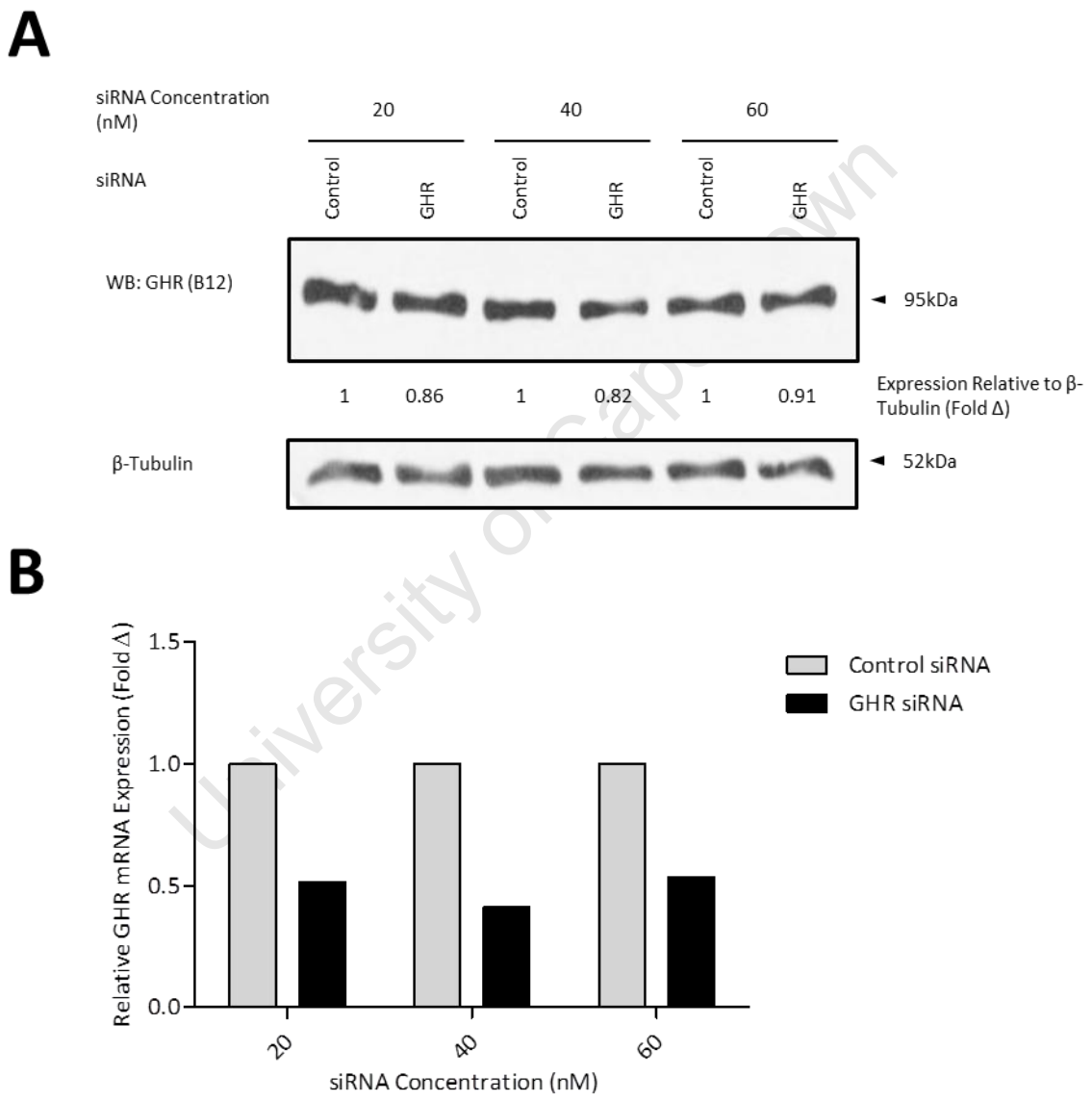


**Figure 18: GHR knockdown in characterising the 95kDa band.** Kyse 180 cells were transfected with 20nM, 40nM, and 60nM GHR and control siRNA as described in materials and methods. Protein and RNA was then isolated 24hrs post-transfection. β-Tubulin was included as a control for protein loading. Sizes of bands are indicated. Depicted results are representative of two separate experiments. **(A)** Immunoblotting of cell lysates with the B12 GHR antibody. Densitometry analysis relative to β-Tubulin is shown. **(B)** Results showing qRT-PCR for GHR after siRNA knockdown.

As evidenced by immunoblotting with the B12 antibody, transfection with increasing concentrations of GHR siRNA failed to induce a decrease in the 95kDa band that was visible to the eye (Fig.18A). However, densitometry analysis performed on the 95kDa band at the differing siRNA concentrations showed an average 15% decrease when normalising to β-Tubulin, indicating a possible link between the 95kDa band and GHR. GHR qRT-PCR analysis on mRNA isolated at the same time point as for protein isolation indicates that GHR mRNA was knocked down, with an approximately 50% decrease in total GHR mRNA transcripts levels irrespective of the concentration of siRNA used (Fig.18B). This decrease in GHR mRNA, however, did not translate in a 50% decrease in the 95kDa band. These findings suggest that while the 95kDa band may be a form of GHR, its protein knockdown does not correlate to mRNA knockdown. This could be indicative of a non-specific protein band also detected by the B12 antibody at 95kDa.Alternatively, the inefficient and short knockdown of GHR mRNA could explain the relatively insignificant decrease in the 95kDa band. It is possible that, if the 95kDa band does represent unglycosylated GHR, a greater decrease in the intensity of the band would have been observed at longer time points following transfection of siRNA, as protein lysates were harvested 24 hours after transfection. Unfortunately this could not be performed due to time constraints, but this certainly warrants further investigation.

### 2.3.3 GHR Expression following Serum Starvation

There is evidence that serum starvation may increase the expression levels of GHR protein, specifically in the T47D cell line (Xu *et al*., 2011). It is possible that expression levels of GHR are too low for the immunoblotting detection system, and serum starvation could increase levels of GHR protein expression by reducing the rate of internalisation. To identify endogenously expressed GHR, T47D cells were subjected to serum starvation, SDS-PAGE, and immunoblotting with the B12 antibody (Fig.19).

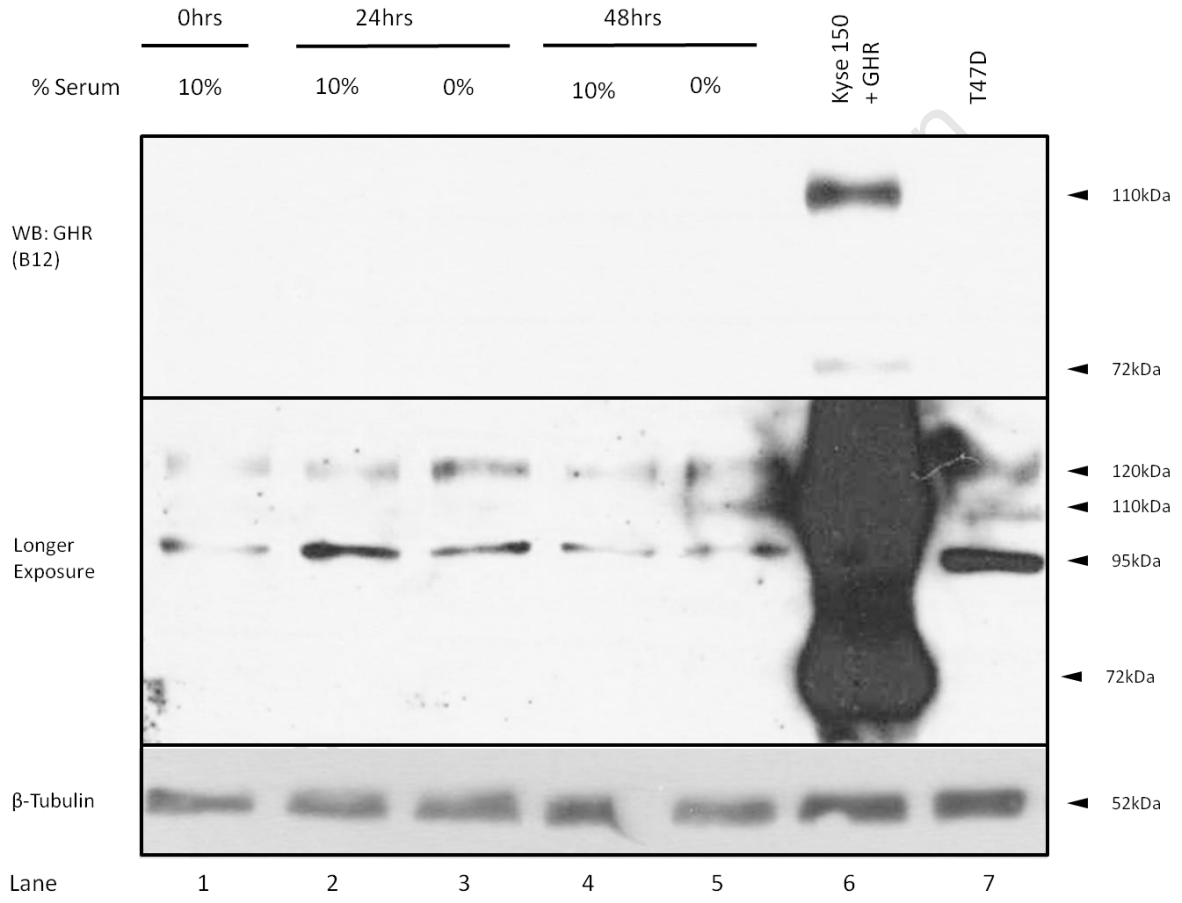


**Figure 19: GHR expression in response to serum starvation.** T47D cells were subjected to serum starvation for the times indicated, protein isolated, electrophoresed, and immunoblotted with the B12 antibody as described in materials and methods. β-Tubulin was included as a control for protein loading. Sizes of bands are indicated. Depicted results are representative of two separate experiments.GHR overexpressing Kyse 150 cells (Kyse 150+GHR) was included as a positive control.

Transfection of the GHR expression plasmid in Kyse 150 cells (Kyse 150+GHR) once again resulted in the detection of the 110kDa and 72kDa bands. Immunoblotting with the B12 antibody revealed 120kDa and 95kDa bands in T47D cells regardless of serum starvation (Lane 1, Fig.19). There was no visible increase in intensity of the 95kDa band in response to serum starvation (Fig.19). Interestingly, the 120kDa showed a slight increase in expression levels following serum starvation at 24hrs and 48hrs (Fig.19). A 110kDa seemed to be induced following 48hrs of serum-starvation, however, as evidenced by the presence of the 110kDa band in the untreated T47D lane (Lane 7), since this band had previously seen no to be expressed by T47D (Lane 1), the introduction of the band may likely be due to overflow of protein while loading the positive control (Lane 6), or signal bleed-through from the adjacent lane, rather than in response to serum starvation (Fig.19). This is supported by other serum-starving experiments which similarly failed to induce the 110kDa band (data not shown).

### 2.3.4 Immunoprecipitation of GHR

To finally deduce whether endogenous levels of GHR may be detected using these two antibodies, and whether endogenous GHR is detectable at 110kDa or 120kDa, 1mg of crude protein lysate isolated from T47D cells. As a control for the immunoprecipitation, 100µg of protein isolated from GHR-overexpressing and untransfected Kyse 150 cells, was subjected to immunoprecipitation by the Mab 263 antibody, and immunoblotted with the B12 antibody (Fig.20). Immunoprecipitation was done on 100µg of lysate rather than the 1mg used for immunoprecipitation for T47D protein in an effort to save reagents, and because it was suspected that 100µg of lysate from GHR-overexpressing cells would contain sufficient GHR to facilitate immunoprecipitation and detection.

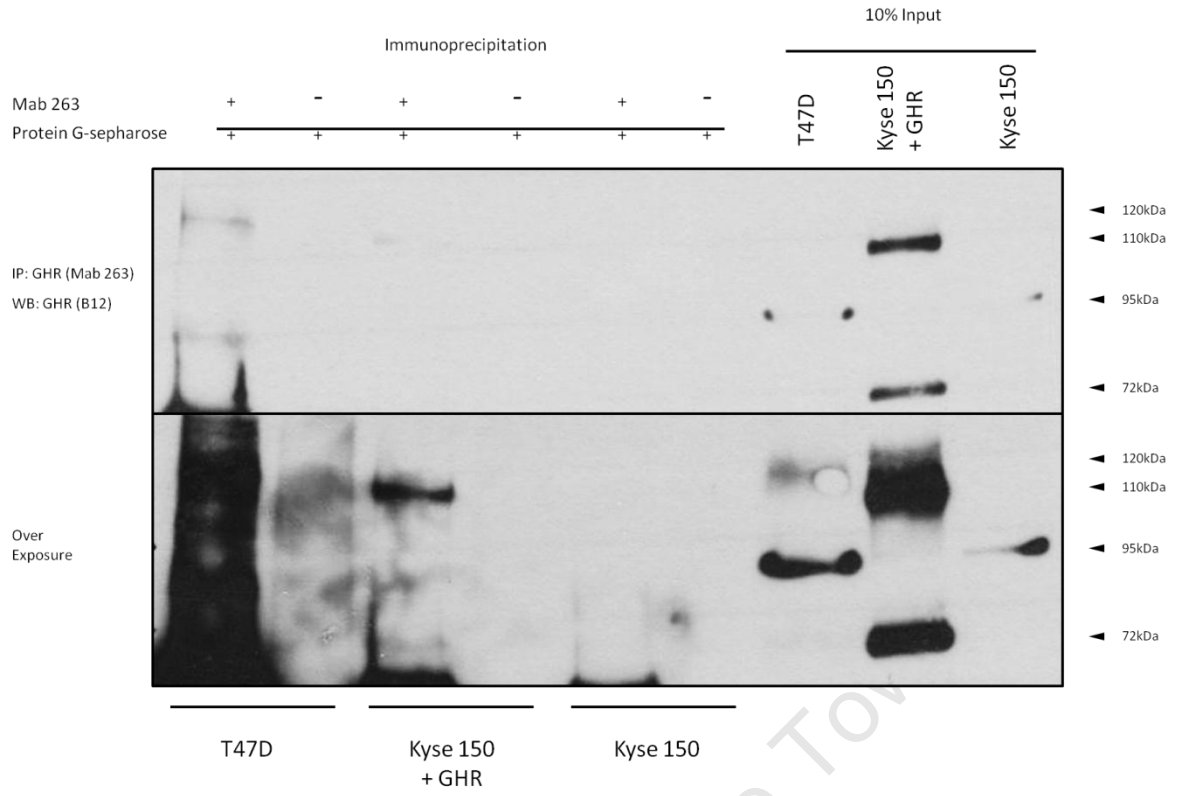


**Figure 20: Immunoprecipitation of GHR:** GHR was immunoprecipitated fromT47D, transiently overexpressing Kyse 150 (Kyse 150+GHR), and untransfected Kyse 150 cells as described in materials and methods. Immunpreciptiations were performed on 1mg T47D, 100µg Kyse 150+GHR, and 100µg Kyse 150 crude protein. The same amount of crude lysate incubated with protein beads only was also included as a control for non-specific protein binding to beads. 10% input of crude lysate used for immunoprecipitation was included.

The expected 110kDa and 72kDa bands were observed when overexpressing GHR by means of transfection with the GHR expression plasmid (Kyse 150+GHR Input lane) (Fig.20). Both bands could be immunoprecipitated (Fig.20). The 95kDa band seen in untransfected cells could not be immunoprecipitated, probably due to the low amount of starting crude protein material from which the immunoprecipitation was performed (Fig.20). The detection of the 110kDa with the B12 antibody following immunoprecipitation with the Mab 263 antibody further confirms the 110kDa band is most likely GHR in cells transfected with the GHR expression plasmid. Immunoprecipitation of the 72kDa band from lysate of GHR transfected cells is not consistent with the assumption that this band represents the ICD remnant following cleavage of the ECD, since the immune precipitating antibody (Mab263) does not recognize the intracellular domain of GHR. However, the ratio of the band intensities in the input and immunoprecipitation indicates that, of the 72kDa protein present in the starting material, only a very small fraction was present following immunoprecipitation. Thus, it is

possible that the presence of this band in the immunoprecipitate Is indicative of a low level of protein cleavage or degradation during the immunoprecipitation experiment.(Fig.17).

Immunoprecipitation of crude lysates isolated from T47D cells show two bands being successfully pull down, at 120kDa and 95kDa (Fig.20). The same 120kDa and 95kDa bands are also seen when immunoblotting the input lysate prior to immunoprecipitation (Fig.20).

Since non-specific binding to the sepharose matrix may be ruled out, as evidenced by the lack of protein bands observed when incubating crude lysate with protein G-sepharose beads only (Fig.20), these results confirm that the 110kDa band observed following GHR overexpression is GHR. Additionally, the 120kDa band seen here to be immunoprecipitated, was observed to increase in expression in response to serum starvation (Fig.19), confirming its possible identity as GHR. Interestingly, the successful immunoprecipitation of a 95kDa band, only visible when overexposing the film and immunoprecipitating from large amounts of crude protein lysates, could also be viewed as evidence for its possible identity as a form of GHR, most likely an unglycosylated, immature form of GHR.

### 2.3.5 Bioactivity Assay

Since the results suggest that the 120kDa and 110kDa bands may be GHR, phosphorylation of these two bands in response to GH stimulation was investigated (Fig.21). Protein lysates from Kyse 180 cells were also included. Since Kyse 180 cells exhibited highest expression of GHR mRNA in all OSCC cell lines tested, it was thought that it may serve as the best candidate for investigating GHR protein expression and response to GH stimulation in OSCC.

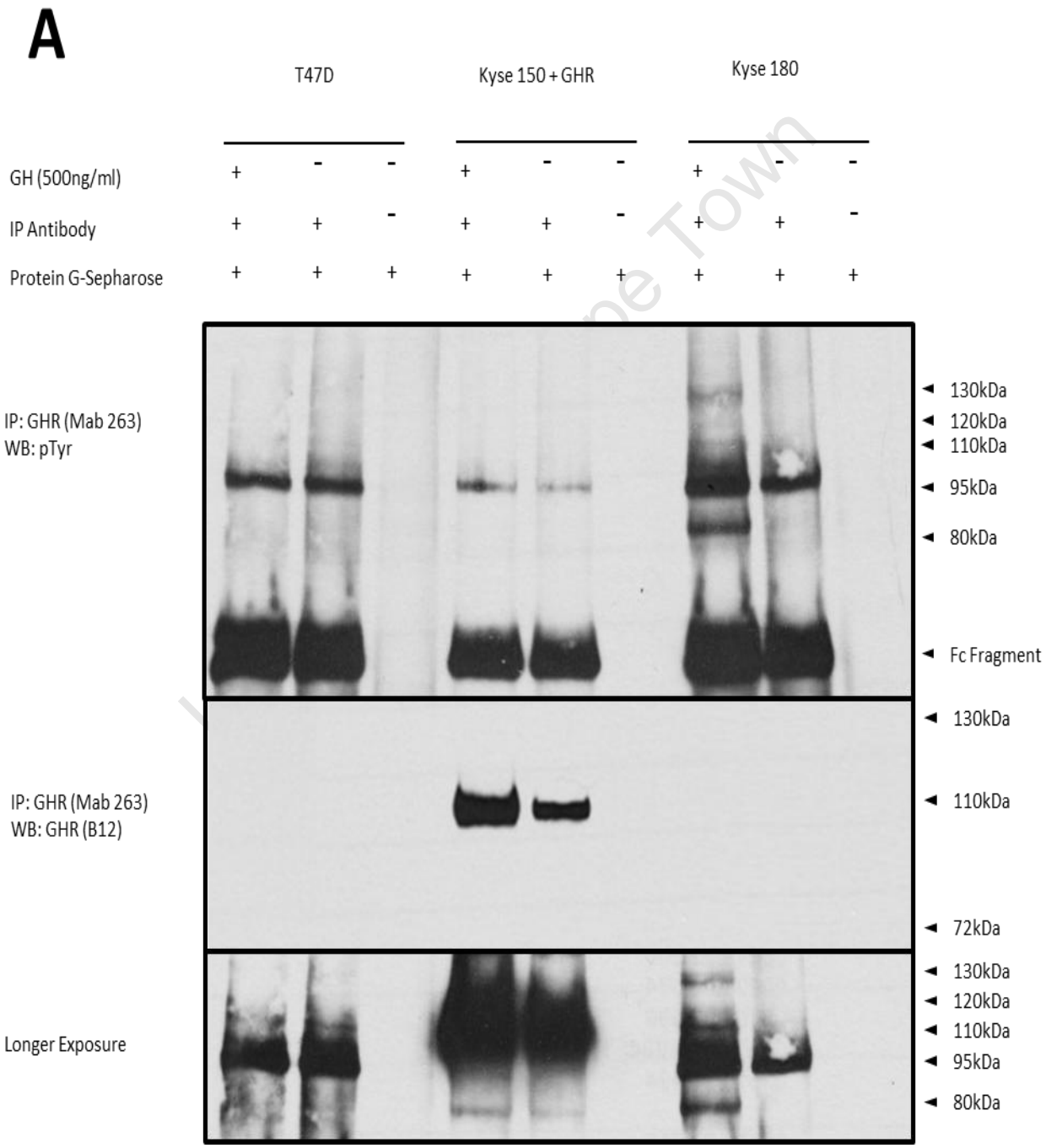

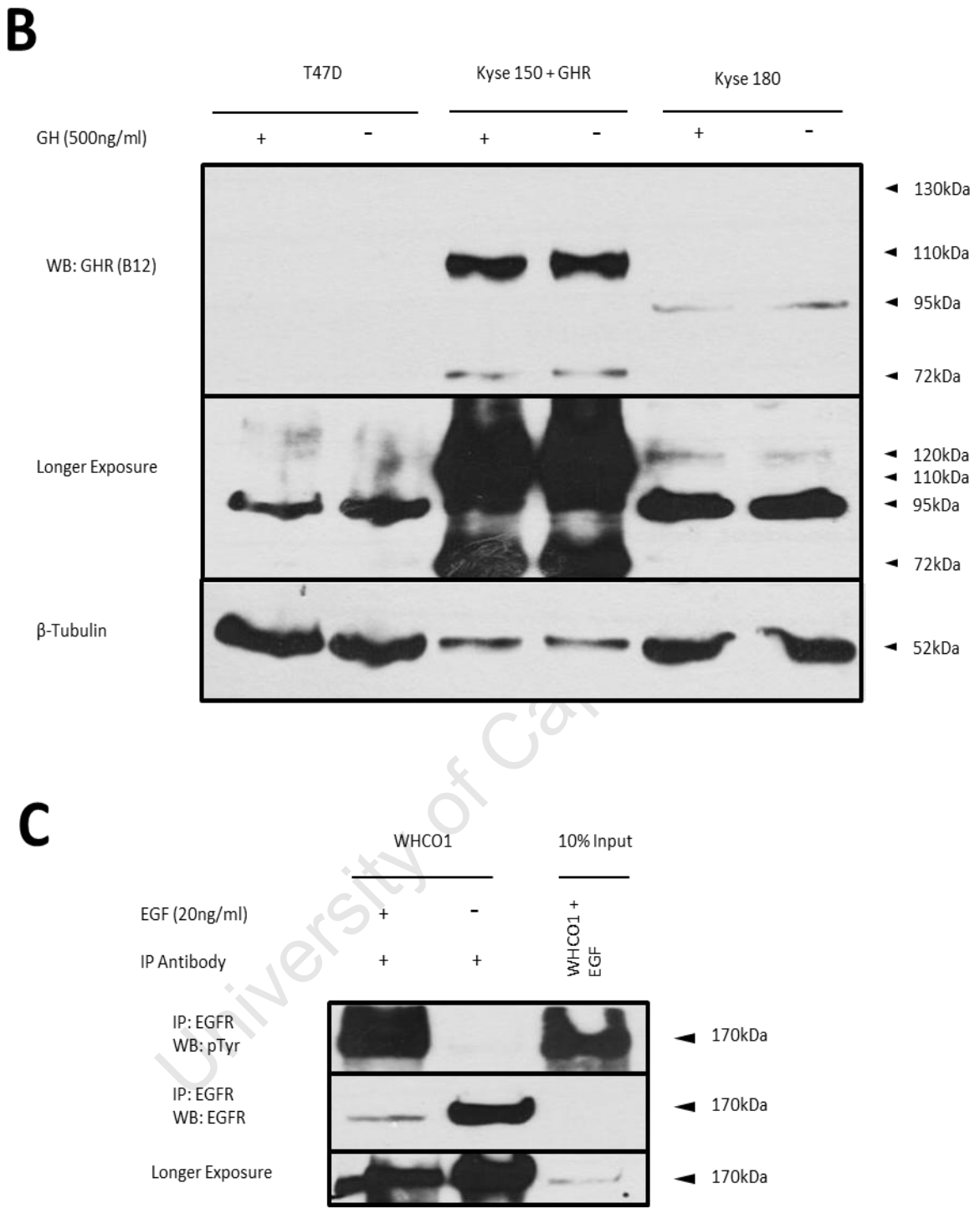




**Figure 21: Protein band phosphorylation in response to 500ng/ml GH stimulation.** Sizes of bands are indicated. Stimulation was performed when cells reached 70% confluency. **(A)** Following serum starvation for 24hrs, 1mg of T47D and Kyse 180 protein, either treated with GH or without for 5min, was immunoprecipitated with the Mab 263 antibody as described in materials and methods. The same was done on 100µg GHR overexpressing cells (Kyse 150+GHR). Following SDS-PAGE electrophoresis, the PDVF membrane was immunoblotted for phosphorylated tyrosine (pTyr) (top panel). The membrane was then stripped, and reprobed for GHR with the B12 antibody (middle and lower panels). **(B)** 10% input for the immunoprecipitations were probed with the B12 antibody. β-Tubulin was included as a control for assessing equal amounts of protein used per immunoprecipitation in the three separate cell lines. **(C)** Protein lysates isolated from WHCO1 treated with or without EGF (20ng/ml) was used as a control for testing the sensitivity of the phosphorylated tyrosine antibody. 300µg of protein was immunoprecipitated using an EGFR antibody, and phosphorylated tyrosine was detected (top panel). The PDVF membrane was then stripped and reprobed for total EGFR levels (middle and lower panels).

Immunoblotting for phosphorylated tyrosines following GHR immunoprecipitation revealed several bands. Firstly, a 95kDa band was immunoprecipitated in all cells tested (Fig.21A, top panel). Faint 110kDa and 120kDa bands were also immunoprecipitated from T47D and Kyse 180 cells tested (Fig.21A, top panel). In addition, two other bands of 130kDa and 80kDa were immunoprecipitated from Kyse 180 cells (Fig.21A, top panel).The 130kDa band could possibly correspond to phosphorylated JAK2, consistent with previous reports (Yin *et al*., 1994), while the 80kDa band may correspond to one of the many transcription factors, kinases, and adaptor proteins known to associate with GHR upon activation by GH respectively. Ideally, to confirm the 130kDa band as phosphorylated Jak2, the membrane should have been probed with a Jak2 antibody, however, since the experiment was done late on in the project, this was unfeasible. None of the bands immunoprecipitated from T47D cells exhibited increased phosphorylation in response to GH treatment (Fig.21A, top panel), whereas the 80kDa, 120kDa, and 130kDa showed increased phosphorylation in response to GH treatment in Kyse 180 cells (Fig.21A, top panel). GHR overexpressing cells (Kyse 150+GHR) only revealed a 95kDa band when immunoblotting for phosphorylated tyrosine, which exhibited no increase in phosphorylation in response to GH treatment. Immunoblotting the same membrane for GHR with the B12 antibody following stripping revealed the same bands in T47D and Kyse 180 when overexposing the film (Fig.21A, lower panel). GHR overexpressing Kyse 150 cells exhibited 110kDa and 80kDa bands when immunoblotting with the B12 antibody (Fig.21A, middle and lower panel).

Immunoblotting 10% inputs used for immunoprecipitations for GHR with the B12 antibody revealed 95kDa bands being detected in all three cell lines (as previously seen in Fig.14B), with the addition of 120kDa bands being observed in T47D and Kyse 180 cells, with the former showing smudging of the 120kDa band (Fig.21B, middle panel). GHR overexpressing cells also exhibited the expected 110kDa and 72kDa bands (Fig.21B, top panel). β-Tubulin immunodetection was then performed on the same PVDF membrane following stripping, and revealed even protein loading between samples of the same cell line (Fig.21B, lower panel).

Since our laboratory has previously observed the phosphorylation of epidermal growth factor receptor (EGFR) in response to epidermal growth factor (EGF) stimulation in WHCO1 cells (unpublished data), protein isolated from WHCO1 cells treated with or without EGF was also immunoprecipitated to test for the activity of the phosphotyrosine antibody (Fig.21C). Epidermal growth factor receptor (EGFR) was immunoprecipitated and tested for phosphorylation in response to EGF stimulation using the same phosphotyrosine antibody as above. The same blot was then stripped and reprobed for total EGFR (Fig.21C, middle and lower panels). A 170kDa band corresponding to EGFR was immunoprecipitated, and showed a high level of phosphorylation of tyrosine residues in response to EGF stimulation (Fig.21C, top panel), indicating that the system used for detecting phosphorylated tyrosine was functional. Difference in level of total EGFR protein being immunoprecipitated between the sample treated with EGF and the sample treated without EGF could be as a result of receptor internalisation and degradation in response to EGF binding rather than uneven amounts of protein used for the immunoprecipitation (Fig.21C, middle and lower panel).

These findings suggest that in Kyse 180, since the 130kDa, 120kDa, 110kDa, and 80kDa exhibited increased phosphorylation in response to GH stimulation, and since all these bands were able to be detected when immunoblotting with the B12 antibody, that these four bands may be variants of GHR and/or proteins associated with GHR in the presence of GH (Fig.21A). Given that endogenous GHR was possibly detected at 120kDa, similar levels of the band was not present in the samples not treated with GH compared to GH-treated samples when detecting GHR (Fig.21A, lower panel).It is possible that unequal amounts of protein were immunoprecipitated, but that seems unlikely considering that β-Tubulin levels in 10% protein input indicated that starting crude protein material was for within these two samples (Fig.21B, lower panel), however, as evidenced by the slight decrease in the Fc fragment between the two sample, amounts of immunoprecipitating antibody used may not be equal, with the sample being treated without GH receiving less Mab 263 than the sample treated with GH (Fig.21A, top panel). Since the same protein bands were seen when immunoblotting for phosphorylated tyrosine residues and GHR, it could also be argued that stripping of the membrane failed to effectively strip previously bound antibodies. It should be noted that given that the experiment was conducted late on in the project, the experiment was unable to be reproduced. Despite the uncertainty regarding the bands immunoprecipitated for Kyse 180 cells, the results above clearly indicate that the 110kDa

band seen following GHR overexpression does not respond to GH treatment, with none of the bands immunoprecipitated in T47D cells also showing no response to GH treatment.

The lack of tyrosine phosphorylation in response to GH stimulation of T47D cells was particularly concerning, since T47D cells have been reported to respond to the same concentration of GH (500ng/ml) by phosphorylating STAT5, and this response was shown to be largely mediated by GHR, and to a lesser extent by PRLR, thus inferring the presence of functional GHR proteins within T47D cells (Xu *et al*., 2011). The above results would also be observed if the GH used in the treatment was ineffective. To test for GH activity, the same crude protein lysates used above underwent immunoblotting for phosphorylation of ERK1/2, a known downstream target of GH signalling (Fig.22).Our laboratory has previously observed that treatment with EGF induces ERK1/2 phosphorylation (pERK1/2) in WHCO1 cells (unpublished data), and this was therefore included as a positive control for the pERK1/2 antibody (Fig.22B).

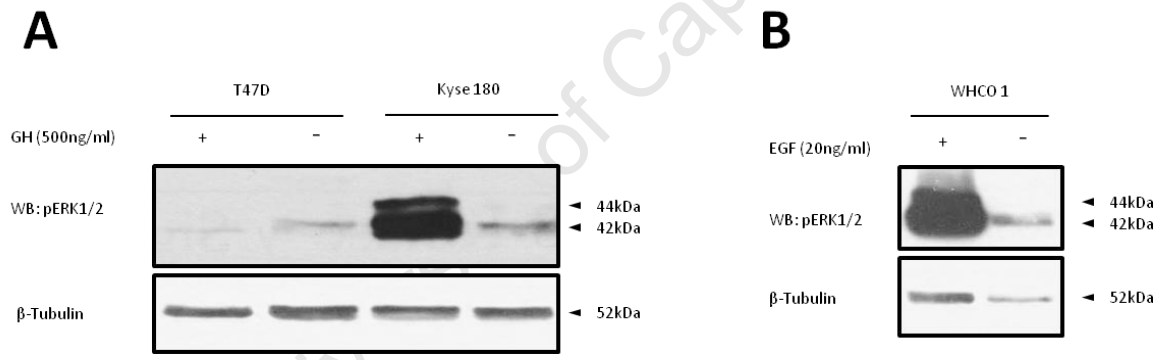


**Figure 22: ERK1/2 phosphorylation in response to ligand.** 30µg of crude protein lysates used in Fig.21 underwent immunoblotting for phosphorylated ERK1/2 (pERK1/2) as described in materials and methods. β-Tubulin was included as a control for protein loading. Sizes of bands are indicated. Results are representative of two separate experiments. Depicted results are representative of two separate experiments. **(A)** pERK1/2 in response to GH treatment (500ng/ml) for 5min in T47D and Kyse 180 cells. **(B)** pERK1/2 response to EGF treatment (20ng/ml) for 5min in WHCO1 cells.

Following immunoblotting for phosphorylated ERK1/2, two bands were observed at 44kDa and 42kDa in size, corresponding to ERK1 and ERK2 respectively (Fig.22). In Kyse 180 cells, GH treatment induced significant phosphorylation of ERK1/2, indicating that GH was functional (Fig.22A), either acting through GHR, PRLR, or both to induce this response. Oddly though, GH failed to induce any phosphorylation of ERK1/2 above that of basal levels in T47D cells (Fig.22A). This was unexpected since T47D cells have been demonstrated to express functional GHR and PRLR protein, both of which respond to GH treatment by activating STAT5 (Xu *et al*., 2011). Given the unexpected non-responsiveness of T47D cells to endogenous GH, cells lines would have to be verified by DNA fingerprinting or otherwise. When treating WHCO1 cells with EGF, a significant pERK1/2 response was observed (Fig.22B), indicating that the pERK1/2 antibody and the system of detection was functional.

Since immunodetection for β-Tubulin revealed even protein loading, these results suggest that GH was functional, and did induce the phosphorylation of ERK1/2 in Kyse 180 cells. The lack of induction in T47D cells, a cell line previously shown to express functional GHR and PRLR proteins, indicated that in our T47D cells, GHR and PRLR may be dysfunctional. Furthermore, the possibility exists that the T47D cells in our laboratory could be contaminated with another cell line. Additionally, differences in culture conditions and/or experimental conditions could also account for differences between results observed here and those previously published.

## CHAPTER THREE

## EFFECT OF GHR KNOCKDOWN ON CANCER CELL BIOLOGY

### 3.1 Effect of GHR Knockdown on Proliferation and $IC_{50}$ in Kyse 180

As stated before, GH has been shown to exert tumourigenic effects in a number of studies using various*in vitro* and *in vivo* models. Additionally, it was found that the effects of GH were largely mediated by GHR in the few studies that investigated possible mechanisms whereby GH may exert its tumourigenic effects. GH mRNA has been shown to be expressed in the majority of OSCC cell lines tested, indicating a possible role for the GH axis in tumourigenesis in these cell lines. In keeping with the literature, since GHR mRNA expression has also been shown, it is possible that the potential tumourigenic effectsof GH may be directly mediated by GHR. To investigate this GHR was knocked down in Kyse 180 cells, a cell line shown to express GH and GHR mRNA, by means of siRNA transfection. Proliferation (Fig.23) and response to chemotherapeutic agents (Fig.24) following GHR knockdown were measured. This served to investigate the role of GHR in regulating proliferation and response of Kyse 180 cells to chemotherapeutic drugs.

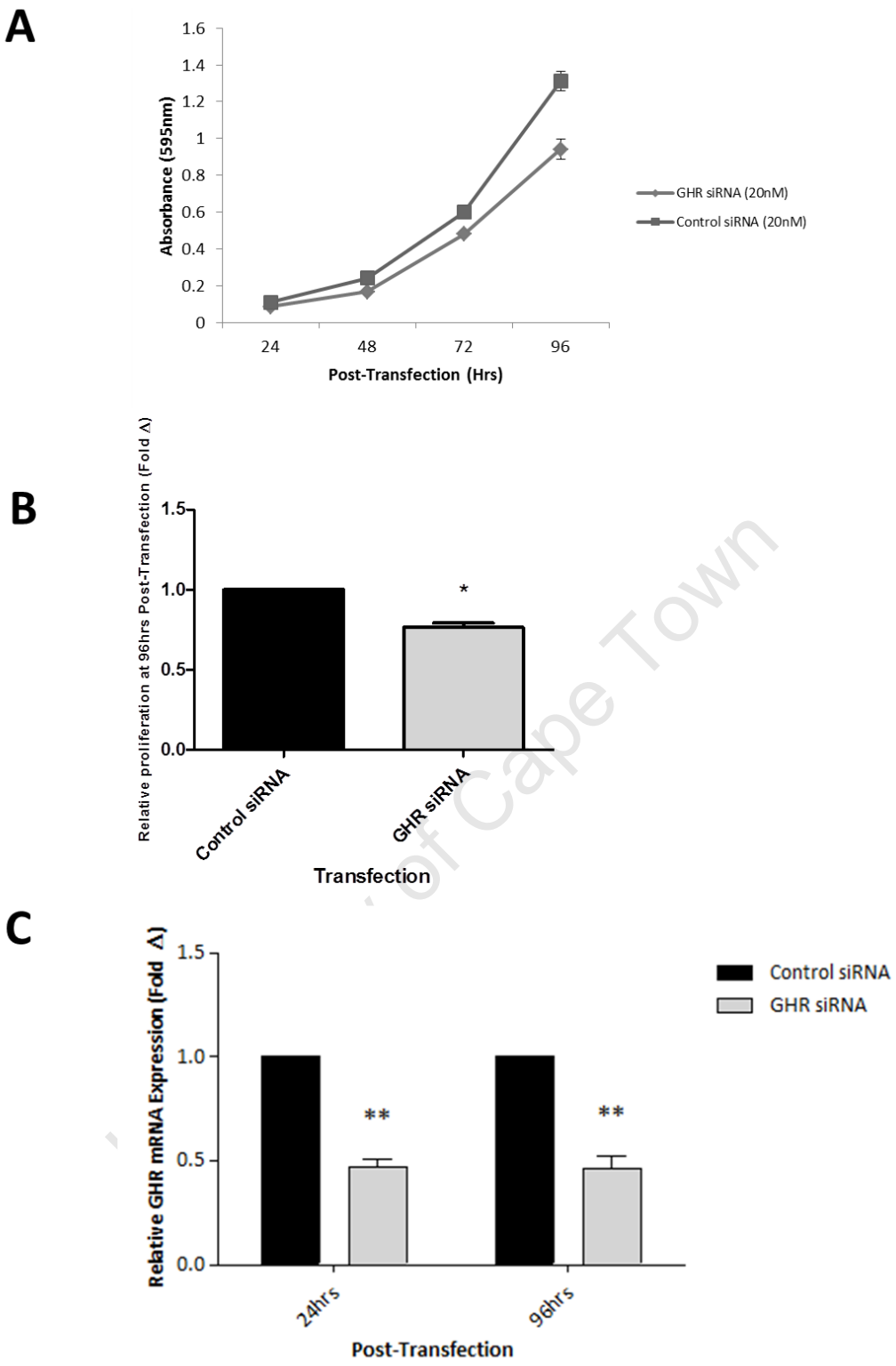


**Figure 23: Proliferation in response to GHR knockdown in Kyse 180 cells.** Kyse 180 cells underwent transfection with 20nM siRNA as described in materials and methods. A proliferation assay was used to measure cell proliferation and RNA was isolated and analysed for GHR expression by means of GHR PCR following cDNA conversion, as described in materials and methods. **(A)** Proliferation of cells transfected with either GHR or controls siRNA. The results are representative of three independent experiments. **(B)** Difference in proliferation at 96hrs post-transfection (n=3, *=p<0.05). Data was normalised to the initial plating at the start of the proliferation assays, and to control siRNA knockdown within the three separate experiments. **(C)** Quantification of GHR mRNA levels relative to control siRNA at 24hrs and 96hrs post-transfection. Pooled results of three separate experiments used in (B) are shown (n=3, **=p<0.005).

Following GHR knockdown, there was a 18% decrease in proliferation at 96hrs post-transfection compared to control siRNA transfected cells (Fig.23A&B). This decrease has been shown to be statistically significant (Fig.23B). The decrease in proliferation was accompanied by a statistically significant 50% decrease in GHR mRNA at 24hrs and 96hrs (Fig23.C). Sensitivity to chemotherapeutic agents in response to GHR knockdown was also measured. This was done by determining the $IC_{50}$ values, the concentration needed to inhibit proliferation by 50%, of the drugs cisplatin and doxorubicin (Fig.23). Furthermore, treatment with a combination of different GHR siRNA sequences or transfection using a lentiviral system could have yielded a better knockdown.

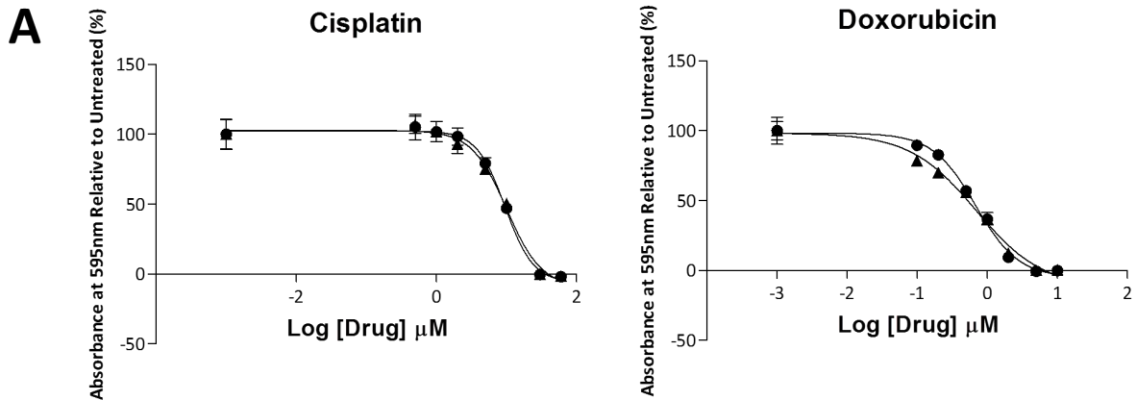


**B**

| | Cisplatin | | Doxorubicin | |
|---|---|---|---|---|
| **Transfection** | **IC50 (μM)** | **95% CI (μM)** | **IC50 (μM)** | **95% CI (μM)** |
| **Control siRNA** | 10.32 | 8.91-11.96 | 0.71 | 0.58-0.87 |
| **GHR siRNA** | 9.61 | 8.74-10.56 | 0.66 | 0.58-0.75 |

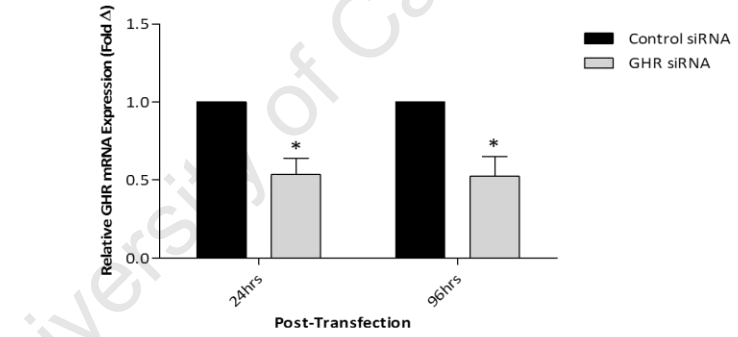




**Figure 24: Effect of GHR knockdown on response to cisplatin and doxorubicin in Kyse 180 cells.** Kyse 180 cells were transfected with siRNA, and treated with a range of concentrations of cisplatin and doxorubicin, as described in materials and methods. RNA was isolated 24hrs post-transfection, and at the end time-point of the drug treatment assays (96hrs post-transfection) as described in materials and methods. **(A)** Pooled dose response curves for cisplatin and doxorubicin following GHR (•) and control (▲) knockdown (n=3). **(B)** Pooled quantification of $IC_{50}$ values for cisplatin and doxorubicin following GHR and control knockdown. 95% confidence intervals (95% CI) are also shown (n=3). **(C)** Quantification and normalisation of GHR mRNA to control knockdown at 24hrs and 96hrs post-transfection for the three separate experiments used in (A) and (B) (n=3, $p<0.05$).

Knockdown of GHR failed to induce a visible shift in $IC_{50}$ graphs for both cisplatin and doxorubicin, indicating that there was no difference in sensitivity to chemotherapy following GHR knockdown compared to control knockdown(Fig.24A). This was further confirmed by quantified $IC_{50}$ values. Although a 7% decrease in $IC_{50}$was observed for both cisplatin and doxorubicin following GHR knockdown, this difference was not statistically significant as 95% confidence intervals are observed to overlap for both GHR and control knockdown (Fig.24B). These results were accompanied by a statistically significant 50% knockdown of GHR mRNA (Fig.24C).

These results suggest that GHR plays a small role in proliferation, while not affecting the response of cells to cisplatin and doxorubicin. The decrease in proliferation was small but significant, with only a 18% decrease in proliferation observed following GHR knockdown, at 96hrs post-transfection. The lack of decrease in $IC_{50}$ values following GHR knockdown seems to be contrary to the literature that shows a protective function of autocrine GH, one that is mediated by GHR (Minoia *et al*., 2012; Zatelli *et al*., 2009). This indicates that while there may be a role of autocrine GH in Kyse 180 cells, as evidenced by the endogenous expression of GH mRNA, these cells seem to be relatively uninfluenced by the disruption of autocrine GH signalling by knocking down GHR. Finally, since these results were observed with only a 50% knockdown of GHR mRNA, it may be argued that the small effect observed on proliferation is a result of the inefficient knockdown of GHR, thereby maintaining the possibility that these cells may be dependent on the intact signalling of autocrine GH through GHR. To further validate the effects of GHR on proliferation in OSCC, GHR knockdown in other OSCC cell lines was investigated.

Addition of exogenous GH to cells that underwent GHR knockdown could have exaggerated the proliferative effect and shown a potential chemoprotective effect of GH, however, when treating cells with exogenous GH, an increase in proliferation was not seen in Kyse 180 cells (data not shown). These results indicate that in Kyse 180 cells, autocrine GH is sufficient to saturate GHR signalling, so that addition of additional exogenous GH does not result in increased efficacy. Although this was only demonstrated in proliferation assays, we speculate that a similar result would be observed in.

### 3.2 Effect of GHR Knockdown on Proliferation and $IC_{50}$ in Kyse 30

GHR knockdown effects on proliferation and $IC_{50}$ concentrations of cisplatin and doxorubicin was also performed on the Kyse 30 cell line (Fig.25 and Fig.26 respectively). The Kyse 30 cell line was selected to elucidate the role of the d3GHR isoform on proliferation and response to chemotherapeutic drugs.

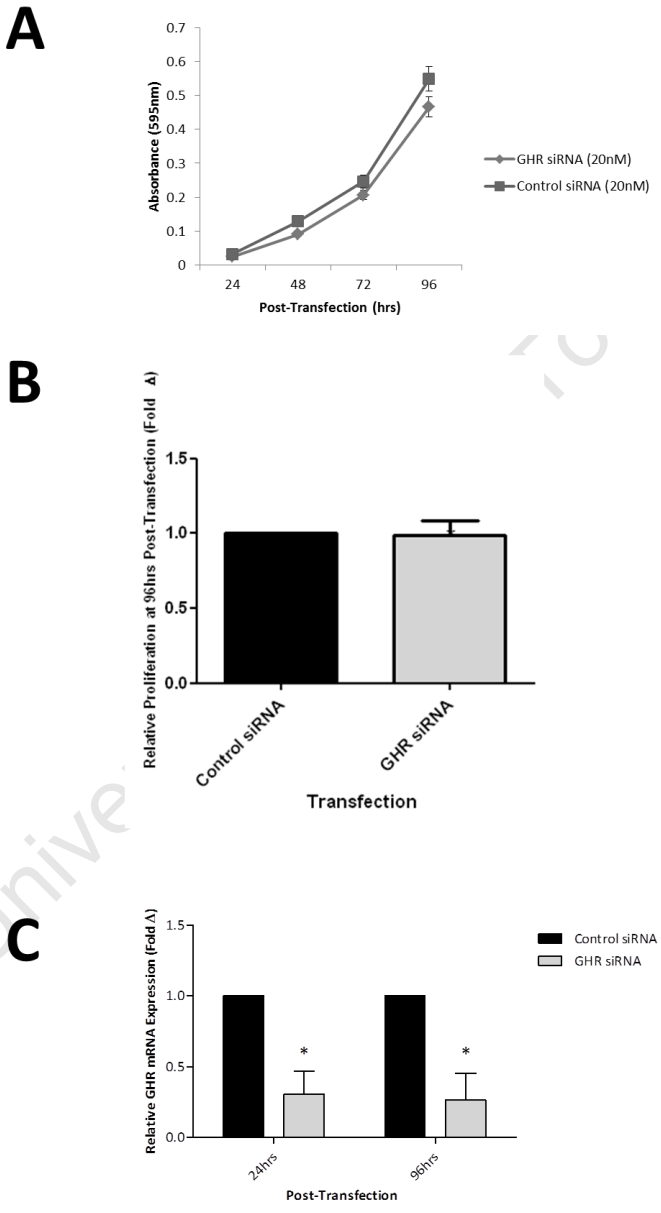


**Figure 25: Proliferation in response to GHR knockdown in Kyse 30 cells.** Kyse 30 cells underwent transfection with 20nM siRNA as described in materials and methods. A proliferation assay was used to measure cell proliferation and RNA was isolated and analysed for GHR expression by means of GHR PCR following cDNA conversion, as described in materials and methods. **(A)** Proliferation of cells transfected with either GHR or controls siRNA. The results are representative of three independent experiments. **(B)** Difference in proliferation at 96hrs post-transfection (n=3). Data was normalised to the initial plating at the start of the proliferation assays, and to control siRNA knockdown within the three separate experiments. **(C)** Quantification of GHR mRNA levels relative to control siRNA at 24hrs and 96hrs post-transfection. Pooled results of three separate experiments used in (B) are shown (n=3, *=p<0.05).

Kyse 30 cells have previously been shown to express only d3GHR mRNA (Fig.12). GHR knockdown inhibited proliferation to a small extent (Fig.25A). However, the decrease in proliferation was not deemed significant when normalised to initial plating densities over the three separate experiments conducted (Fig.25B), despite achieving a 70% knockdown of GHR mRNA in these three experiments (Fig.25C). Concurrently to the proliferation assays, drug treatments assays for cisplatin and doxorubicin were also performed (Fig.26).

**A**

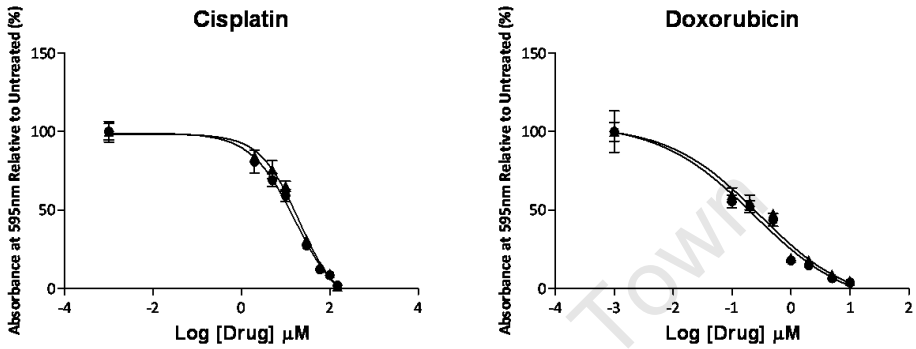


**B**

| | Cisplatin | | Doxorubicin | |
|---|---|---|---|---|
| Transfection | IC50 (µM) | 95% CI (µM) | IC50 (µM) | 95% CI (µM) |
| Control siRNA | 19.54 | 16.86-22.64 | 0.29 | 0.17-0.48 |
| GHR siRNA | 17.36 | 13.55-22.24 | 0.26 | 0.17-0.39 |

**C**

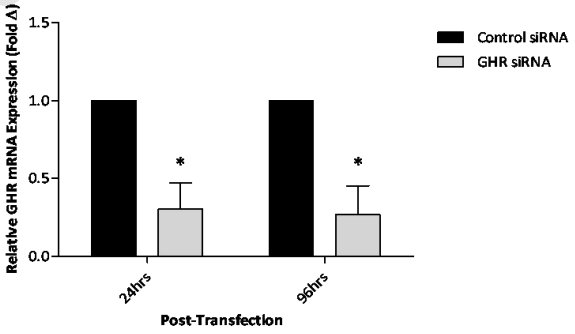




**Figure 26: Effect of GHR knockdown on response to cisplatin and doxorubicin in Kyse 30 cells.** Kyse 30 cells were transfected with siRNA, and treated with a range of concentrations of cisplatin and doxorubicin, as described in materials and methods. RNA was isolated 24hrs post-transfection, and at the end time-point of the drug treatment assays (96hrs post-transfection) as described in materials and methods. **(A)** Pooled dose response curves for cisplatin and doxorubicin following GHR (•) and control (▲) knockdown (n=3). **(B)** Pooled quantification of $IC_{50}$ values for cisplatin and doxorubicin following GHR and control knockdown. 95% confidence intervals (95% CI) are also shown (n=3). **(C)** Quantification and normalisation of GHR mRNA to control knockdown at 24hrs and 96hrs post-transfection for the three separate experiments used in (A) and (B) (n=3, $p<0.05$).

There was no shift in $IC_{50}$ curves for both cisplatin and doxorubicin, indicating no change in $IC_{50}$values following GHR knockdown compared to control knockdown (Fig.26A). This was confirmed by the overlapping 95% CI intervals for both drugs and overlapping $IC_{50}$ values for doxorubicin, despite observing a 12% decrease in $IC_{50}$ concentration for cisplatin following GHR knockdown (Fig.26B). These results were observed despite a 70% decrease in GHR mRNA levels (Fig.26C), as calculated following qRT-PCR with the flGHR gene-specific primers that also bind d3GHR cDNA. Since K30 has been shown to express d3GHR exclusively, the 70% knockdown seen following flGHR qRT-PCR thus correlates to a 70% decrease in d3GHR mRNA. The d3GHR primers could not be used for qRT-PCR since it is able to amplify and distinguish two products, flGHR and d3GHR.

Since knocking down d3GHR failed to induce any change in proliferation or $IC_{50}$ concentrations of both cisplatin and doxorubicin, it can be inferred that Kyse 30 cells do not rely on d3GHR for proliferation, and knockdown does not potentiate the effects of cisplatin and doxorubicin. It can be further inferred that, since these experiments were conducted in 10% foetal bovine serum and is therefore likely to be exposed to levels of GH, the GH/IGF1 axis possibly does not play a role in proliferation or chemoresistance in the Kyse 30 cell line. Possible explanations could include the translation of dysfunctional d3GHR or lack of mRNA translation. Additionally, the relatively inefficient knockdown of GHR may not be ignored it is possible that a change in proliferation and/or chemosensitivity would have been seen if a higher degree of knockdown had been achieved.

### 3.3 Effect of GHR Knockdown on Proliferation and $IC_{50}$ in Kyse 450

GHR knockdown effects on proliferation and $IC_{50}$ concentrations of cisplatin and doxorubicin was also performed on the Kyse 450 cell line (Fig.27 and Fig.28 respectively), a cell line similar to Kyse 180 in that Kyse 450 cells likely express flGHR mRNA predominantly, with no expression of d3GHR (Fig.12). However, as with Kyse 180, possible 1-279 and 1-277GHR isoforms within Kyse 450 cells may not be ignored.

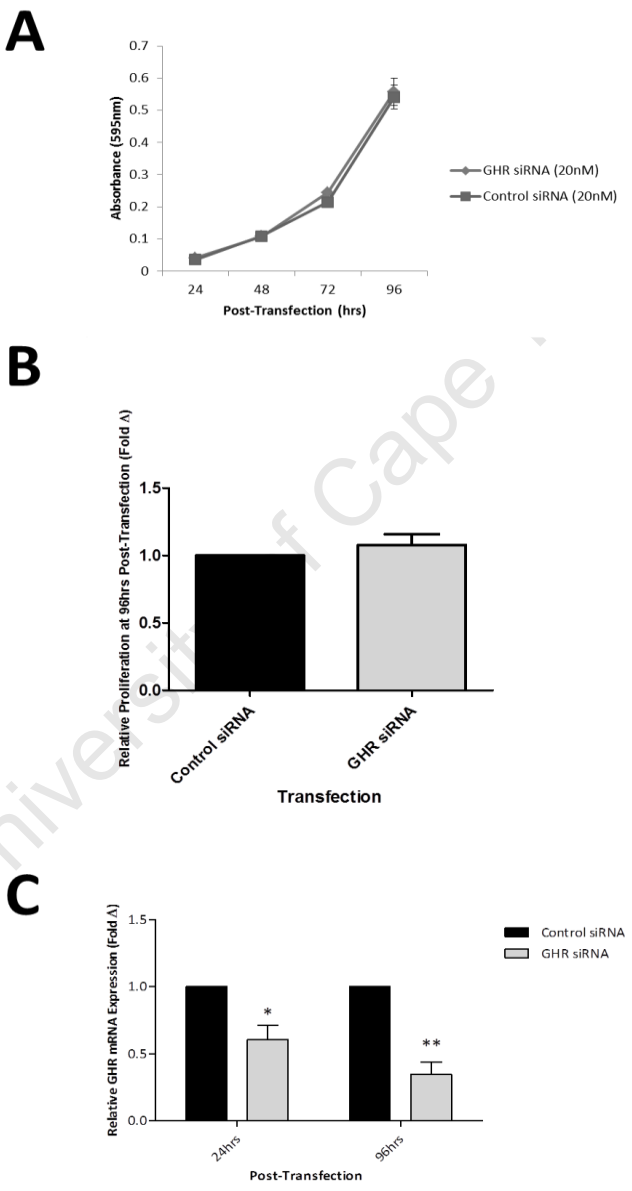


**Figure 27: Proliferation in response to GHR knockdown in Kyse 450 cells.** Kyse 450 cells underwent transfection with 20nM siRNA as described in materials and methods. A proliferation assay was used to measure cell proliferation and RNA was isolated and analysed for GHR expression by means of GHR PCR following cDNA conversion, as described in materials and methods. **(A)** Proliferation of cells transfected with either GHR or controls siRNA. The results are representative of three independent experiments. **(B)** Difference in proliferation at 96hrs post-transfection (n=3). Data was normalised to the initial plating at the start of the proliferation assays, and to control siRNA knockdown within the three separate experiments. **(C)** Quantification of GHR mRNA levels relative to control siRNA at 24hrs and 96hrs post-transfection. Pooled results of three separate experiments used in (B) are shown (n=3, *=p<0.05, **=p<0.005).

Unlike in the case of Kyse 180 cells, knockdown of GHR mRNA failed to induce a change in proliferation (Fig.27A&B). Responses to doxorubicin and cisplatin were also conduced concurrently to the proliferation assays (Fig.28).

**A**

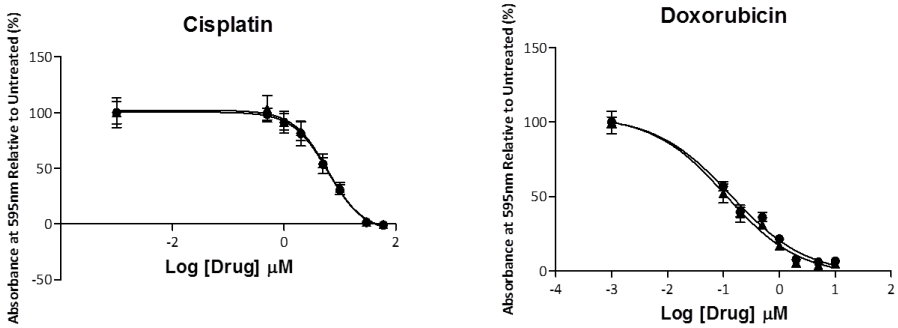


**B**

| | Cisplatin | | Doxorubicin | |
|---|---|---|---|---|
| **Transfection** | **IC50 (μM)** | **95% CI (μM)** | **IC50 (μM)** | **95% CI (μM)** |
| **Control siRNA** | 6.57 | 5.67-7.61 | 0.12 | 0.09-0.16 |
| **GHR siRNA** | 6.14 | 5.20-7.26 | 0.15 | 0.12-0.20 |

**C**

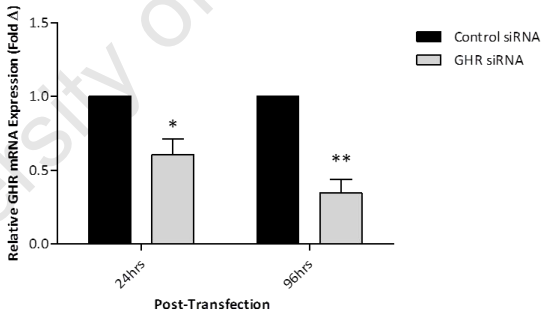




**Figure 28: Effect of GHR knockdown on response to cisplatin and doxorubicin in Kyse 450 cells.** Kyse 450 cells were transfected with siRNA, and treated with a range of concentrations of cisplatin and doxorubicin, as described in materials and methods. RNA was isolated 24hrs post-transfection, and at the end time-point of the drug treatment assays (96hrs post-transfection) as described in materials and methods. **(A)** Pooled dose response curves for cisplatin and doxorubicin following GHR (•) and control ( ▲) knockdown (n=3). **(B)** Pooled quantification of $IC_{50}$ values for cisplatin and doxorubicin following GHR and control knockdown. 95% confidence intervals (95% CI) are also shown (n=3). **(C)** Quantification and normalisation of GHR mRNA to control knockdown at 24hrs and 96hrs post-transfection for the three separate experiments used in (A) and (B) (n=3, *=p<0.05, **=p<0.005).

Once again, knockdown of GHR failed to induce a change in $IC_{50}$ concentrations of both cisplatin and doxorubicin, as evidenced by the lack of shift in $IC_{50}$ curves (Fig 28A), and overlapping of 95% CI for both drugs (Fig.28B), regardless of achieving an average knockdown of 60% during the course of the three separate drug treatment assays (Fig28C).

These results suggest, as in the case of Kyse 30 cells, that GHR is not important for the proliferation of Kyse 450 cells, and knockdown does not potentiate the effects of cisplatin and doxorubicin. As in the case of Kyse 30 cells, it may also be further inferred that, since these experiments were conducted in 10% foetal bovine serum and is therefore likely to be exposed to levels of GH, the GH/IGF1 axis possibly does not play a role in the Kyse 450 cell line. Additionally, the translation of dysfunctional GHR may not be disproved, therefore explaining the above results. Also, despite Kyse 450 cells expressing GHR mRNA, this necessarily does not translate to the translation into protein, therefore also explaining the above results.

### 3.4 ERK1/2 Phosphorylation following GHR Knockdown

To test whether GHR is functional within the Kyse 30, Kyse 180, and Kyse 450 cell lines, ERK1/2 phosphorylation was investigated following GHR knockdown (Fig.29).

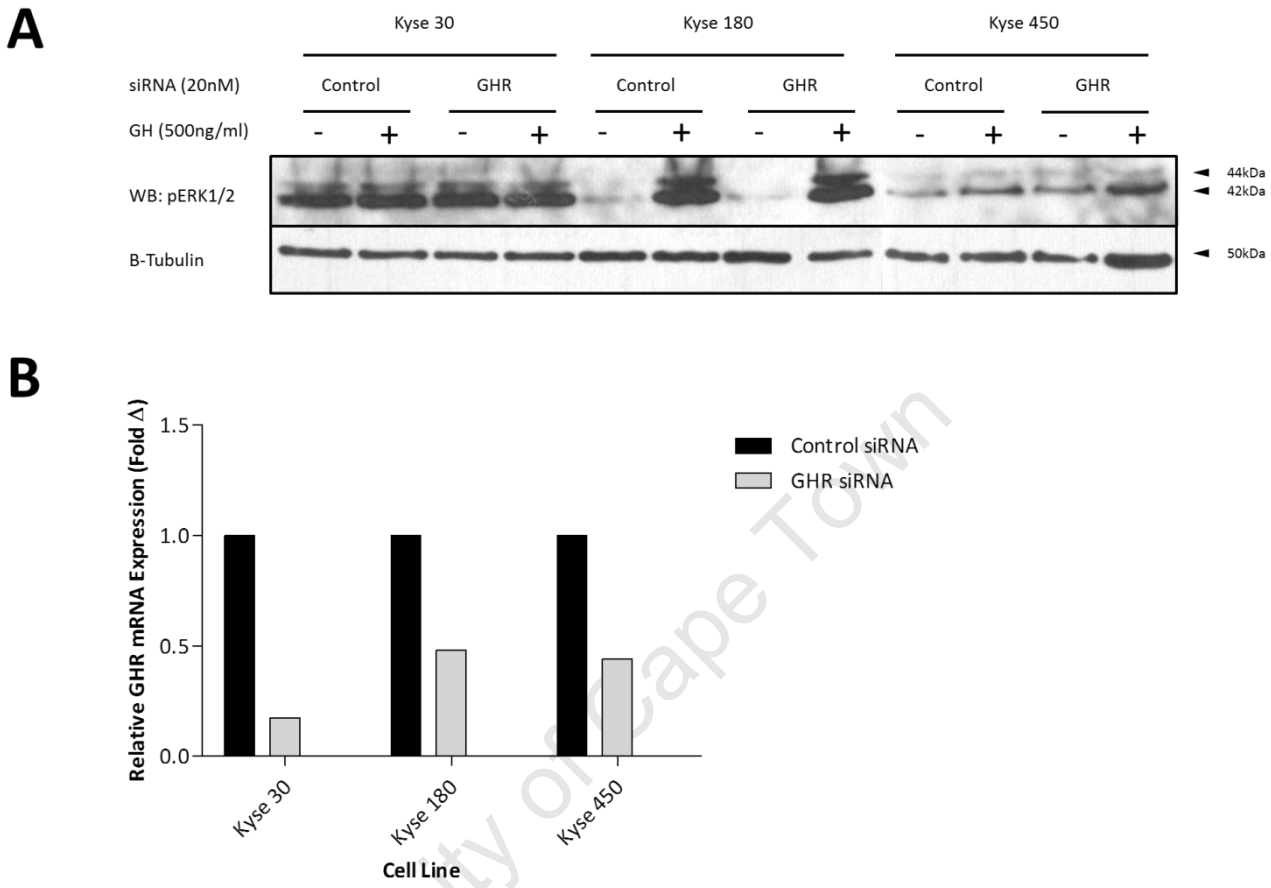


**Figure 29: ERK1/2 phosphorylation in response to GH following GHR knockdown.** Kyse 30, Kyse 180, and Kyse 450 cells were transfected with either GHR or control siRNA (20nM), serum starved for 24hrs, and treated with GH (500ng/ml) for 5min before protein isolation and SDS-PAGE. **(A)** Immunoblotting for pERK1/2.β-Tubulin was included as a control for protein loading. Sizes of bands are indicated. **(B)** Quantification and normalisation of GHR mRNA to control knockdown at end-time point for assay for each cell line.

GH was able to induce ERK1/2 phosphorylation in Kyse 180 cells, but not in Kyse 30 or Kyse 450 cells, indicating that either GHR was not functional in these cell lines, or not expressed at all as protein (Fig.29A). The slight increase in pERK1/2 observed in Kyse 450 cells following GH treatment and GHR knockdown could be as a result of uneven protein loading, as evidenced by immunoblotting for β-Tubulin, rather than as a response to GH (Fig 29A). Furthermore, since GH failed to induce phosphorylation of ERK1/2, it can be further inferred that function PRLR are not expressed in Kyse 30 and Kyse 450 cells.

Once again, GH induced phosphorylation of ERK1/2 in Kyse 180 cells, however, knockdown of GHR failed to reduce pERK1/2. Since only 50% knockdown was achieved, inefficient knockdown of GHR may not be overlooked. If this is the case, 50% of original GHR levels may be enough to still saturate the ERK1/2 pathway in response to the high level of GH used for treatment in Kyse 180 cells. Alternatively, GH may be possibly acting through PRLR in order to achieve ERK1/2 phosphorylation. However, since PRLR expression within OSCC is beyond the scope of this project, the PRLR-mediated ERK1/2 phosphorylation in response to GH was not explored further.

# CHAPTER FOUR

# DISCUSSION AND CONCLUSION

## 4.1 Discussion

The tumourigenic effects of autocrine GH are well documented. Early studies have shown that administration of GH induced neoplasms in rats (Moon *et al*., 1950), while transgenic mice overexpressing human GH showed higher incidences of cancers (Törnell et al., 1992). *In vitro* studies showed that forced autocrine signalling of GH resulted in carcinogenesis in a number of cancer models (Brunet-Dunand *et al*., 2009; Kaulsay *et al*., 1999; Minoia *et al*., 2012; Pandey *et al*., 2008; Segard *et al*., 2003; Zatelli *et al*., 2009). Previous studies have shown that the tumourigenic effects of autocrine GH are largely mediated by GHR (Goffin *et al*., 1999; Kaulsay *et al*., 1999; Minoia *et al*., 2012; Pandey *et al*., 2008). The objective of this study was to therefore determine whether GH/GHR signalling axis plays any role in the tumourigenic phenotype of OSCC.

To establish whether available OSCC cell lines have established a possible GH/GHR signalling loop, nine OSCC cell lines were tested for GH mRNA expression. Endogenous, extra-pituitary expression of GH mRNA in 56% of OSCC cell lines tested reveals the possible role of GH signalling in OSCC (Fig.12). Of course, GH protein expression would have served as the ideal indicator of its potential role in OSCC, but went beyond the scope of this project. Furthermore, it is possible that these cells expressing endogenous GH may affect stromal cells by activating GH/GHR axis signalling within these cells in a paracrine manner, in addition to the possible role of GH autocrine signalling in OSCC. However, the experiments performed in this study would not expose this potential paracrine signalling of GH, and would require analysis of biopsy tissue.

Another approach to determine the possible tumourigenic effects of GH signalling in OSCC was to investigate whether any typical tumourigenic markers of OSCC cells show dependency on GHR signalling. For this, GHR expression would firstly need to be investigated. Given that GHR is expressed on many target tissues (Frank and Messina, 2002), it is unsurprising that 78% of OSCC cell lines tested expressed GHR mRNA, either that of full-length GHR, or its more active isoform d3GHR (Binder *et al*., 2006; van der Klaauw *et al*.,

2008; Dos Santos *et al*., 2004) (Fig.12). Using the d3GHR gene-specific primers, only 33% of OSCC cell lines tested expressed d3GHR mRNA (Fig.12), indicating that while the potential tumourigenic effects of autocrine GH signalling may be mediated by full-length GHR in a majority of cases, the d3GHR may play a role in a subset of patients.

Immunoblotting for GHR proved challenging, most likely due to the insensitivity of the commercially-available GHR antibodies, lending credence to the use of antibodies produced in-house in other studies (Asa *et al*., 2007; Xu *et al*., 2011; Yang *et al*., 2007). Despite this, exogenous GHR induced by GHR overexpression by means of expression plasmid transfection indicated that exogenous GHR was detected at 110kDa (Fig.13A&B).A second band of 72kDa was also observed, which corresponds to the size of the intracellular domain following cleavage of the extracellular domain as observed by previous studies (Schantl *et al*., 2004) (Fig.13A).Expression plasmid PCR indicated that the insert was that of human GHR cDNA (Appendix A). Tunicamycin treatment indicated that the 110kDa band was most likely fully-mature, glycosylated, full-length GHR (Fig.17). Regardless of this, the 110kDa size was smaller than the 120-130kDa size corresponding to mature GHR seen in previous studies (Asa *et al*., 2007; Kerkhof *et al*., 2007; Ross *et al*., 1997; Stubbart *et al*., 1991; Wang *et al*., 1992). Additionally, the overexpressed 110kDa GHR band was dysfunctional, as evidenced by the lack of phosphorylation in response to GH stimulation (Fig.21). This, coupled with the smaller than expected size of overexpressed GHR, may indicate that the expression plasmid was not cloned correctly.

Endogenous GHR was detected at 120kDa (Fig.19, Fig.20, Fig.21), in agreement to the size of mature GHR detected in other studies (Asa *et al*., 2007; Kerkhof *et al*., 2007; Ross *et al*., 1997; Stubbart *et al*., 1991; Wang *et al*., 1992). This band was only seen in one of the nine OSCC cell lines tested (Fig.15), further indicating the possible insensitivity of commercially-available GHR antibodies.

Interestingly, the 95kDa band deemed to be GHR by a previous study using the same antibody (Arturi *et al*., 2011), despite it being smaller than the reported 120-130kDa size seen in other studies, was detected in all OSCC cell lines tested. The same study, however, did not indicate whether the 95kDa band was mature GHR, and isoform, or a precursor form of GHR. Tunicamycin treatment indicates that this band is likely an unglycosylated, precursor form of GHR (Fig.17), while it is also likely a cytosolic protein (Fig.15). GHR knockdown by

means of siRNA did little to alter expression levels of the 95kDa band, however, inefficient knockdown may not be excluded. Also, the detection of a non-specific protein band of 95kDa may also explain the above knockdown results. Successful immunoprecipitations using the two GHR antibodies further confirm that the 95kDa band is that of GHR, albeit at much lower levels than prior to immunoprecipitation, further indicating the possible detection of an additional non-specific protein band at 95kDa. Taken together, this indicates while unglycosylated, precursor GHR is detected at 95kDa, the possible detection of a non-specific band also at 95kDa does not allow the conclusive detection of precursor GHR in OSCC. Additionally, only the Kyse 180 cell line exhibited detectable levels of mature GHR expression (Fig.15, Fig.21B). This could be due to the possible insensitivity of commercially-available GHR antibodies, and/or the very short half-life of mature GHR (Baxter, 1985; Murphy and Lazarus, 1984).

GHR knockdown by means of siRNA indicated that GHR plays a significant role in proliferation in Kyse 180 cells. A statistically significant decrease of 18% was seen compared to control knockdown (Fig.23B). Similar results were seen when antagonising GHR in GH-expressing breast cancer cells, albeit to a greater extent (Kaulsay *et al*., 1999). $IC_{50}$ values for both cisplatin and doxorubicin remain unchanged following GHR knockdown (Fig.24), in contradiction to previous studies showing that the anti-apoptotic effects of autocrine GH signalling are mediated by GHR (Minoia *et al*., 2012). These results suggest that while GHR plays a role in proliferation in Kyse 180 cells, the response of these cells to cisplatin and doxorubicin remain largely uninfluenced by the disruption of autocrine GH signalling by GHR, inferring that autocrine GH signalling mediated by GHR is not important for the chemosensitivity of these cells. Also, this could further infer that the potential tumourigenic effects of GH in these cells may be mediated by PRLR, a receptor that binds GH (Somers *et al*., 1994), and not by GHR. Additionally, since the above results were seen with only a 50% knockdown of total GHR mRNA levels (Fig.23C, Fig.24C), inefficient knockdown may not be excluded.

Kyse 30 and Kyse 450 cells showed no changes in proliferation and $IC_{50}$ following GHR knockdown (Fig.25-28), indicating that GH signalling via GHR, an in the case of Kyse 30 cells, via d3GHR is not important in these cells for proliferation and sensitivity to cisplatin and doxorubicin. Downstream ERK1/2 phosphorylation in response to GH stimulation revealed that GH signalling was not being transduced in both Kyse 30 and Kyse 450 cells (Fig.29). This

could be as a result of either the translation of dysfunctional GHR, or the lack of translation of GHR mRNA into protein.

### 4.2 Conclusion

RNA analysis indicates the ectopic expression of GH in a majority of OSCC cell lines. Several cell lines expressed mRNA for full-length GHR while few express mRNA for the d3GHR isoform, indicating a possible role of autocrine and/or paracrine GH signalling that may be mediated by full-length GHR in a majority of cell lines tested. While GHR knockdown did cause a decrease in proliferation in Kyse 180 cells, there was no change in $IC_{50}$ values for cisplatin and doxorubicin, indicating that disruption of autocrine GH signalling through GHR only affects proliferation when investigating the effects of GH on only proliferation and chemoresistance. The failure of GH to elicit downstream signalling in several cell lines indicates that while a majority of OSCC cell lines express GHR mRNA, this does not correlate to the expression of functional GHR protein. These results suggest that while the GH axis acting through GHR may play an important role in proliferation in a subset of patients, in a majority of cases GHR plays a very limited role, and may not be expressed as a functional protein. However, since only proliferation and chemoresistance were investigated, this cannot serve as an indication of the potential tumourigenic effects of GH in OSCC, and investigating additional tumourigenic markers are needed. Additionally, the inability to detect endogenous levels of mature and functional GHR is an indication of the insensitivity of commercially available GHR antibodies and/or the short half-life of mature GHR.

### 4.3 Future Perspectives

Given the ectopic expression of GH mRNA in OSCC, it would be interesting to investigate whether autocrine GH signalling plays a role in OSCC tumourigenesis, and whether it is mediated by PRLR. For this, the use of a PRLR-specific antagonist is needed (Xu *et al*., 2011).Also, GHR and PRLR have shown to form functional heterodimers which are able to activate downstream signalling in response to GH (Xu *et al*., 2011). To test whether the potential tumourigenic effects of endogenous GH in OSCC is mediated by these heterodimers, antagonists will have to be used (Xu *et al*., 2011), given the inefficient knockdown achieved by siRNA transfection.

As evidenced by this project, GHR did not play a role in chemoresistance in any of the three OSCC cell lines tested, and only contributed towards proliferation in one out of the three cell lines tested. This could be confirmed in a wider panel of cell lines using a GHR antagonist. Additionally, knockdown of GHR did not significantly reduce activation of downstream signalling in response to GH, possibly indicating that effects of GH are not mediated exclusively by GHR. This could also be better explored by using antagonists specific to GHR. Additionally, since only proliferation and chemoresistance were investigated in this project and therefore cannot be a true reflection of the potential tumourigenic effects of GH in OSCC, it would be interesting to investigate whether GH/GHR signalling may play a role in other tumourigenic markers such as metastasis, invasion, angiogenesis, epithelial-to-mesenchymal transition, and anchorage-independent growth.

Given the possible identity of the 120kDa band detected in Kyse 180 as that of mature GHR, tunicamycin treatment within this cell line would be needed to investigate its glycosylation status and thus further confirm its identity as mature, glycosylated GHR. The band's response to serum starvation in Kyse 180 cells would further confirm this. Additionally, given the possible identity of the 95kDa band as unglycosylated, precursor GHR, a time and dose-dependent knockdown of GHR in differing cell lines would serve to confirm this. To minimise the effects of inefficient knockdown in such experiments, a suitable cell line shown to respond to GHR knockdown by greatly decreasing GHR mRNA levels would be needed.

Evidence in this project suggests that the 75kDa band detected by Mab 263 is likely a non-specific protein band. However, there is also evidence suggesting its identity as a previously uncharacterised dominant negative of GHR, given that Kyse 30 and Kyse 450 cells exhibit no

downstream signalling when stimulated with GH (Fig.29), while expressing relative low levels of full-length and/or d3GHR mRNA (Fig.12, panel flGHR/d3GHR) and relatively high levels of the 75kDa band (Fig.14A) when compared to Kyse 180, a cell line shown to respond to GH stimulation. Additionally, this dominant negative isoform of GHR would function in a similar manner to that of the 1-279GHR isoform, since it lacks the necessary intracellular domain for downstream signal transduction, as evidenced by the lack of detection by the B12 antibody. To further investigate the possible identity of the 75kDa band as a dominant negative isoform of GHR, knockdown of GHR mRNA and immunoblotting with the Mab 263 antibody will be needed. Additionally, it would be interesting to investigate its dominant negative role in OSCC by selecting two cell lines, one expressing low levels of the 75kDa band, and one expressing high levels, and investigating the difference in ERK1/2 phosphorylation in response to GH between the two.

As final confirmation of the potential tumourigenic role of endogenously-produced GH in OSCC, it would be interesting to investigate patient material for GH mRNA expression by qRT-PCR, and, if possible, GH protein expression. Additionally, it would be interesting to investigate GHR mRNA expression by qRT-PCR and localisation by either immunohistochemistry and/or immunoblotting of nuclear-fractionalised protein lysates obtained from patient material. This would be done for both normal, and tumour biopsies and serve as an indicator for the possible role of GH in OSCC.

# CHAPTER FIVE

# MATERIALS AND METHODS

## 5.1 Transformation and Plasmid Isolation

### 5.1.1 Transformation

Competent JM109 *E.coli* cells (Promega, USA) were transformed with the GHR expression vector (kindly supplied by Andrew Brooks). The JM109 strain of *E.coli* cells allows for better transformation efficiency and improved plasmid yield since endonuclease A activity is abolished within this strain(Taylor *et al*., 1993).

Plasmids arrived by mail blotted on filter paper. The filter paper was then immersed in TE buffer (pH 8) (Appendix B) allowing the resuspension of the expression plasmids. The plasmid concentration within the suspensions was then quantified using the NanoDrop™ 2000c spectrophotometer (Thermo Scientific, USA). 50ng of each plasmid was then used to transform 20µl of JM109 *E.coli* cells. Upon the addition of the plasmid suspension to the cells, the mixture was allowed to chill on ice for 10min. Cells were then transformed at 42$^{o}$C for 2min before chilling on ice for 2min. 900µl of Luria broth (LB) (no ampicillin) (Appendix B) was then added prior to incubation at 37$^{o}$C in a shaker set at 275rpm for 1hr. 20µl, 100µl, and 500µl of cells were then plated on ampicillin-containing agar plates (100µg/ml) (Appendix B) which were incubated overnight at 37$^{o}$C. Colonies were then selected and inoculated in 5ml ampicillin-containing (100µg/ml) LB. Plasmid from these colonies were then isolated using the PureYield™ Plasmid Miniprep System kit (Promega, USA) following overnight incubation at 37$^{o}$C shaking at 200rpm. Following confirmation of desired transformation, 1ml aliquots of 15% glycerol transformed *E.coli* cells were made and stored at -80$^{o}$C for long-term storage.

### 5.1.2 Plasmid Isolation, Restriction Enzyme Digest, and Agarose Gel Electrophoresis

The plasmid isolation was performed as manufacturer's instructions and is based on alkaline lysis of bacterial cells followed by the adsorption of DNA onto silica in the presence of high salt. Successful colonies containing desired GHR plasmid were initially confirmed using restriction enzyme digest on the plasmids isolated from the colonies (*SspI*). Additionally, 100 copies of each GHR, d3GHr, and GH expression plasmid underwent PCR using gene-specific primers for GHR, d3GHR, and GH respectively, to further confirm desired colonies. Digested and PCR products from each expression vector underwent agarose gel electrophoresis as described below.

For transfections in mammalian cells, plasmid stocks of GHR expression plasmid was made using the PureYield™ Plasmid Midiprep System kit (Promega, USA), as per manufacturer's instructions. This kit allowed for more plasmid to be isolated from more transformed *E.coli* cells than would have been possible with the PureYield™ Plasmid Miniprep System kit. Final plasmid stocks of all 3 expression vectors were finally quantified using the NanoDrop™ 2000c spectrophotometer and stored at -20$^{o}$C for long term-storage.

### 5.2 RNA Isolation and Quantification

### 5.2.1 RNA Isolation

Ribonucleic acid (RNA) was isolated from cells using the QAIzol™Lysis Reagent (QAIGEN, GER) as per manufacturer's instructions. The lysis reagent, consisting of phenol and guanidine thiocyanate, is designed to optimally extract RNA from cells and tissue by facilitating lysis of fatty tissues and cell membranes, and inhibiting RNases.

Briefly, the protocol entailed washing the cells with 4$^{o}$C 1x phosphate buffered saline (PBS) (Appendix B) before adding QAIzol (volumes of QAIzol added to size of culture dishes bellow), transferring the lysate to a Diethylpyrocarbonate (DEPC)-treated Eppendorf tube, and allowing 5min incubation at RT. This was then stored at -80$^{o}$C prior to RNA isolation. RNA was then isolated by means of a chloroform separation and isopropanol precipitation. The addition of chloroform (one-fifth the volume of QAIzol used) allowed the dissociation of two phases, the upper aqueous phase and the lower organic phase following centrifugation at 12000g for 15min at 4$^{o}$C. RNA was contained within the aqueous phase. Following the

transfer of the aqueous phase to a new DEPC-treated Eppendorf tube, isopropanol was added (half the volume of QAIzol used) to allow precipitation of the RNA. The RNA was then centrifuged out of solution at 12000g for 15min at 4$^{o}$C and washed with 75% ethanol made up in DEPC-treated $H_2O$ (Appendix B). The RNA pellet was then allowed to air-dry before being resuspended in 20µl DEPC-treated water and stored at -80$^{o}$C.

**Table 1:** Volumes of QAIzol added per size of dish used.

| Dish Diameter (mm) | Volume of QAIzol used (µl) |
|---|---|
| 35 | 300 |
| 60 | 600 |
| 1000 | 1000 |

### 5.2.2 RNA Quantification

The RNA was quantified using the NanoDrop™ 2000c spectrophotometer (Thermo Scientific, USA). Absorbance readings at 280nm, 260nm, and 230nm were used to determine protein contamination and organic solvent contamination. Protein contamination was investigated using the 260/280 ratio. Pure RNA achieves a value of 2, and lower values are an indication of protein contamination within the sample. Contamination by organic solvents used in RNA extraction could also be investigated by means of the 260/230 ratio. A pure sample of RNA would achieve a value of 1.8, with lower values indicating possible organic sample contamination which could interfere with downstream processes such as cDNA conversion. RNA of good quality was routinely used for further analysis.

### 5.2.3 RNA Agarose Gel Electrophoresis

To assess the integrity of the isolated RNA, 1µg was analysed by RNA gel (Appendix B) electrophoresis. RNA was suspended in RNA loading buffer (Appendix B) and heated at 55$^{o}$C for 5min. The heated sample then underwent electrophoresis at 70V for 1hr and was visualised by means of ultraviolet light (UV) transilluminator. The absence of smearing and a clear ratio of 2:1 for the 28S:18S ribosomal RNA subunits indicated that the RNA was of good quality and did not harbour significant degradation.

### 5.3 DNase Treatment

Since genomic DNA (gDNA) contamination is common to QAIzol-isolated RNA, isolated RNA underwent DNase treatment using the TURBO™ DNA-free DNase Treatment Kit (Applied Biosystems, USA) as per manufacturer's instructions. The kit allows for degradation of DNA by an engineered version of the wild type DNase I enzyme which has a greater catalytic efficiency, followed by the removal of the enzyme and divalent cations that may catalyse RNA degradation by means of the DNase Inactivation Reagent, without heating of the sample.

5µg of RNA was diluted to a concentration of 200ng/µl and subjected to DNase digest by 1u of the TURBO™DNase I enzyme. The catalytic reaction occurred at 37$^{o}$C for 30min followed by the addition of 2.5µl of the DNase Inactivation Reagent. The sample was then centrifuged at 10000g at RT for 1.5min, and the supernatant containing the DNase-treated RNA was transferred to a clean DEPC-treated Eppendorf tube. DNase-treated RNA was stored at -80$^{o}$C.

**5.4 First-strand cDNA Synthesis**

DNase-treated RNA was subjected first-strand complementary DNA (cDNA) synthesis using the ImProm-II™ Reverse Transcription System kit (Promega, USA) as per manufacturer's instructions. The kit allows for efficient synthesis of cDNA using an optimised set of reagents and entails the annealing of either random hexomer primers (RHP) or Oligo(dT) subsequent to cDNA synthesis by the ImProm-II™ Reverse Transcriptase enzyme, followed by heat-inactivation of the enzyme.

Briefly, 1µg of DNase-treated RNA was added to 0.5µg RHP and allowed to denature at 70$^{o}$C for 5min. The reaction was then chilled on ice for 5min. A mastermix of $MgCl_2$ and the 4 deoxyribonucleotides to a final concentration of 2mM and 0.5mM respectively, was made along with 1µl ImProm-II™ Reverse Transcriptase enzyme and 20U Recombinant RNasin® Ribonuclease Inhibitor and added to the primer-RNA reaction. The sample was then allowed to incubate at 25$^{o}$C for 5min to allow primer annealing. cDNA synthesis was then achieved by subjecting the reaction to 42$^{o}$C incubation for 1hr. Following reverse transcription, the transcriptase enzyme was heat-inactivated at 70$^{o}$C for 5min. cDNA was then stored at -80$^{o}$C.

**5.5 Quantitative Real-time Polymerase Chain Reaction**

mRNA expression was investigated and quantified by means of quantitative real-time polymerase chain reaction (qRT-PCR), following reverse transcription. This procedure involved the use of primers that anneal specifically to sequences within a template to amplify the desired product. This is achieved by exposing the reaction to several cycles of temperatures to allow primer annealing, product extension, and denaturation.The comparative threshold cycle ($C_T$) method was used for the calculation of expression fold changes between samples.

Gene-specific primers were used and were synthesized by the Oligonucleotide Synthesis Facility, University of Cape Town, and 20µM stocks for each primer were prepared. GHR, d3GHR, GH, and GAPDH gene-specific primer sequences, final concentration used, annealing temperatures, PCR cycles, and PCR product sizes are indicated below. 2µl of converted cDNA was added to a reaction already containing gene-specific primers, 9.5µl Fast SYBR® Green Master Mix (Invitrogen, USA) and made up to a total volume of 20µl with SABAX® water (Adcock Ingram, USA) per sample. qRT-PCR was performed on the StepOne™ Real-Time PCR System (Applied Biosystems, USA). For all PCRs, initial denaturation occurred at 95$^{o}$C for 3min, primer annealing occurred at the indicated temperatures for 20sec, and denaturing after each cycle occurred at 95$^{o}$C for 1sec. Extension occurred during the temperature increase from primer annealing to denaturation. mRNA was then quantified after standardising to the housekeeping gene, GAPDH. Relative $C_T$ values were then analysed using the Microsoft Office Excel.

**Table 2:** Gene-Specific Primer sequences and PCR conditions

| Target | Primer | Sequence (5'-3') | Final Concentration (µM) | Annealing Temperature (°C) | Cycles | Product Size (bp) | Reference |
|---|---|---|---|---|---|---|---|
| flGHR | Forward | CTC AAC TGG ACT TTA CTG AAC G | 1 | 62 | 30 | 454 | (Kaulsay *et al.*, 1999) |
| | Reverse | AAT CTT TGG AAC TGG AAC TGG G | | | | | |
| d3GHR | Forward | CCT ACA GGT ATG GAT CTC TGG | 1 | 60 | 40 | flGHR: 420 | (Sobrier *et al.*, 1993) |
| | Reverse | CCA CCA TTG CTA GTT AGC TT | | | | d3GHR: 354 | |
| GH | Forward | CCG ACA CCC TCC AAC AGG GA | 0.2 | 62 | 40 | 343 | (Kaulsay *et al.*, 1999) |
| | Reverse | CCT TGT CCA TGT CCT TCC TG | | | | | |
| GAPDH | Forward | GCC TGC TTC ACC ACC TTC | 1 | 55 | 40 | 201 | Unpublished |
| | Reverse | GGC TCT CCA GAA CAT CAT CC | | | | | |

## 5.6 Agarose Gel Electrophoresis

PCR products generated from cDNA samples and expression plasmids were visualised by means of ethidium bromide staining and observation by means of a UV transilluminator, since ethidium bromide intercalates within DNA and is fluorescent under UV. PCR products were separated by electrophoresis in either a 2% or 3% agarose gel containing 10mg/ml ethidium bromide for 1hr at 100V following the addition of 6X DNA loading dye (Appendix B) to the PCR reaction. Additionally, digested GHR expression plasmidwas subjected to electrophoresis in a 0.8% agarose gel containing 10mg/ml ethidium bromide following digestion by their respective restriction enzymes.

## 5.7 Sequencing

Appropriate amounts of PCR products were used as templates for labelling and sequencing using the BigDye® Terminator v3.1 Cycle Sequencing Kit (Applied Biosystems, USA) and ABI PRISM® 3100 Genetic Analyzer (Applied Biosystems, USA). Provided protocols were followed accordingly.

The sequencing reaction works on the principle of cycle sequencing. This involves the denaturation of double-stranded DNA at 96°C for one minute, annealing of the primers, and extension by incorporation of either deoxynucleotides or fluorescent dideoxynucleotides to form a fluorescent dye-labelled product. Once a dideoxynucleotide is randomly incorporated, elongation of that particular strand is terminated. Therefore, after the PCR of 25 cycles is complete, one is left with PCR fragments all of different sizes depending on when a dideoxynucleotide was incorporated.

Before the sequencing reaction could take place, the PCR product band was cut out of the agarose gel and purified using the Wizard® SV Gel and PCR Clean-Up System (Promega, USA) as per manufacturer's instructions. The kit allowed for the removal of free deoxynucleotides and primers that could interfere with the sequencing. Briefly, the protocol entailed melting the agarose gel slice in the Membrane Binding Solution supplied with the kit, followed by passing the DNA-solution mix through a DNA-binding silica membrane, washing the membrane with the provided Membrane Wash Solution, and eluting the bound DNA with DNase-free water. The eluted DNA was then quantified using theNanoDrop™ 2000c spectrophotometer and stored at -20$^{o}$C.

An appropriate amount of purified PCR product was then added to 2µl of BigDye® Terminator Mix, 4µl BigDye® Buffer, and 4µM of either the forward or the reverse primer used to generate that PCR product. The BigDye® Terminator Mix contained the necessary deoxynucleotides and dideoxynucleotides. The sequencing reaction then underwent PCR with an initial denaturing step at 96$^{o}$C for 3min, followed by 25 cycles of 96$^{o}$C for 30sec, primer annealing at 50$^{o}$C for 15sec, finally followed by extension at60$^{o}$C for 4min.

The sequencing reaction was then analysed using ABI PRISM® 3100 Genetic Analyzer (Department of Human Genetics, University of Cape Town) which works on the principle of capillary electrophoresis. Briefly, this involves the separation of differently-sized fluorescently-labelled sequences. The shorter fragments are the first to be detected by the laser followed by larger fragments. This results in the fragment being sequenced in the 5' to 3' direction. Since each of the four possible dideoxynucleotidesare independently labelled, a computer is then able to assemble a chromatogram, from which the sequence of the PCR fragments can be read. The generated sequence was then compared to the expected PCR product sequence using the program Bioedit.

## 5.8 Cell Culture

### 5.8.1 Cell Lines

The human oesophageal squamous-cell carcinoma cell lines WHCO1, WHCO5 andWHCO6, derived from South African patients, were a gift from Prof. R. Veale(University of Witwatersrand). All Kyse cell lines used were previously established(Shimada *et al*., 1992),and purchased from German ResourceCentre for Biological Material, DSMZ GmbH (Braunschweig, GER).

### 5.8.2 Cell Culture

All cell lines used were cultured at 37$^{o}$C in a humidified incubator which was also supplied with a 5% carbon dioxide and 95% air gas mixture. Cells were cultured Gibco® Dulbecco's Modified Eagle Medium (DMEM) (Invitrogen, USA) containing 10% heat-inactivated foetal bovine serum (FBS), penicillin (100U/ml), and streptomycin (100µg/ml) (Appendix B). Media with these additives will be called complete media from here on.

Frozen stocks of cells were prepared by allowing cells to reach 80% confluency, before media was removed and washed with trypsin/EDTA (Difco, USA) heated up to 37$^{o}$C. After washing, cells were then trypsinised with 5ml trypsin/EDTA at 37$^{o}$C for 2min. Trypsin/EDTA was then inactivated by adding an equal amount of complete media, followed by transfer of the cells into a sterile 12 ml tube. Cells were then centrifuged at 1000rpm for 5min. The supernatant was then removed from the cell pellet and resuspended in 2.7ml complete media. 0.3ml of DMSO was then added to achieve a final concentration of DMSO of 10% (v/v). 1ml of the cell/DMSO mixture was then aliquoted per cryotube and stored at -80$^{o}$C for 24hrs. Frozen cells were then placed into liquid nitrogen for long-term storage.

### 5.8.3 Cell Culture Passaging

Frozen cell stocks were thawed by incubation in a water bath set at 37$^{o}$C. Once completely thawed, cells were added to a 10cm cell culture dish containing 10ml of complete media already pre-warmed to 37$^{o}$C. Cells were then incubated overnight at 37$^{o}$C, followed by a change of complete media. Cells were then cultured in this state with regular changing of media for future experiments, or trypsinised and split into new cell culture dishes as needed.

### 5.8.3 Mycoplasma Testing

Cells were tested for Mycoplasma contamination twice a year. The test briefly involved culturing cells in penicillin and streptomycin-free DMEM for 3 days, before being plated on flamed coverslips. Cells were then allowed to settle and culture for 2 days. Cells were then fixed with fixing solution (Appendix B) and stained with Hoechst fluorescent DNA-binding stain (Appendix B) for 30sec. Coverslips were then washed with water and mounted on slides. Stained cells were visualised on the Zeiss Axiovert 200 Fluorescent microscope (Carl Zeiss, Germany). The absence of small fluorescent spots between stained nuclei indicated that cells were negative for Mycoplasma contamination.

**5.9 Expression Plasmid and siRNA Transfections**

The Kyse 150 cell line was transfected with the GHR expression plasmid using GeneCellin™ Transfection Reagent (BioCellChallenge, USA). The reagent allows for higher delivery efficiencies of plasmid DNA into cell lines and primary cells compared to other lipid and polymer based transfection reagents, with reduced cytotoxicity.

100000 cells were plated per 35mm cell culture dish and incubated at 37$^{o}$C overnight. The next day, cells were transfected overnight using 0.5µg of plasmid as follows; 0.5µg of plasmid was diluted in 50µl of serum-free DMEM media in a 1.5ml Eppendorf tube. 2µl of GeneCellin™ Transfection Reagent was then immediately added and allowed to incubate at RT for 15min. The mixture was then added to the cells in 2ml of complete media drop-wise and incubated overnight at 37$^{o}$C. The next day, protein and/or RNA was either isolated or the media changed to 2ml complete media for future use.

GHR siRNA (Sigma, USA) was transfected using the Transfectin™ Lipid Reagent (BIO RAD, USA). The lipid-based transfection reagent, which is a mixture of a proprietary cationic compound and a co-lipid, allows for optimised intracellular delivery of nucleic acids into cultured mammalian cells.

150000 cells were plated per 35mm cell culture dish and incubated at 37$^{o}$C overnight. The next day, cells were transfected for 6hrs using 20nM amounts of siRNA as follows; 0.625µl of the Transfectin™ Lipid Reagent was added to 50µl of serum and penicillin and streptomycin-free media in a 1.5ml Eppendorf tube and allowed to incubate at RT for 5min. siRNA was added to the mixture to a final concentration of 20nM and incubated at RT for 20min. The mixture was then added drop-wise to cells in 1ml complete media and allowed to transfect for 6hrs, followed by the removal of the media and the replacement with 2ml complete media.

If different sized culture dishes were used for transfection other than the 35mm dishes, the protocols above were scaled down/up according to area of the dish used compared to the area of a 35mm cell culture dish.

### 5.10 Protein Isolation

Protein was isolated from plated cells (with varying densities according to the experiments needed) by firstly removing existing media and washing cells twice with 1xPBS cooled at 4$^{o}$C (volumes of 1xPBS used per wash was exactly half of the volume of complete media used to culture the cells in that specific dish). Radioimmnoprecipitation assay buffer (RIPA) with the indicated additives (Appendix B) (volume of RIPA buffer used to culture dish size table below) was added to the cells. Cells were then scraped using a cell scraper and transferred to a 1.5ml Eppendorf tube. Cells were then subjected to sonication for 15sec on ice, followed by centrifugation at 10000g at 4$^{o}$C for 10min. The supernatant was then transferred to a clean Eppendorf tube, and protein concentration was quantified using the Bichinchoninic acid (BCA) Protein Assay Kit (Thermo Scientific, USA) as per manufacturer's instructions. Absorbance at 595nm was then measured, and protein concentration was calculated using a set of standard bovine serum albumin (BSA) concentrations. Isolated protein was stored at -80$^{o}$C for long-term storage.

**Table 3:** Volume of RIPA used to size of dish

| Dish Diameter (mm) | Volume of RIPA used (µl) |
|---|---|
| 35 | 50 |
| 60 | 100 |
| 100 | 300 |
| 200 | 300 |

## 5.11 Immunoblotting

### 5.11.1 Sodium dodecyl-sulphate Polyacrylamide Gel Electrophoresis (SDS-PAGE)

Protein samples were prepared by adding a specific amount of protein to 5X loading dye (Appendix B) and made up to a specific volume with RIPA buffer. The prepared samples were then heated at $85^0$C for 5min before loading onto a 7.5% polyacrylamide gel (Appendix B). Heating of the sample in the presence of β-mercaptoethanol and SDS ensured that the proteins were in their denatured, reduced state allowing for the separation of the proteins present in the sample based only on their respective sizes. Proteins were then electrophoresed at 150V for 2hrs in 1X Running Buffer (Appendix B). Following this, separated proteins within the gel were then transferred onto a Hybond™-ECL™ nitrocellulose membrane (Amersham Life Sciences, UK) at 100V for 1.5hrs in 1X Transfer Buffer (Appendix B).

### 5.11.2 Immunoblotting

Following protein transfer onto the nitrocellulose membrane, the membrane was then blocked for 1hr at RT in blocking solutions described below. All blocking solutions were diluted in 0.1% Tween TBS (TBST). Membranes were then probed with the desired primary antibody at $4^o$C O/N with agitation. Membranes were then washed 3 times with TBST (Appendix B) for 5min each, before the addition and incubation with HRP-conjugated secondary antibody. Incubations with secondary antibody occurred at RT for 1hr with agitation. Following incubation with the secondary antibody, the membrane was once again washed 3 times with TBST for 5min each with agitation. Below is a table summarising the blocking conditions for all primary antibodies used, along with primary and secondary antibody conditions;

**Table 4:** Blocking and Immunoblotting Conditions for Antibodies

| Primary Antibody | Type | Species | Block | Dilution | Diluent | Company | Catalogue Number |
|---|---|---|---|---|---|---|---|
| **GHR (B12)** | monoclonal | Mouse | 5%Milk+2.5%BSA | 1:250 | 5%Milk/TBST | Santa Cruz | sc-137184 |
| **GHR (Mab263)** | monoclonal | Mouse | 5%Milk | 1:1000 | TBST | Abcam | Ab11380 |
| **β-Tubulin** | polyclonal | Rabbit | 5%Milk | 1:1000 | TBST | Santa Cruz | sc-9104 |
| **HA** | polyclonal | Mouse | 5%Milk | 1:5000 | 5%Milk/TBST | Santa Cruz | sc-805 |
| **pTyr** | monoclonal | Mouse | 5%Milk | 1:1000 | 5%BSA/TBST | Cell Signalling | 9411S |
| **pERK1/2** | monoclonal | Mouse | 5%Milk | 1:500 | 5%BSA/TBST | Cell Signalling | 9106 |
| **EGFR** | polyclonal | Rabbit | 5%Milk | 1:1000 | 2.5%Milk/TBST | Santa Cruz | sc-03 |

**Table 5:** Immunoblotting Conditions for Secondary Antibodies

| Secondary Antibody | Dilution | Diluent | Company | Catalogue Number |
|---|---|---|---|---|
| **Goat α-Mouse** | 1:1000 | 5%Milk/TBST | Abcam | 170-6516 |
| **Goat α-Rabbit** | 1:1000 | 5%Milk/TBST | Abcam | 170-6515 |

### 5.11.3 Immunodetection

Protein bands of interest were detected using SuperSignal® West Pico Chemoluminescent Substrate (Thermo Scientific, USA) as per manufacturer's instructions. This involved incubating the membrane for 5min at RT before detection. For detection, AGFA CU-BR Medical X-ray film (AGFA, Belgium) were exposed to the membrane. The X-ray films were then developed until bands of interest were seen, before being fixed using a fixative agent.

### 5.11.4 Membrane Stripping

Membranes could be reprobed for different proteins following stripping. Membranes were stripped in β-mercaptoethanol stripping buffer (Appendix B) for 30min at RT with agitation, after prior heating of the stripping buffer at 50$^{o}$C for 30min. Following stripping, membranes were washed 3 times with TBST for 5min at RT each time with agitation. Membranes were then processed as above starting with blocking according to the conditions stipulated above for the primary antibody.

### 5.11.5 Densitometry Analysis

Following autoradiographic detection of the membranes, the band intensities of bands of interest were quantified by densitometry using the software ImageJ. Protein expression was quantified relative to intensity of β-Tubulin bands.

### 5.12 Immunoprecipitation

GHR was immunoprecipitated from 1000µg of protein using the 10µg of the Mab 263 antibody in a total volume of 500µl made up with RIPA buffer containing the phosphatase and protease inhibitors. The protein-antibody mix was incubated at 4$^{o}$C O/N with continuous rotation. 100µl of Protein G-Sepharose beads (Calbiochem, USA) was then added to allow binding of the protein-antibody complex to the beads, and allowed to incubate at 4$^{o}$C O/N also with continuous rotation. The protein-antibody-bead solution was then centrifuged at 3000rpm at 4$^{o}$C for 2min. The supernatant was then removed leaving only the protein-antibody-bead complex. The complex was then washed 3 times with 1XPBS chilled at 4$^{o}$C at 3000rpm at 4$^{o}$C for 2min. 35µl of 2X loading dye (Appendix B) was added, followed by heating at 95$^{o}$C to allow dissociation of the protein-antibody-bead complex. Following centrifugation at RT at 3000rpm for 2min, 30µl of supernatant was electrophoresed and immunoblotted using the GHR B12 antibody as described above. The protocol was scaled down according to crude lysate used for immunoprecipitation

**5.13 Immunocytochemistry**

GHR expression and localisation was determined by means of immunocytochemistry. The method allows for detection and localisation of native proteins within fixed cells by means of antigen detection by specific antibodies.

100000 cells were plated per 35mm cell culture dish the day before on coverslips sterilised by means of flaming. Cells were then fixed with either 4% paraformaldehyde (PFA) (Appendix B) or absolute methanol. In the case of PFA fixation, cells were washed with 1xPBS, and coverslips were immersed in 4% PFA and incubated at RT for 20min. In the case of methanol fixation, cells were washed with 1xPBS, and coverslips were immersed in absolute methanol chilled at -20$^{o}$C, and allowed to incubate at -20$^{o}$C for 5min. Cells were then washed 3 times with 1xPBS for 10min per wash on shaker at RT. When cells were fixed with PFA, they underwent permeablisation by means of incubating cells at RT for 5min in 0.5% Triton-X 100 made up in 1xPBS. Permeabilised cells were then quenched with 50mM $NH_4Cl$ made up in 1xPBS for 5min at RT.

Cells were then blocked in either 0.2% gelatin or 1%BSA, both made up in 1xPBS. Two different blocking conditions were used, either 1hr or O/N. In the case of 1hr blocking, cells were immersed in either blocking solution and allowed to incubate for 1hr at RT on a shaker. When cells were blocked O/N, cells were immersed in either blocking solution and allowed to incubate O/N at 4$^{o}$C on a shaker.

Following blocking, cells were then incubated with a range of primary antibody concentrations (1:50 to 1:500, made up in blocking solution) for either 1hr at RT or O/N at 4$^{o}$C, by means of inverting the coverslips on 100µl drops of antibody dilutions. The primary antibody used for GHR localisation was Mab 263 (Abcam, USA). All antibody incubations were done in a humidifying chamber in the dark. Following incubation with primary antibody, cells were washed 3 times for 10min each wash in 1xPBS. Coverslips were then incubated in 1:500 dilution of Alex Fluor® 488 goat anti-mouse secondary antibody (Invitrogen, USA) at RT for 90min in a humidifying chamber. Nuclei were counterstained with 100ng/ml4',6-diamidino-2-phenylindole (DAPI) (Sigma Aldrich, USA) diluted in 1xPBS, at RT for 5min. Coverslips were finally washed once with 1xPBS for 10min and mounted on slides

with Mowiol®4-88 (Polysciences Inc., USA) (Appendix B). Slides were kept at 4$^{o}$C in a dark chamber for long-term storage.

**5.14 Proliferation Assay**

The 3-[4,5-Dimethylthiazol-2-yl]-2,5-diphenyltetrazolium bromide (MTT) (Sigma Aldridge, USA) colourimetric assay was used as a measure for cellular proliferation. Upon incubation of live cells with the MTT reagent, the yellow tetrazolium salt within the reagent is converted into purple formazan crystals in the mitochondria of living cells. The use of MTT is therefore strictly an indication of mitochondrial activity within living cells only at a specific time point, however, when the assay is conducted over a number of time points, the increase/decrease in mitochondrial activity is directly proportional to the cellular proliferation/death experienced by those cells within that range of time points.

1500 cells were plated in complete media per well in a 96-well plate. Cells were plated in triplicate for each condition tested, and 10µl MTT (5µg/ml) (Appendix B) was added per well at the predetermined time points. The cells were then allowed to incubate for 4hrs at 37$^{o}$C in a humidified incubator before the addition of 100µl solubilising solution (Appendix B). The solubilising solution allowed for the lysing of the cells and the solubilisation of the formazan crystals. Once the solubilising solution was added, cells were allowed to incubate O/N at 37$^{o}$C in a humidified incubator. Absorbance at 595nm was then read using the Bio-Tek EL800 Microplate reader (Labtech, UK) in conjunction with the Gen5 Data Analysis software. The absorbance value measured was a quantification of mitochondrial activity at that time point. This was then done at several predetermined time points, and the increase/decrease in absorbance was a representation of the proliferation/death experienced by those cells within that range of time points. Proliferation/death curves were then plotted and analysed using the GraphPad Prism® software.

### 5.15 Growth Hormone Stimulation

Cells were plated and allowed to culture O/N in complete media. Cells were then serum starved with DMEM media supplemented with 0.1% FBS, penicillin (100U/ml), and streptomycin (100µg/ml) for 24hrs. Recombinant human GH (500ng/ml) (Sigma Aldrich, USA) was then added and allowed to incubate at 37$^{o}$C for 5min before extracting RNA/protein as described above.

### 5.16 Chemotherapeutic Drug Treatments

Cisplatin was prepared to a final concentration of 1.6mM in 1xPBS and stored at -80$^{o}$C. Doxorubicin was prepared to a final concentration of 50mM in sterile $dH_2O$ and stored at -80$^{o}$C. Cells used in drug treatment assays were plated at 3000 cells in complete media per well in a 96-well plate, and allowed to incubate O/N at 37$^{o}$C in a humidified incubator. A range of drug concentrations was then added and allowed to incubate at 37$^{o}$C for 48hrs in a humidified incubator before the addition of MTT and the analysis of absorbance at 595nm as described above. Concentrations used for cisplatin treatments ranged from untreated to 150µM while concentrations used for doxorubicin treatments ranged from untreated to 10µM . Cells were plated in triplicate per concentration of drug used. Absorbance readings were then used for analysis using the GraphPad Prism® software, to generated dose response curves and $IC_{50}$ values.

## References


Adams, T.E., Hansen, J.A., Starr, R., Nicola, N.A., Hilton, D.J., and Billestrup, N. (1998). Growth Hormone Preferentially Induces the Rapid, Transient Expression of SOCS-3, a Novel Inhibitor of Cytokine Receptor Signaling. Journal of Biological Chemistry *273*, 1285–1287.

Alele, J., Jiang, J., Goldsmith, J.F., Yang, X., Maheshwari, H.G., Black, R.A., Baumann, G., and Frank, S.J. (1998). Blockade of growth hormone receptor shedding by a metalloprotease inhibitor. Endocrinology *139*, 1927–1935.

Allevato, N.G., Billestraup, N., Goujon, L., Galsgaard, E.D., Norstedt, G., Postel-Vinay, M.C., Kelly, P.A., and Nielsen, J. (1995). Identification of Phenylalanine 346 in the Rat Growth Hormone Receptor as Being Critical for Ligand-mediated Internalization and Down-regulation. Journal of Biological Chemistry *270*, 17210–17214.

Amit, T., Bergman, T., Dastot, F., Youdim, M.B., Amselem, S., and Hochberg, Z. (1997). A membrane-fixed, truncated isoform of the human growth hormone receptor. The Journal of Clinical Endocrinology and Metabolism *82*, 3813–3817.

Argetsinger, L.S., Campbell, G.S., Yang, X., Witthuhn, B.A., Silvennoinen, O., Ihle, J.N., and Carter-Su, C. (1996). Identification of JAK2 as a growth hormone receptor-associated tyrosine kinase. Journal of Biological Chemistry *271*, 29415–29421.

Arturi, F., Succurro, E., Procopio, C., Pedace, E., Lugarà, G.C., Marina, M., Procopio, T., Andreozzi, F., Sciacqua, A., Hribal, M.L., et al. (2011). Nonalcoholic Fatty Liver Disease Is Associated with Low Circulating Levels of Insulin-Like Growth Factor-I. Journal of Clinical Endocrinology & Metabolism *96*, E1640.

Asa, S.L., Digiovanni, R., Jiang, J., Ward, M.L., Loesch, K., Yamada, S., Sano, T., Yoshimoto, K., Frank, S.J., and Ezzat, S. (2007). A growth hormone receptor mutation impairs growth hormone autofeedback signaling in pituitary tumors. Cancer Research *67*, 7505–7511.

Ballesteros, M., Leung, K.C., Ross, R.J., Iismaa, T.P., and Ho, K.K. (2000). Distribution and abundance of messenger ribonucleic acid for growth hormone receptor isoforms in human tissues. The Journal of Clinical Endocrinology and Metabolism *85*, 2865–2871.

Baumann, G., Amburn, K., and Buchanan, T. (1987). The Effect of Circulating Growth Hormone-Binding Protein on Metabolic Clearance, Distribution, and Degradation of Human Growth Hormone. Journal of Clinical Endocrinology & Metabolism *4*, 657–660.

Baumann, G., Amaburn, K., and Shaw, M. (1988). The Circulating Growth Hormone (GH)-Binding Protein Complex: A Major Constituent of Plasma GH in Man. Endocrinology *3*, 976–984.

Baumann, G., Lowman, H.B., Mercado, M., and Wells, J.A. (1994). The stoichiometry of growth hormone-binding protein complexes in human plasma: comparison with cell surface receptors. Journal of Clinical Endocrinology & Metabolism *78*, 1113–1118.

Baumbach, W.R., Horner, D.L., and Logan, J.S. (1989). The growth hormone-binding protein in rat serum is an alternatively spliced form of the rat growth hormone receptor. Genes and Development *3*, 1199–1205.

Baxter, R.C. (1985). Measurement of growth hormone and prolactin receptor turnover in rat liver. Endocrinology *117*, 650–655.

Bazan, J.F. (1990). Structural design and molecular evolution of a cytokine receptor superfamily. Proceedings of the National Academy of Sciences of the United States of America *87*, 6934–6938.

Bergad, P.L., Shih, H.-M., Towle, H.C., Schwarzenberg, S.J., and Berry, S.A. (1995). Growth Hormone Induction of Hepatic Serine Protease Inhibitor 2.1 Transcription Is Mediated by a Stat5-related Factor Binding Synergistically to Two γ-Activated Sites. Journal of Biological Chemistry *270*, 24903–24910.

Bergmann, U., Funatomi, H., Yokoyama, M., Beger, H., and Korc, M. (1995). Insulin-like Growth Factor I Overexpression in Human Pancreatic Cancer: Evidence for Autocrine and Paracrine Roles1. Cancer Research *55*, 2007–2011.

Binder, G., Baur, F., Schweizer, R., and Ranke, M.B. (2006). The d3-growth hormone (GH) receptor polymorphism is associated with increased responsiveness to GH in Turner syndrome and short small-for-gestational-age children. The Journal of Clinical Endocrinology and Metabolism *91*, 659–664.

Blobel, G., and Dobberstein, B. (1975). Transfer of proteins across membranes. The Journal of Cell Biology *65*, 835–851.

Brooks, A.J., Wooh, J.W., Tunny, K.A., and Waters, M.J. (2008). Growth hormone receptor; mechanism of action. The International Journal of Biochemistry & Cell Biology *40*, 1984–1989.

Brown, R.J., Adams, J.J., Pelekanos, R.A., Wan, Y., William J McKinstry, K.P., Seeber, R.M., Monks, T.A., Eidne, K.A., Parker, M.W., and Waters, M.J. (2005). Model for growth hormone receptor activation based on subunit rotation within a receptor dimer. Nature Structural & Molecular Biology *12*, 814–821.

Brunet-Dunand, S.E., Vouyovitch, C., Araneda, S., Pandey, V., Vidal, L.J.-P., Print, C., Mertani, H.C., Lobie, P.E., and Perry, J.K. (2009). Autocrine human growth hormone promotes tumor angiogenesis in mammary carcinoma. Endocrinology *150*, 1341–1352.

Carter-Su, C., Schwartz, J., and Smit, L.S. (1996). Molecular mechanism of growth hormone action. Annual Review of Physiology *58*, 187–207.

Chen, X.P., Losman, J.A., and Rothman, P. (2000). SOCS proteins, regulators of intracellular signaling. Immunity *13*, 287–290.

Chen, Y., Li, D., Wang, D., Liu, X., Yin, N., Song, Y., Lu, S.H., Ju, Z., and Zhan, Q. (2012). Quiescence and attenuated DNA damage response promote survival of esophageal cancer stem cells. Journal of Cellular Biochemistry *113*, 3643–3652.

Chetty, R., and Simelane, S. (1999). p53 and cyclin A protein expression in squamous carcinoma of the oesophagus. Pathology Oncology Research *5*, 193–196.

Cheung, N.W., and Boyages, S.C. (1997). Increased incidence of neoplasia in females with acromegaly. Clinical Endocrinology *47*, 323–327.

Chhabra, Y., Waters, M.J., and Brooks, A.J. (2011). Role of the growth hormone–IGF-1 axis in cancer. Expert Review of Endocrinology & Metabolism *6*, 71–84.

Chiesa, J., Ferrer, C., Arnould, C., Vouyovitch, C.M., Diaz, J., Gonzalez, S., Mares, P., Morel, G., Wu, Z.-S., Zhu, T., et al. (2011). Autocrine proliferative effects of hGH are maintained in primary cultures of human mammary carcinoma cells. The Journal of Clinical Endocrinology and Metabolism *96*, 1418–1426.

Cho, H.-S., Mason, K., Ramyar, K.X., Stanley, A.M., Gabelli, S.B., Denney, D.W., and Leahy, D.J. (2003). Structure of the extracellular region of HER2 alone and in complex with the Herceptin Fab. Nature *421*, 765–60.

Clark, R.G., Mortensen, D.L., Carlsson, L.M., Spencer, S.A., McKay, P., Mulkerrin, M., Moore, J., and Cunningham, B.C. (1991). Recombinant human growth hormone (GH)-binding protein enhances the growth-promoting activity of human GH in the rat. Endocrinology *10*, 4308–4315.

Colao, a, Marzullo, P., Ferone, D., Spiezia, S., Cerbone, G., Marinò, V., Di Sarno, a, Merola, B., and Lombardi, G. (1998). Prostatic hyperplasia: an unknown feature of acromegaly. The Journal of Clinical Endocrinology and Metabolism *83*, 775–779.

Conway-Campbell, B.L., Wooh, J.W., Brooks, A.J., Gordon, D., Brown, R.J., Lichanska, A.M., Chin, H.S., Barton, C.L., Boyle, G.M., Parsons, P.G., et al. (2007). Nuclear targeting of the growth hormone receptor results in dysregulation of cell proliferation and tumorigenesis. Proceedings of the National Academy of Sciences of the United States of America *104*, 13331–13336.

Cosman, D., Lyman, S., Idzerda, R, L., Beckmann, P., Park, L., Goodwin, R., and March, C. (1990). A new cytokine receptor superfamily. Trends in Biochemical Sciences *15*, 265–270.

Costoya, J.A., Finidori, J., Moutoussamy, S., Seãris, R., Devesa, J., and Arce, V.M. (1999). Activation of growth hormone receptor delivers an antiapoptotic signal: evidence for a role of Akt in this pathway. Endocrinology *140*, 5937–5943.

Cummings, D.E., Weigle, D.S., Frayo, R.S., Breen, P.A., Ma, M.K., Dellinger, E.P., and Purnell, J.Q. (2002). Plasma ghrelin levels after diet-induced weight loss or gastric bypass surgery. The New England Journal of Medicine *346*, 1623–1630.

Cunningham, B.C., Ultsch, M., De Vos, A.M., Mulkerrin, M.G., Clauser, K.R., and Wells, J.A. (1991). Dimerization of the extracellular domain of the human growth hormone receptor by a single hormone molecule. Science *254*, 821–825.

Daly, J.M., Fry, W. a, Little, a G., Winchester, D.P., McKee, R.F., Stewart, a K., and Fremgen, a M. (2000). Esophageal cancer: results of an American College of Surgeons Patient Care Evaluation Study. Journal of the American College of Surgeons *190*, 562–72; discussion 572–3.

Date, Y., Kojima, M., Hosoda, H., Sawaguchi, a, Mondal, M.S., Suganuma, T., Matsukura, S., Kangawa, K., and Nakazato, M. (2000). Ghrelin, a novel growth hormone-releasing acylated peptide, is synthesized in a distinct endocrine cell type in the gastrointestinal tracts of rats and humans. Endocrinology *141*, 4255–4261.

Davey, H., Xie, T., McLachlan, M., Wilkins, R., Waxman, D., and Grattan, D. (1999). STAT5b Is Required for GH-Induced Liver Igf-I Gene Expression. Endocrinology *9*, 3836–3841.

Decouvelaere, C., Peyrat, J.-P., Bonneterre, J., Djiane, J., and Jammes, H. (1995). Presence of the Two Growth Hormone RNA Isoforms in Human Breast Cancer. Cell Growth & Differentiation *6*, 477–483.

Dehari, R., Nakamura, Y., Okamoto, N., and Nakayama, H. (2008). Increased nuclear expression of growth hormone receptor in uterine cervical neoplasms of women under 40 years old. The Tohoku Journal of Experimental Medicine *216*, 165–172.

Deng, L., He, K., Wang, X., Yang, N., Thangavel, C., Jiang, J., Fuchs, S.Y., and Frank, S.J. (2007). Determinants of growth hormone receptor down-regulation. Molecular Endocrinology (Baltimore, Md.) *21*, 1537–1551.

Divisova, J., Kuiatse, I., Lazard, Z., Weiss, H., Vreeland, F., Hadsell, D.L., Schiff, R., Osborne, C.K., and Lee, A. V (2006). The growth hormone receptor antagonist pegvisomant blocks both mammary gland development and MCF-7 breast cancer xenograft growth. Breast Cancer Research and Treatment *98*, 315–327.

Edens, A., and Talamantes, F. (1998). Alternative Processing of Growth Hormone Receptor Transcripts. Endocrine Reviews *19*, 559–582.

Edens, A., Southard, J.N., and Talamantes, F. (1994). Mouse growth hormone-binding protein and growth hormone receptor transcripts are produced from a single gene by alternative splicing. Endocrinology *135*, 2802.

Eisenhauer, K.M., Chun, S.Y., Billig, H., and Hsueh, a J. (1995). Growth hormone suppression of apoptosis in preovulatory rat follicles and partial neutralization by insulin-like growth factor binding protein. Biology of Reproduction *53*, 13–20.

Elkas, J., Gray, K., Howard, L., Petit, N., Pohl, J., and Armstrong, A. (1998). The effects of tamoxifen on endometrial insulin-like growth factor-1 expression. Obstetrics & Gynecology *91*, 25–29.

Enzinger, P.C., and Mayer, R.J. (2003). Esophageal cancer. The New England Journal of Medicine *349*, 2241–2252.

Ezzat, S., Strom, C., and Melmed, S. (1991). Colon polyps in acromegaly. Annals of Internal Medicine *114*, 754–755.

Ferlay, J., Shin, H.-R., Bray, F., Forman, D., Mathers, C., and Parkin, D.M. (2010). Estimates of worldwide burden of cancer in 2008: GLOBOCAN 2008. International Journal of Cancer. Journal International Du Cancer *127*, 2893–2917.

Finidori, J. (2000). Regulators of growth hormone signaling. Vitamins & Hormones *59*, 71–97.

Frank, S.J., and Messina, J.L. (2002). Growth Hormone Receptor. Cytokine Reference.

Frank, S.J., Gilliland, G., Kraft, A.S., and Arnold, C.S. (1994). Interaction of the growth hormone receptor cytoplasmic domain with the JAK2 tyrosine kinase. Journal of Biological Chemistry *270*, 14776–14785.

Fuh, G., Mulkerrin, M.G., Bass, S., Bourellg, J.H., Light, D.R., and Well, J.A. (1990). The human growth hormone receptor. Secretion from Escherichia coli and disulfide bonding pattern of the extracellular binding domain. The Journal of Biological Chemistry *265*, 3111–3115.

Fuh, G., Cunningham, B.C., Fukunaga, R., Nagata, S., Goeddel, D. V, and Wells, J.A. (1992). Rational design of potent antagonists to the human growth hormone receptor. Science *256*, 1677–1680.

Gadd, S.L., and Clevenger, C. V (2006). Ligand-independent dimerization of the human prolactin receptor isoforms: functional implications. Molecular Endocrinology (Baltimore, Md.) *20*, 2734–2746.

Galsgaard, E.D., Gouilleux, F., Groner, B., Serup, P., Nielsen, J.H., and Billestrup, N. (1996). Identification of a growth hormone-responsive STAT5-binding element in the rat insulin 1 gene. Molecular Endocrinology *10*, 652–660.

Garcia-Fernandez, M.O., Schally, A. V, Varga, J.L., Groot, K., and Busto, R. (2003). The expression of growth hormone-releasing hormone (GHRH) and its receptor splice variants in human breast cancer lines; the evaluation of signaling mechanisms in the stimulation of cell proliferation. Breast Cancer Research and Treatment *77*, 15–26.

Gebre-medhin, M., Kindblom, L., Wennbo, H., Tornell, J., and Meis-Kindblom, J. (2001). Growth Hormone Receptor is Expressed in Human Breast Cancer. American Journal of Pathology *158*, 1217–1222.

Gent, J., Kerkhof, P. van, Roza, M., Bu, G., and Strous, G.J. (2002). Ligand-independent growth hormone receptor dimerization occurs in the endoplasmic reticulum and is required for ubiquitin system-dependent endocytosis. Proceedings of the National Academy of Sciences of the United States of America *99*, 9858–9863.

Godowski, P.J., Leung, D.W., Meachamt, L.R., Galganit, J.P., Hellmiss, R., Keret, R., Rotwein, P.S., Parkst, J.S., Laron, Z.V.I., and Wood, W.I. (1989). Characterization of the human growth hormone receptor gene and demonstration of. Proceedings of the National Academy of Sciences of the United States of America *86*, 8083–8087.

Goffin, V., Bernichtein, S., Carrière, O., Bennett, W.F., Kopchick, J.J., and Kelly, P.A. (1999). The Human Growth Hormone Antagonist B2036 Does Not Interact with the Prolactin Receptor. Endocrinology *140*, 3853–3856.

Goh, E.L., Pircher, T.J., Wood, T.J., Norstedt, G., Graichen, R., and Lobie, P.E. (1997). Growth hormone-induced reorganization of the actin cytoskeleton is not required for STAT5 (signal transducer and activator of transcription-5)-mediated transcription. Endocrinology *138*, 3207–3215.

Gooch, J.L., Van Den Berg, C.L., and Yee, D. (1999). Insulin-like growth factor (IGF)-I rescues breast cancer cells from chemotherapy-induced cell death--proliferative and anti-apoptotic effects. Breast Cancer Research and Treatment *56*, 1–10.

Gorin, E., and Goodman, M. (1985). Turnover of Growth Hormone Receptors in Rat Adipocytes. Endocrinology *116*, 1796–1805.

Gurland, G., Ashcom, G., Cochran, B.H., and Schwartz, J. (1990). Rapid Events in Growth Hormone Action. Induction of c-fos and c-jun Transcription in 3T3-F442A Preadipocytes. Endocrinology *127*, 3187–3195.

Hanahan, D., and Weinberg, R.A. (2011). Hallmarks of cancer: the next generation. Cell *144*, 646–674.

Harvey, S. (2010). Extrapituitary growth hormone. Endocrine *38*, 335–359.

Heifetz, A., Keenan, R.W., and Elbein, A.D. (1978). Mechanism of Action of Tunicamycin on the UDP-G1cNAc:DolichyLPhosphate GlcNAc- 1 -Phosphate Transferase. Biochemistry *18*, 2186–2192.

Hendricks, D., and Parker, M.I. (2002). Oesophageal Cancer in Africa. IUBMB Life *53*, 263–268.

Heron, M. (2011). Deaths: leading causes for 2007. National Vital Statistics Reports *59*, 1–95.

Herrington, J., Smit, L.S., Schwartz, J., and Carter-Su, C. (2000). The role of STAT proteins in growth hormone signaling. Oncogene *19*, 2585–2597.

Hodge, C., Liao, J., Stofega, M., Guan, K., Carter-Su, C., and Schwartz, J. (1998). Growth hormone stimulates phosphorylation and activation of elk-1 and expression of c-fos, egr-1, and junB through activation of extracellular signal-regulated kinases 1 and 2. The Journal of Biological Chemistry *273*, 31327–31336.

Holt, R.I.G. (2002). Fetal programming of the growth hormone–insulin-like growth factor axis. Trends in Endocrinology and Metabolism *13*, 392–397.

Ihle, J.N. (1996). STATs: signal transducers and activators of transcription. Cell *84*, 331–334.

Jemal, A., Bray, F., and Ferlay, J. (2011). Global Cancer Statistics. Cancer Journal for Clinicians *61*, 69–90.

Johnston, J.A., Kawamura, M., Kirken, R.A., Chen, Y.-Q., Blake, T.B., Shibuya, K., Ortaldo, J.R., McVicar, D.W., and O'Shea, J.J. (1994). Phosphorylation and activation of the Jak-3 Janus kinase in response to interleukin-2. Nature *370*, 151–153.

Kaabi, Y.A. (2012). Growth hormone and its receptor: A molecular insight. Saudi Journal for Health Sciences *1*, 61–68.

Kaulsay, K.K., Mertani, H.C., Törnell, J., Morel, G., Lee, K.O., and Lobie, P.E. (1999). Autocrine stimulation of human mammary carcinoma cell proliferation by human growth hormone. Experimental Cell Research *250*, 35–50.

Kerkhof, P., Putters, J., and Strous, G.J. (2007). The ubiquitin ligase SCF(βTrCP) regulates the degradation of the growth hormone receptor. The Journal of Biological Chemistry *282*, 20475–20483.

Van der Klaauw, A. a, Van der Straaten, T., Baak-Pablo, R., Biermasz, N.R., Guchelaar, H.-J., Pereira, A.M., Smit, J.W., and Romijn, J. (2008). Influence of the d3-growth hormone (GH) receptor isoform on short-term and long-term treatment response to GH replacement in GH-deficient adults. The Journal of Clinical Endocrinology and Metabolism *93*, 2828–2834.

Kojima, M., Hosoda, H., Date, Y., Nakazato, M., Matsuo, H., and Kangawa, K. (1999). Ghrelin is a growth-hormone-releasing acylated peptide from stomach. Nature *402*, 656–660.

Lau, J.S., Yip, C.W., Law, K.M., and Leung, F.C. (2007). Cloning and characterization of chicken growth hormone binding protein (cGHBP). Domestic Animal Endocrinology *33*, 107–121.

Leung, D.W., Spencer, S.A., Cachianes, G., Hammonds, R.G., Collins, C., Hazel, W.J., Barnard, R., and Waters, M.J. (1987). Growth hormone receptor and serum binding protein: purification, cloning and expression. Nature *330*, 537–543.

Lewis, T.S., Shapiro, P.S., and Ahn, N.G. (1998). Signal Transduction through MAP Kinase Cascades. Advances in Cancer Research *74*, 49–139.

Li, H., Gao, Q., Guo, L., and Lu, S.H. (2011). The PTEN/PI3K/Akt pathway regulates stem-like cells in primary esophageal carcinoma cells. Cancer Biology & Therapy *11*, 950–958.

Lin, C.J.I.A., Mendonca, B.B., Lucon, A.M., Cristina, I., Guazzelli, D.E.M., Nicolau, W., Mara, S., and Villares, F. (1997). in Normal and Pathologic Human Adrenocortical Tissues — An Analysis by Quantitative Polymerase Chain Reaction Technique. *82*, 2671–2676.

Lincoln, D.T., Sinowatz, F., Temmim-Baker, L., Baker, H.I., Kölle, S., and Waters, M.J. (1998). Growth hormone receptor expression in the nucleus and cytoplasm of normal and neoplastic cells. Histochemistry and Cell Biology *109*, 141–159.

Lincoln, D.T., Sinowatz, F., Kolle, S., Takahashi, H., Parsons, P., and Waters, M. (1999). Up-regulation of growth hormone receptor immunoreactivity in human melanoma. Anticancer Research *19*, 1919–1931.

Lin-Su, K., and Wajnrajch, M.P. (2002). Growth Hormone Releasing Hormone (GHRH) and the GHRH Receptor. Reviews in Endocrine & Metabolic Disorders *84*, 313–323.

Lobie, P.E., Wood, T.J., Chen, C.M., Waters, M.J., and Norstedt, G. (1994). Nuclear translocation and anchorage of the growth hormone receptor. The Journal of Biological Chemistry *269*, 31735–31746.

McCutcheon, I., Flyvbjerg, A., Hill, H., Li, J., Bennett, W., Scarlett, J., and Friend, K. (2001). Antitumor activity of the growth hormone receptor antagonist pegvisomant against human meningiomas in nude mice. Journal of Neuroscience *94*, 487–492.

Meyer, D.J., Campbell, G.S., Cochran, B.H., Argetsinger, L.S., Larner, A.C., Finbloom, D.S., Carter-Su, C., and Schwartz, J. (1994). Growth hormone induces a DNA binding factor related to the interferon-stimulated 91-kDa transcription factor. Journal of Biological Chemistry *269*, 4701–4704.

Minoia, M., Gentilin, E., Mole, D., Rossi, M., Filieri, C., Tagliati, F., Baroni, A., Ambrosio, M.R., Uberti, E., and Zatelli, M.C. (2012). Growth Hormone Receptor Blockade Inhibits Growth Hormone-Induced Chemoresistance by Restoring Cytotoxic-Induced Apoptosis in Breast Cancer Cells Independently of Estrogen Receptor Expression. Clinical Endocrinology *97*, 907–916.

Minuto, F., Del Monte, P., Barreca, a, Fortini, P., Cariola, G., Catrambone, G., and Giordano, G. (1986). Evidence for an increased somatomedin-C/insulin-like growth factor I content in primary human lung tumors. Cancer Research *46*, 985–988.

Moon, H.D., Simpson, M.E., and Li, C.H. (1950). Neoplasms in Rats Treated with Pituitary Growth Hormon. Cancer Research *10*, 549–556.

Moutoussamy, S., Renaudi, F., Lago, F., Kelly, P.A., and Finidori, J. (1998). Grb10 Identified as a Potential Regulator of Growth Hormone ( GH ) Signaling by Cloning of GH Receptor Target Proteins. Journal of Biological Chemistry *273*, 15906–15912.

Murphy, L.J., and Lazarus, L. (1984). The mouse fibroblast growth hormone receptor: ligand processing and receptor modulation and turnover. Endocrinology *115*, 1625–1632.

Murphy, L.J., and Lazarus, L. (1987). The Mouse Fibroblast Growth Hormone Receptor: Ligand Processing and Receptor Modulation and Turnover. Endocrinology *115*, 1625.

Murphy, L.J., Bell, G.I., and Friesen, H.G. (1987). Growth Hormone Stimulates Sequential Induction of c-myc and Insulin-Like Growth Factor I Expression in Vivo. Endocrinology *120*, 1806–1812.

Nagasawa, S., Onda, M., Sasajima, K., Makino, H., Yamashita, K., Takubo, K., and Miyashita, M. (2001). Cyclin D1 overexpression as a prognostic factor in patients with esophageal carcinoma. Journal of Surgical Oncology *78*, 208–214.

Ooi, G.T., Cohen, F.J., Tseng, L.Y.-H., Rechler, M.M., and Boisclair, Y.R. (1997). Growth Hormone Stimulates Transcription of the Gene Encoding the Acid-Labile Subunit (ALS) of the Circulating Insulin-Like Growth Factor-Binding Protein Complex and ALS Promoter Activity in Rat Liver. Molecular Endocrinology *10*, 997–1007.

Pandey, V., Perry, J.K., Mohankumar, K.M., Kong, X.-J., Liu, S.-M., Wu, Z.-S., Mitchell, M.D., Zhu, T., and Lobie, P.E. (2008). Autocrine human growth hormone stimulates oncogenicity of endometrial carcinoma cells. Endocrinology *149*, 3909–3919.

Pantel, J., Machinis, K., Sobrier, M.L., Duquesnoy, P., Goossens, M., and Amselem, S. (2000). Species-specific alternative splice mimicry at the growth hormone receptor locus revealed by the lineage of retroelements during primate evolution. The Journal of Biological Chemistry *275*, 18664–18669.

Parkin, D.M., Pisani, P., and Ferlay, J. (1999). Estimates of the worldwide incidence of 25 major cancers in 1990. International Journal of Cancer *80*, 827–841.

Pekhletsky, R.I., Chernov, B.K., and Rubtsov, P.M. (1992). Variants of the 5'-untranslated sequence of human growth hormone receptor mRNA. Molecular and Cellular Endocrinology *90*, 103–109.

Pilecka, I., Whatmore, A., Huijsduijnen, R.H. van, Destenaves, B., and Clayton, P. (2007). Growth hormone signalling: sprouting links between pathways, human genetics and therapeutic options. Trends in Endocrinology and Metabolism *18*, 12–18.

Ram, P. a, and Waxman, D.J. (1997). Interaction of growth hormone-activated STATs with SH2-containing phosphotyrosine phosphatase SHP-1 and nuclear JAK2 tyrosine kinase. The Journal of Biological Chemistry *272*, 17694–17702.

Ram, P.A., Park, S., Choi, H.K., Waxman, D.J., and Chem, H.K.J.B. (1996). Growth Hormone Activation of Stat 1, Stat 3, and Stat 5 in Rat Liver. Journal of Biological Chemistry *271*, 5929–5940.

Rinaldi, S., Cleveland, R., Norat, T., Biessy, C., Rohrmann, S., Linseisen, J., Boeing, H., Pischon, T., Panico, S., Agnoli, C., et al. (2010). Serum levels of IGF-I, IGFBP-3 and colorectal cancer risk: results from the EPIC cohort, plus a meta-analysis of prospective studies. International Journal of Cancer *126*, 1702–1715.

Risk, J.M., Mills, H.S., Garde, J., Dunn, J.R., Evans, K.E., Hollstein, M., and Field, J.K. (1999). Molecular biology and esophageal cancer The tylosis esophageal cancer ( TOC ) locus: more than just a familial cancer gene. Disease of the Esophagus *12*, 173–176.

Rosenfeld, R.G., Belgorosky, A., Camacho-Hubner, C., Savage, M.O., Wit, J.M., and Hwa, V. (2007). Defects in growth hormone receptor signaling. Trends in Endocrinology and Metabolism: TEM *18*, 134–141.

Ross, R.J. (1999). Truncated growth hormone receptor isoforms. Acta Paediatrica *88*, 164–6;

Ross, R.J., Esposito, N., Shen, X.Y., Von Laue, S., Chew, S.L., Dobson, P.R., Postel-Vinay, M.C., and Finidori, J. (1997). A short isoform of the human growth hormone receptor functions as a dominant negative inhibitor of the full-length receptor and generates large amounts of binding protein. Molecular Endocrinology (Baltimore, Md.) *11*, 265–273.

Le Roux, C.W., Monson, J.P., Chew, S.L., Grossman, A.B., Besser, G.M., and Jenkins, P.J. (2000). Increased serum prostate-specific antigen in acromegaly–a cross-sectional study. Journal of Endocrinology *164*, 128.

Rowlands, M.-A., Gunnell, D., Harris, R., Vatten, L.J., Holly, J.M.P., and Martin, R.M. (2009). Circulating insulin-like growth factor peptides and prostate cancer risk: a systematic review and meta-analysis. International Journal of Cancer. Journal International Du Cancer *124*, 2416–2429.

Saharinen, P., Takaluoma, K., and Silvennoinen, O. (2000). Regulation of the Jak2 Tyrosine Kinase by Its Pseudokinase Domain. Molecular and Cell Biology *20*, 3387–3395.

Dos Santos, C., Essioux, L., Teinturier, C., Tauber, M., Goffin, V., and Bougnères, P. (2004). A common polymorphism of the growth hormone receptor is associated with increased responsiveness to growth hormone. Nature Genetics *36*, 720–724.

Sarbia, M., Stahl, M., Fink, U., Heep, H., Dutkowski, P., Willers, R., Seeber, S., and Gabbert, H.E. (1999). Prognostic significance of cyclin D1 in esophageal squamous cell carcinoma patients treated with surgery alone or combined therapy modalities. International Journal of Cancer *84*, 86–91.

Schantl, J. a, Roza, M., Van Kerkhof, P., and Strous, G.J. (2004). The growth hormone receptor interacts with its sheddase, the tumour necrosis factor-alpha-converting enzyme (TACE). The Biochemical Journal *377*, 379–384.

Scott, J., Dai, C.D., and Baxter, R.C. (1994). Regulation of the acid-labile subunit of the insulin-like growth factor complex in cultured rat hepatocytes. Endocrinology *135*, 1066–1072.

Segard, H.B., Moulin, S., Boumard, S., De Cremiers, C., and Kelly, P.A. (2003). Autocrine growth hormone production prevents apoptosis and inhibits differentiation in C2C12 myoblasts. Cellular Signalling *15*, 615 – 623.

Shimada, Y., Imamura, M., Wagata, T., Yamaguchi, N., and Tobe, T. (1992). Characterization of 21 newly established esophageal cancer cell lines. Cancer *69*, 277–284.

Siewert, J.R., Stein, H.J., Feith, M., Bruecher, B.L., Bartels, H., and Fink, U. (2001). Histologic tumor type is an independent prognostic parameter in esophageal cancer: lessons from more than 1,000 consecutive resections at a single center in the Western world. Annals of Surgery *234*, 360–7; discussion 368–9.

Slamon, D., Godolphin, W., Jones, L., Holt, J., Wong, S., Keith, D., WJ, L., Stuart, S., Udove, J., and Ullrich, A. (1989). Studies of the HER-2/neu proto-oncogene in human breast and ovarian cancer. Science *244*, 707–712.

Smit, L.S., Meyer, D.J., Billestrup, N., Norstedt, G., Schwartz, J., and Carter-Su, C. (1996). The role of the growth hormone (GH) receptor and JAK1 and JAK2 kinases in the activation of Stats 1, 3, and 5 by GH. Molecular Endocrinology *10*, 519.

Smith, B.D., Smith, G.L., Hurria, A., Hortobagyi, G.N., and Buchholz, T.A. (2009). Future of cancer incidence in the United States: burdens upon an aging, changing nation. Journal of Clinical Oncology *27*, 2758–2765.

Snibson, K.J., Bhathal, P.S., and Adams, T.E. (2001). Overexpressed growth hormone (GH) synergistically promotes carcinogen-initiated liver tumour growth by promoting cellular proliferation in emerging hepatocellular neoplasms in female and male GH-transgenic mice. Liver *21*, 149–158.

Sobrier, M.-L., Duquesnoy, P., Duriez, B., Amselem, S., and Goossens, M. (1993). Expression and binding properties of two isoforms of the human growth hormone receptor. Federation of European Biochmical Societies *319*, 16–20.

Somers, W., Ultsch, M., Vos, A.M. DE, and Kossaikoff, A.A. (1994). The X-ray structure of a growth hormone–prolactin receptor complex. Nature *372*, 478–481.

Sotiropoulos, A., Moutoussamy, S., Renaudie, F., Clauss, M., Kayser, C., Gouilleux, F., Kelly, P.A., and Finidori, J. (1996). Differential activation of Stat3 and Stat5 by distinct regions of the growth hormone receptor. Molecular Endocrinology *10*, 998–1009.

Strous, G.J., Van Kerkhof, P., Govers, R., Ciechanover, A., and Schwartz, A.L. (1996). The ubiquitin conjugation system is required for ligand-induced endocytosis and degradation of the growth hormone receptor. The EMBO Journal *15*, 3806–3812.

Stubbart, J.R., Barton, D.F., Tai, P., Stred, E., Gorin, E., Goodman, M., and Carter-Su, C. (1991). Antibodies to Cytoplasmic Sequences of Cloned Liver Growth Hormone (GH) Receptors Recognize GH Receptors Associated with Tyrosine Kinase Activity. Endocrinology *129*, 1659–1670.

Taylor, R.G., Walker, D.C., and Mclnnes, R.R. (1993). E.coli host strains. Nucleic Acid Research *21*, 1677–1678.

Tollet-Egnell, P., Flores-morales, A., Sahlin, L., and Norstedt, G. (1999). Growth Hormone Regulation of SOCS-2, SOCS-3, and CIS Messenger Ribonucleic Acid Expression in the Rat. Endocrinology *140*, 3693–3704.

Törnell, J., Carlsson, B., Pohjanen, P., Wennbo, H., Rymo, L., and Isaksson, O. (1992). High frequency of mammary adenocarcinomas in metallothionein promoter-human growth hormone transgenic mice created from two different strains of mice. The Journal of Steroid Biochemistry and Molecular Biology *43*, 237–242.

Urbanek, M., Russell, J.E., Cooke, N.E., and Liebhaber, S.A. (1993). Functional characterization of the alternatively spliced, placental human growth hormone receptor. The Journal of Biological Chemistry *268*, 19025–19032.

VanderKuur, J., Allevato, G., Billestrup, N., Norstedt, G., and Carter-Su, C. (1995). Growth Hormone-promoted Tyrosyl Phosphorylation of SHC Proteins and SHC Association with Grb2. Journal of Biological Chemistry *270*, 7587–7593.

Varki, A., Cummings, R., Esko, J., Freeze, H., Hart, G., and Marth, J. (2009). Essentials of Glycobiology (New York: Cold Spring Harbor Laboratory Press).

Vleurick, L., Pezet, A., Kühn, E.R., Decuypere, E., and Edery, M. (1999). A beta-turn endocytic code is required for optimal internalization of the growth hormone receptor but not for alpha-adaptin association. Molecular Endocrinology *13*, 1823–1831.

Wan, Y., Zheng, Y.Z., Harris, J.M., Brown, R., and Waters, M.J. (2003). Epitope map for a growth hormone receptor agonist monoclonal antibody, MAb 263. Molecular Endocrinology (Baltimore, Md.) *17*, 2240–2250.

Wang, X., Uhler, M., Billestraup, N., Norstedt, G., Talamantes, F., Nielsen, J., and Carter-Su, C. (1992). Evidence for Association of the Cloned Liver Growth Hormone Receptor with a Tyrosine Kinase. Journal of Biological Chemistry *267*, 17390–17396.

Waxman, D.J., Ram, P.A., Park, S.-H., and Choi, H.K. (1995a). Intermittent Plasma Growth Hormone Triggers Tyrosine Phosphorylation and Nuclear Translocation of a Liver-Expressed, Stat 5-related DNA Binding Protein. Journal of Biological Chemistry *270*, 13262–13270.

Waxman, D.J., Ram, P.A., Pampori, N.A., and Shapiro, B.H. (1995b). Growth hormone regulation of male-specific rat liver P450s 2A2 and 3A2: induction by intermittent growth hormone pulses in male but not female rats rendered growth hormone deficient by neonatal monosodium glutamate. Molecular Pharmacology *48*, 790–797.

Wehrenberg, W., Ling, N., Bőhlen, P., Esch, F., Brazeau, P., and Guillemin, R. (1982). Physiological roles of somatocrinin and somatostatin in the regulation of growthhormonesecretion. Biochemical and Biophysical Research Communications *109*, 562–567.

Winston, L.A., and Hunter, T. (1995). JAK2 , Ras , and Raf Are Required for Activation of Extracellular activated Protein Kinase by Growth Hormone. Journal of Biological Chemistry *270*, 30837–30840.

Xu, J., Zhang, Y., Berry, P.A., Jiang, J., Lobie, P.E., Langenheim, J.F., Chen, W.Y., and Frank, S.J. (2011). Growth Hormone Signaling in Human T47D Breast Cancer Cells : Potential Role for a Growth Hormone Receptor-Prolactin Receptor Complex. Molecular Endocrinology *25*, 597–610.

Yamauchi, T., Ueki, K., Tobe, K., Tamemoto, H., Sekine, N., Wada, M., Honjo, M., Takahashi, M., Takahashi, T., Hirai, H., et al. (1997). Tyrosine phosphorylation of the EGF receptor by the kinase Jak2 is induced by growth hormone. Nature *390*, 91–96.

Yamauchi, T., Kaburagi, Y., Ueki, K., Tsuji, Y., Stark, G.R., Kerr, I.M., Tsushima, T., Akanuma, Y., Komuro, I., Tobe, K., et al. (1998). Growth hormone and prolactin stimulate tyrosine phosphorylation of insulin receptor substrate-1, -2, and -3, their association with p85 phosphatidylinositol 3-kinase (PI3-kinase), and concomitantly PI3-kinase activation via JAK2 kinase. The Journal of Biological Chemistry *273*, 15719–15726.

Yang, N., Wang, X., Jiang, J., and Frank, S.J. (2007). Role of the growth hormone (GH) receptor transmembrane domain in receptor predimerization and GH-induced activation. Molecular Endocrinology (Baltimore, Md.) *21*, 1642–1655.

Yang, X., Liu, F., Xu, Z., Chen, C., Li, G., Wu, X., and Li, J. (2004). Growth hormone receptor expression in human colorectal cancer. Digestive Diseases and Sciences *49*, 1493–1498.

Yasukawa, H., Misawa, H., Sakamoto, H., Masuhara, M., Sasaki, a, Wakioka, T., Ohtsuka, S., Imaizumi, T., Matsuda, T., Ihle, J.N., et al. (1999). The JAK-binding protein JAB inhibits Janus tyrosine kinase activity through binding in the activation loop. The EMBO Journal *18*, 1309–1320.

Yee, D., Paik, S., Lebovic, G.S., Marcus, R.R., Favoni, R.E., Cullen, K.J., Lippman, M.E., and Rosen, N. (1989). Analysis of Insulin-Like Growth Factor I Gene Expression in Malignancy: Evidence for a Paracrine Role in Human Breast Cancer. Molecular Endocrinology *3*, 509–517.

Yenush, L., and White, M.F. (1997). The IRS-signalling system during insulin and cytokine action. BioEssays *19*, 491–500.

Yin, T., Yasukawa, H., Taga, T., Kishimoto, T., and Yang, Y.C. (1994). Identification of a 130-kilodalton tyrosine-phosphorylated protein induced by interleukin-11 as JAK2 tyrosine kinase, which associates with gp130 signal transducer. Experimental Hematology *22*, 467–472.

Zatelli, M.C., Minoia, M., Mole, D., Cason, V., Tagliati, F., Margutti, A., Bondanelli, M., Ambrosio, M.R., and Uberti, E. (2009). Growth Hormone Excess Promotes Breast Cancer Chemoresistance. Clinical Endocrinology *94*, 3931–3938.

Zhang, Y.U.E., Jiang, J., Black, R.O.Y.A., Baumann, G., Frank, S.J., and Biology, C. (2000). Tumor Necrosis Factor-a Converting Enzyme (TACE) Is a Growth Hormone Binding Protein (GHBP) Sheddase: The Metalloprotease TACE/ADAM-17 Is Critical for (PMA-Induced) GH Receptor Proteolysis and GHBP Generation. Endocrinology *141*, 4342–4348.

Zhu, T., Goh, E.L.K., and Lobie, P.E. (1998). Growth Hormone Stimulates the Tyrosine Phosphorylation and Association of p125 Focal Adhesion Kinase ( FAK ) with JAK2. Journal of Biological Chemistry *273*, 10682–10689.

Zhu, T., Goh, E.L., Graichen, R., Ling, L., and Lobie, P.E. (2001). Signal transduction via the growth hormone receptor. Cellular Signalling *13*, 599–616.

Zhu, T., Sarling-Emerald, B., Zhang, X., Lee, K.O., Gluckman, P.D., Mertani, H.C., and Lobie, P.E. (2005). Oncogenic Transformation of Human Mammary Epithelial Cells by Autocrine Human Growth Hormone. Cancer Research *65*, 317–324.

# Appendix

## Appendix A- PCR Product Sequences and Additional Immunoblots

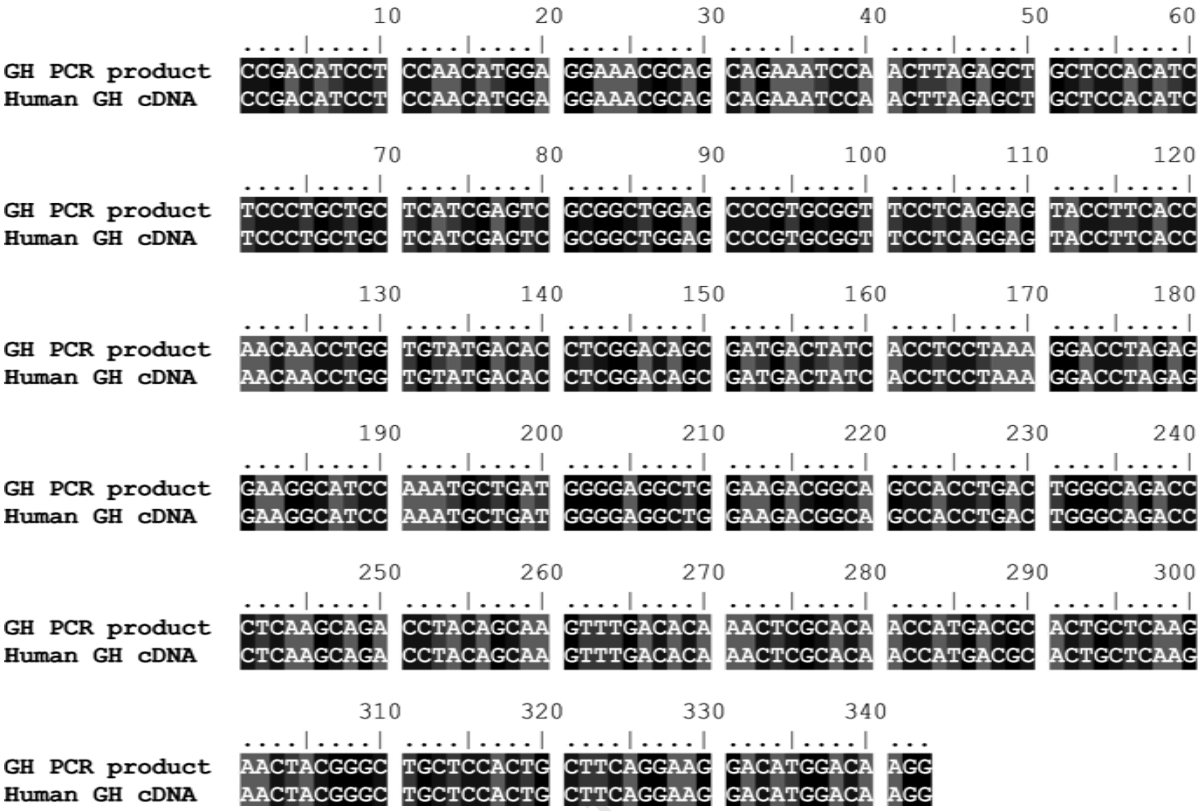


**Figure 29: Sequencing and alignment of the GH PCR product to human GH cDNA.** The PCR product generated using T47D cDNA as template and GH-specific primers, and its alignment to human GH cDNA, indicates that the 343bp product corresponds to human GH.

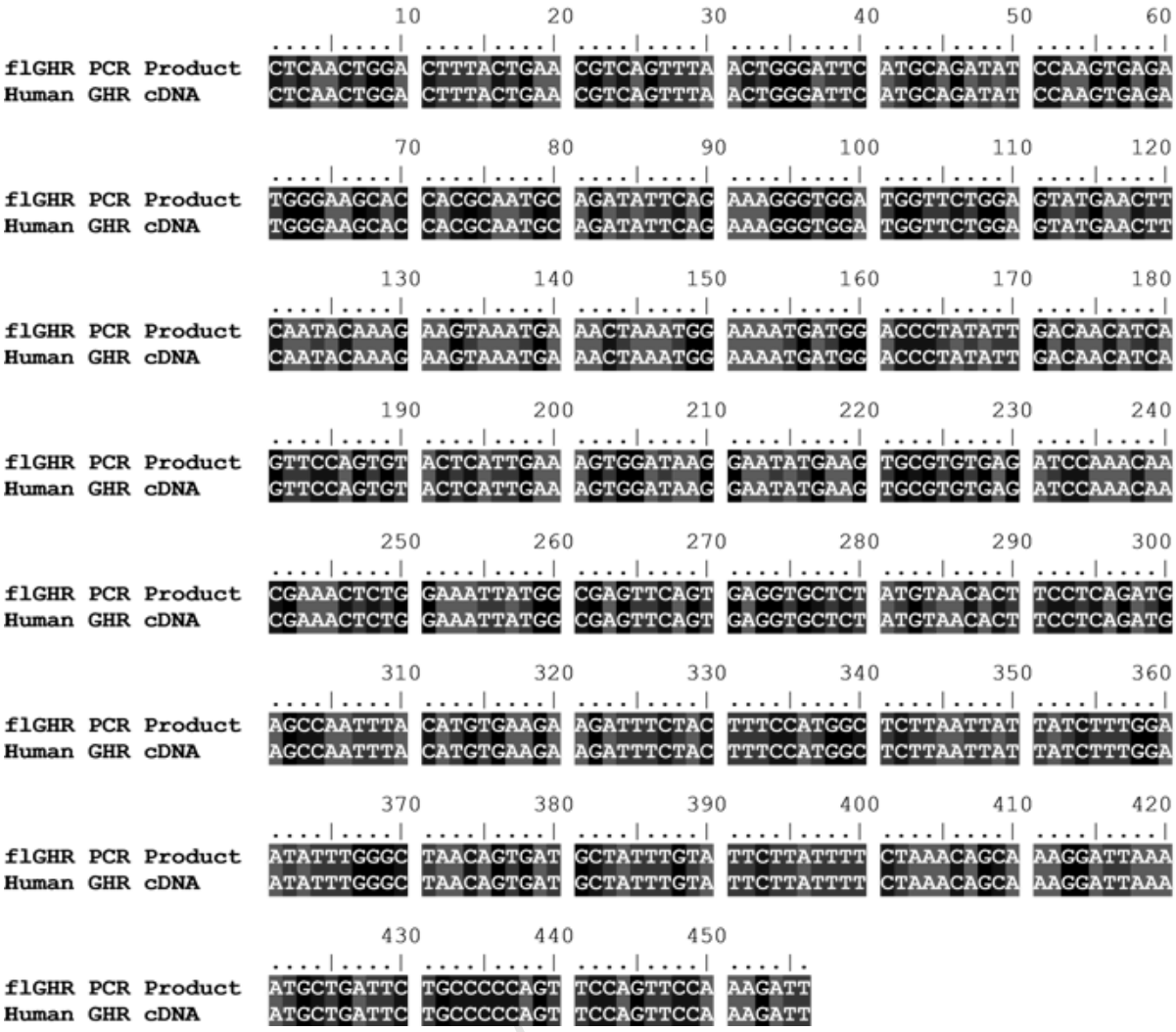


**Figure 30: Sequencing and alignment of the flGHR PCR product to human GHR cDNA.** The PCR product generated using T47D cDNA as template and flGHR-specific primers, and its alignment to human GHR cDNA, indicates that the 456bp product corresponds to human GHR.

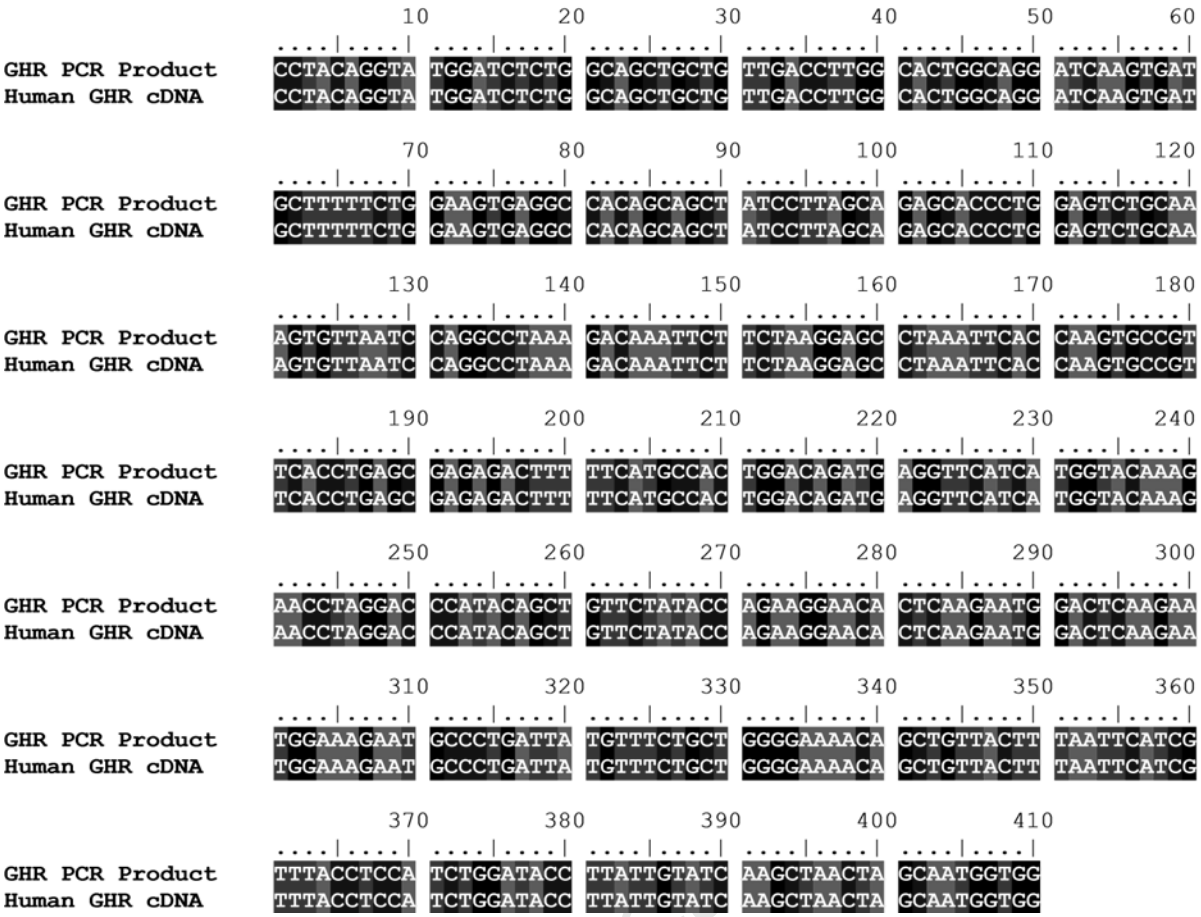


**Figure 31: Sequencing and alignment of the GHR PCR product using the d3GHR-specific primers to human GHR cDNA.** The PCR product generated using T47D cDNA as template and d3GHR-specific primers, and its alignment to human GHR cDNA, indicates that the 410bp product corresponds to human GHR.

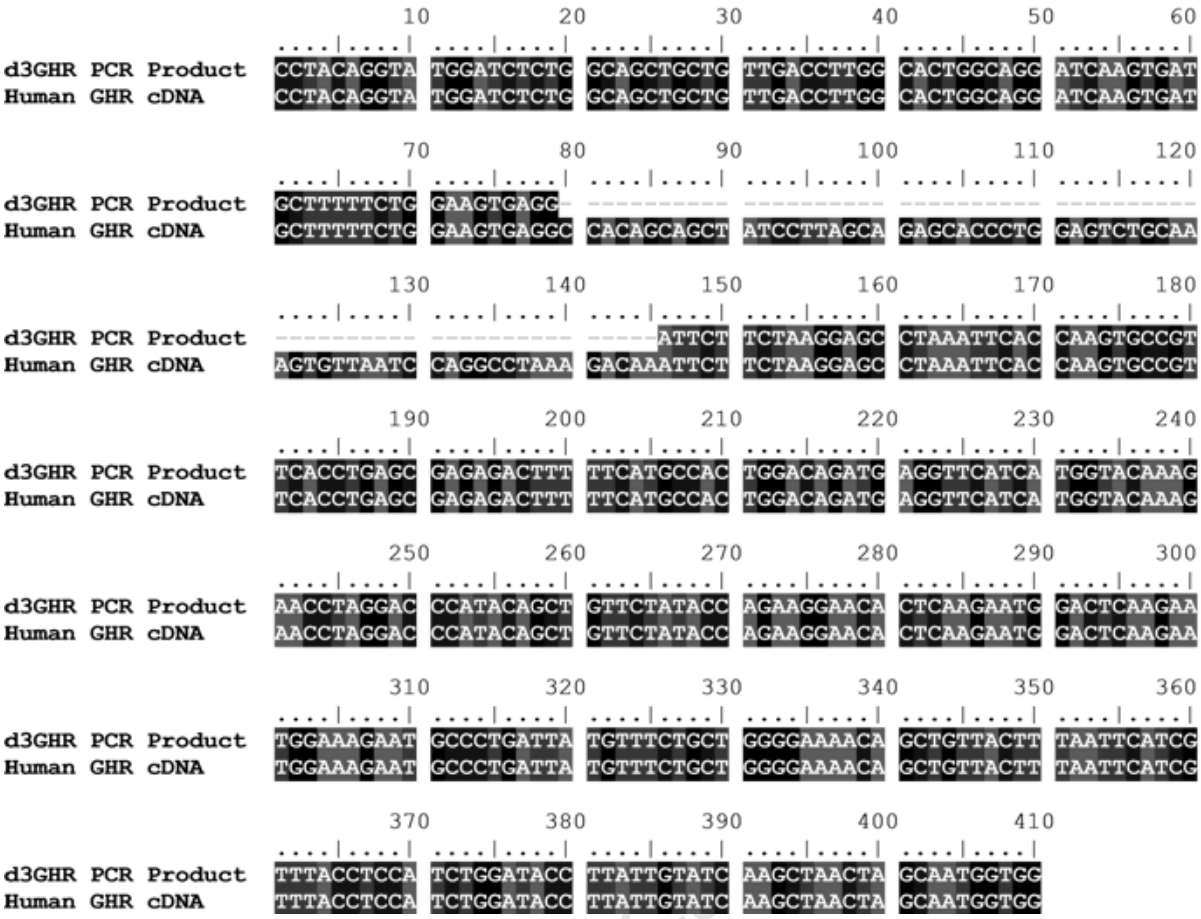


**Figure 32: Sequencing and alignment of the d3GHR PCR product using the d3GHR-specific primers to human GHR cDNA.** The PCR product generated using T47D cDNA as template and d3GHR-specific primers, and its alignment to human GHR cDNA, indicates that the 354bp product corresponds to human d3GHR. The missing 66bp in the PCR product sequence compared to the GHR cDNA sequence correlates to the loss of the 66bp-long exon 3 of GHR

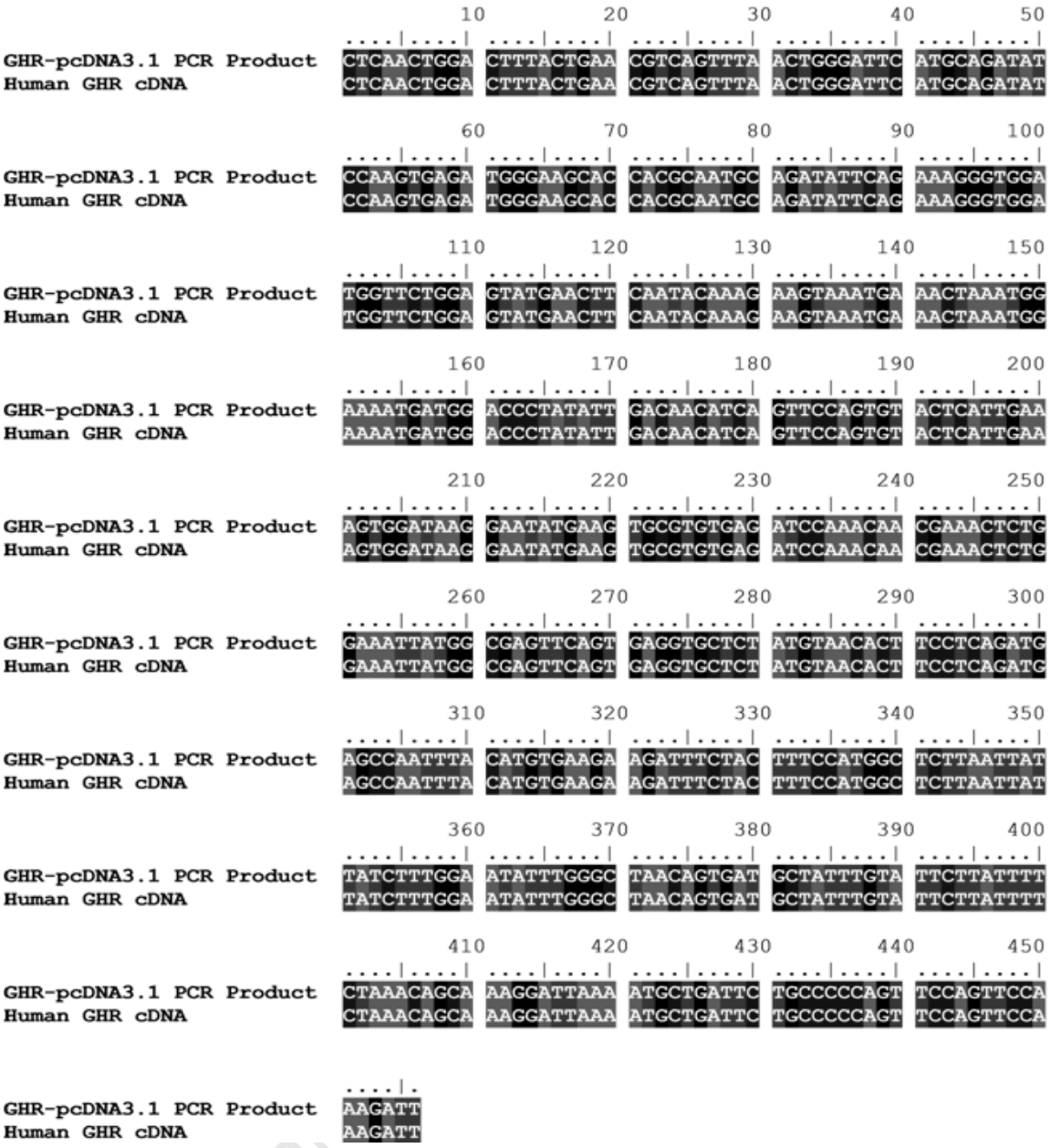


**Figure 30: Sequencing and alignment of the GHR-pcDNA3.1 expression plasmid and human GHR cDNA.** 100 copies of the GHR expression plasmid underwent PCR using the flGHR-specific primers. The PCR product was sequenced and aligned to the human GHR cDNA sequence. Alignment reveals that the insert of the GHR expression plasmid was most likely that of human GHR cDNA.

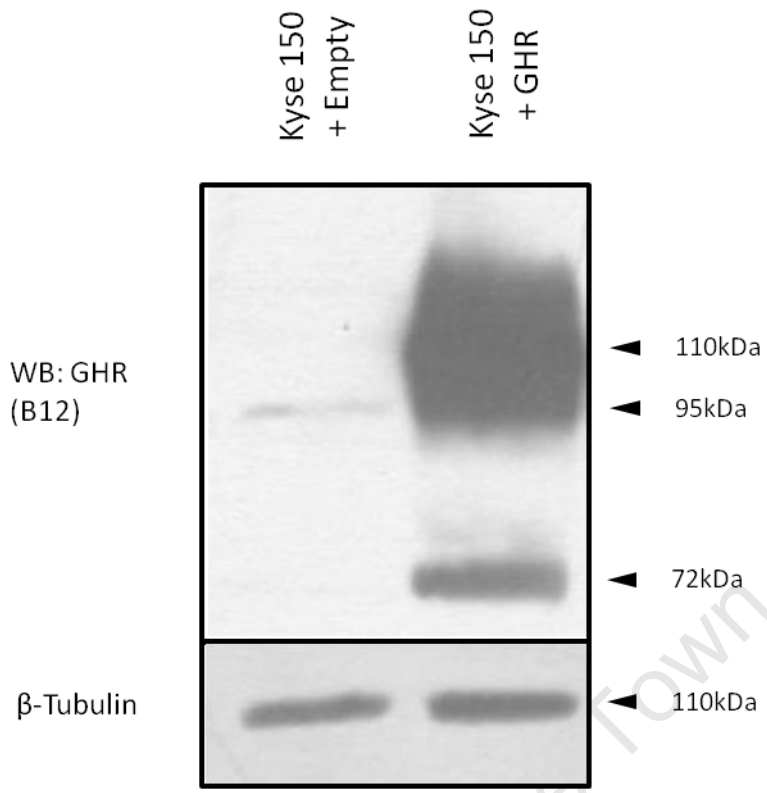


**Figure 31: Immunoblotting Kyse 150 cells transfected with GHR and empty expression vector.** Kyse 150 cells were either transfected with the GHR-pcDNA3.1 (Kyse 150+GHR) or empty pcDNA3.1 (Kyse 150+Empty) expression vector and protein lysates were immunoblotted as described in materials and methods. Sizes of bands are indicated. β-Tubulin was included as a control for protein loading.

**Appendix B- Solutions**

## 1. Transformation and Plasmid Isolation

**TE Buffer (pH8.0) 500ml**

5ml 1M Tris-HCl (pH8.0)

1ml 0.5M EDTA (pH 8.0)

**Luria Broth (LB) (100ml)**

10g Bactro-Tryptone

5g Bacto-Yeast

10g $NaCl_2$

900ml $H_2O$

Sterilize by autoclaving

Store at room temperature

**Ampicillin-containing LB**

1:1000 dilution of filter-sterilized ampicillin (100mg/ml) into LB

Store at room temperature

**Ampicillin-containing Agar (200ml)**

3g Agar

200ml LB

Sterilize by autoclaving

Add 200µl ampicillin (100mg/ml) once cool

Pour approximately 20ml into Petri dish

## 2. RNA Isolation and Electrophoresis

**DEPC-Treatment**

0.1% DEPC in distilled $H_2O$

Stir for one hour

Soak pipette tips and microfuge tubes in DEPC-treated $H_2O$ overnight

Remove as much water as possible and autoclave

**DEPC-Treaded $H_2O$**

0.1% DEPC in distilled $H_2O$

Stir for one hour

Autoclave

**RNA Gel (50ml)**

0.75g Agarose

42ml $dH_2O$

Heat and allow to cool

5ml 10X MOPS

2.7ml Formaldehyde

**10X MOPS (1000ml)**

41.86g MOPS

16.6ml 3M NaAcetate

20ml 0.5M EDTA (pH8.0)

Dilute to 1x MOPS as needed

**2x RNA Loading Dye**

0.72ml Formamide

0.16ml 10X MOPS

0.26ml Formaldehyde

0.18ml $dH_2O$

0.1ml 80% Glyerol

0.08ml Bromophenol Blue

Store at -80$^{o}$C

### 3. DNA Electrophoresis

**2% Agarose Gel (50ml)**

1g Agarose

50ml 1X TAE

3µl Ethiduim Bromide (10mg/ml)

**0.8% Agarose Gel (50ml)**

0.4g Agarose

50ml 1X TAE

3µl Ethidium Bromide (10mg/ml)

**50xTAE (500ml)**

121g Tris

28.5ml Glacial Acetic acid

50ml 0.5M EDTA (pH8.0)

Make up to 500ml with $dH_2O$

**6X DNA Loading Dye**

25mg Bromophenol Blue

25mg Xylene Cyanol

3.3ml Glycerol

6.7ml $dH_2O$

Add Tris until blue

## 4. Cell Culture

**10X PBS (500ml)**

40g NaCl

1g KCl

5.75g $Na_2HPO_4.7H_2O$

1g $KH_2PO_4$

Make up to 500ml with $dH_2O$

Dilute to 1x PBS when needed

**Complete DMEM Media**

450ml DMEM

5ml P/S

50ml FBS

**Trypsonisation Solution (1000ml)**

0.5g Trypsin

8g NaCl

1.45g $NaHPO4.2H_2O$

0.2g KCl

0.2g $KH_2HPO_4$

10mM EDTA

Make up to 1000ml with 1xPBS

**Freezing Media (10ml)**

9ml Complete DMEM Media

1ml 99% DMSO

## 5. Immunoblotting

**RIPA Buffer (200ml)**

1.752g NaCl

2ml TritonX100

0.2g SDS

2ml 1M Tris (pH 7.5)

2g Na deoxycholate

**Complete RIPA (1ml)**

825µl RIPA

100µl 10X Protease Inhibitor (Sigma, USA) (104mM AEBSF. 80µM Aprotinin, 4mM Bestatin, 1.4mM E-46, 2mM Leupeptin, 1.5mM Pepstatin)

50µl 1MNaF

20µl 0.1M $Na_3VO_4$

5µl 100mM PMSF

**Resolving Gel Buffer (200ml)**

36.2g Tris

0.8g SDS

pH 8.9 and make upto 200ml with $dH_2O$

Store at $4^oC$

**Stacking Gel Buffer (100ml)**

5.9g Tris

0.4g SDS

pH 8.0 and make up to 100ml with $dH_2O$

Store at $4^oC$

**7.5% Denaturing Polyacrylamide Separating Gel**

3ml Resolving Gel Buffer

2.25ml 30% Acrylamide

3.75ml $dH_2O$

180µl 0.1% APS

18µl TEMED

**5% Denaturing Polyacrylamide Stacking Gel**

1.5ml Stacking Gel Buffer

1ml 30% Acrylamide

3.5ml $dH_2O$

60µl 0.1% APS

6µl TEMED

**5X Protein Loading Dye (50ml)**

1.75g Tris

30ml Glycerine

pH 6.8 and make up to 40ml with $dH_2O$

5g SDS

Make up to 50ml with $dH_2O$

**2X Protein Loading Dye (10ml)**

4ml 5x Protein Loading Dye

6ml 1X PBS

**10X Running Buffer (1000ml)**

30.2g Tris

144g Glycine

10g SDS

Make up to 1000ml with $dH_2O$

Dilute to 1X Running Buffer when needed

**10X Transfer Buffer**

144g Glycine

38g Tris

Make up to 1000ml with $dH_2O$

**1X Transfer Buffer (1000ml)**

100ml 10X Trasfer Buffer

200ml Methanol

700ml $dH_2O$

**10X TBS (1000ml)**

60.5g Tris

87.6g NaCl

pH7.5 and make up to 1000ml with $dH_2$)

**TBST (1000ml)**

100ml 10X TBS

900ml $dH_2O$

1ml Tween 20

**B-Mercaptoethanol Stripping Buffer (200ml)**

1.4ml β-Mercaptoethanol

4g SDS

12.5ml 1M Tris (pH6.7)

Make up to 200ml with $dH_2O$

## 6. Immuncytochemistry

**4% Paraformaldehyde (PFA)**

16g PFA

80ml $dH_2O$

Cover with foil and stir for 1hr not letting temperature exceed 60$^{o}$C

Add 10M NaOH until clear

Filter-sterilise

Adjust to pH 7.0

Store in 2.5ml aliquots at -20$^{o}$C

Add 7.5ml 1X PBS to make 4% PFA

**50mM $NH_4Cl$**

0.265g $NH_4Cl$

100ml 1X PBS

**Mowiol 4-88**

2g Mowiol 4-88

2ml Glycerol

4ml $dH_2O$

Leave at RT O/N

8ml 0.2M Tris (pH8.5)

Incubate at50$^{o}$C for 1hr

Store in 2ml aliquots at -20$^{o}$C

Add 2.5% Anti-Fading Agent (N-propyl gallate) day before use

## 7. Proliferation and Drug Treatment Assays

**MTT (5ml)**

25mg MTT

5ml 1X PBS

Vortex mixture and incubate at 37$^{o}$C for 30min

Filter-sterilise

Store in dark at 4$^{o}$C

Use within one month

**Solubilisation Solution (500ml)**

50g SDS

153ml HCl

Make up to 500ml with $dH_2O$

## Appendix C – DNA and Protein Markers

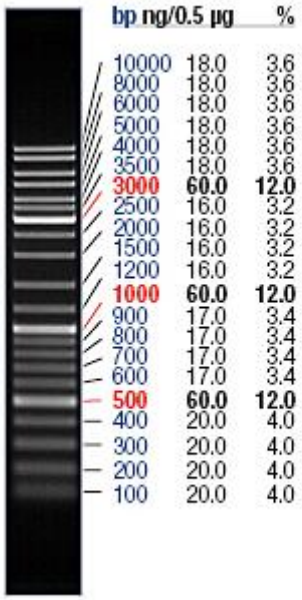


**Figure 31: DNA molecular weight marker: O'GeneRuler DNA Ladder Mix (Thermo Scientific)** used to determine the size of qRT-PCR products.

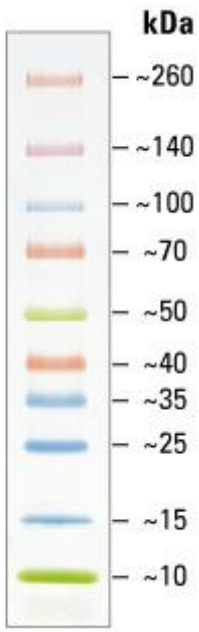


**Figure 32: Protein molecular weight marker: Spectra Multicolour Broad Range Protein Ladder** used to determine size of proteins subjected to polyacrylamide gel electrophoresis and western blot analysis.